VYSOKÉ UČENÍ TECHNICKÉ V BRNĚ
BRNO UNIVERSITY OF TECHNOLOGY

FAKULTA ELEKTROTECHNIKY
A KOMUNIKAČNÍCH TECHNOLOGIÍ
FACULTY OF ELECTRICAL ENGINEERING AND COMMUNICATION

ÚSTAV BIOMEDICÍNSKÉHO INŽENÝRSTVÍ
DEPARTMENT OF BIOMEDICAL ENGINEERING

INTEGRACE A TESTOVÁNÍ REAL-TIME ŘÍDICÍ JEDNOTKY PRO SIMULACI PLIC
INTEGRATION AND TESTING OF A REAL TIME PROCESSING UNIT FOR LUNG SIMULATION

DIPLOMOVÁ PRÁCE
MASTER'S THESIS

AUTOR PRÁCE   Bc. Richard Paštěka
AUTHOR

VEDOUCÍ PRÁCE   Ing. Jiří Sekora
SUPERVISOR

BRNO 2016

BRNO UNIVERSITY OF TECHNOLOGY

&

UNIVERSITY OF APPLIED SCIENCES TECHNIKUM WIEN

ACKNOWLEDGEMENT

This Master's Thesis and the corresponding tasks have been performed within the Double Degree agreement between the study programs Biomedical and Ecological Engineering at Brno University of Technology & Biomedical Engineering Sciences at University of Applied Sciences Technikum Wien.

Brno   ……………….   ……..…………………

                                                              (author's signature)

BRNO FACULTY OF ELECTRICAL
UNIVERSITY ENGINEERING
OF TECHNOLOGY AND COMMUNICATION

Master's Thesis

Master's study field **Biomedical and Ecological Engineering**
Department of Biomedical Engineering

Student:	Bc. Richard Paštěka	*ID:* 134379
Year of study:	2	*Academic year:* 2015/16

TITLE OF THESIS:

Integration and testing of a real time processing unit for lung simulation

INSTRUCTION:

1) Study the physiology of human lungs and respiratory processes. 2) Study the simulator pulmonary lung module (the project AlveoPic output). Learning the sensors module simulator. 3) Adjust and adapt created control unit to cooperate with other units of simulator. 4) Implement the designed controller into simulator. 5) Verify the functioning of the unit and the designed algorithms. The topic is dealt in cooperation with the FH Technikum Wien. For compliance with semester project; it is necessary to develop at least items 1) to 3).

RECOMMENDED READING:

[1] JANKOVSKÝ, Michal. Návrh některých programových systémů pracujících v reálném čase. Brno: Vysoké učení technické, 1999, 30 s. Vědecké spisy Vysokého učení technického v Brně. ISBN 80-214-1416-2.

[2] ŠOLC, František, František ZEZULKA, Ivo VESELÝ, Jiří SEKORA, Martin MÉZL, Anton ESCHLI a Ivo PROVAZNÍK. The mathematical model of a LUNG simulator. MEFANET journal. Brno: Facta Medica, 2014, (2). ISSN 1805-9163.

Date of project specification:	8.2.2016	*Deadline for submission:* 20.5.2016

Leader: Ing. Jiří Sekora
Consultant Master's Thesis: Mathias Forjan, MSc., FH-Prof. DI Dr. Stefan Sauermann, Ing. Ivo Veselý

prof. Ing. Ivo Provazník, Ph.D., *Subject Council chairman*

ABSTRACT

An active mechanical lung simulator (iLung) provides the possibility of simulating human breathing patterns. The aim of this thesis is to implement and test an real time embedded control and acquisition system cRIO as iLung control unit. Resulting connections are documented in tables and also by labelling assembly drawings with corresponding pin functions. One of the major improvements was made by tuning the motor and modifying the proportional-integral controller in the software. Those modifications resulted in significantly reduced motor oscillations around zero value. In order to increase usability and accessibility of the simulator a user manual and corresponding laboratory experiment were additionally created. The Validation of cRIO implementation was not limited to simple testing routines, but also extended on testing the simulator as a whole functioning unit. The results of simulator based measurements were compared and discussed to the spirometry measurements, taken from 20 subjects. Measurements showed a high degree of similarity between breathing patterns simulated by iLung and normal human breathing supporting the possibility for further research applications.

KEYWORDS

Human breathing patterns, active mechanical lung simulation, motor tuning, cRIO

ABSTRAKT

Aktivní mechanický plicní simulátor (iLung) nabízí možnost simulace lidského dýchání. Cílem této práce je implementovat a otestovat řídící a akviziční systém cRIO pracující v reálném čase, jako řídící jednotku simulátoru. Výsledné propojení obou zařízení je zdokumentováno ve formě tabulek a původních osazovacích výkresů, které jsou doplněny o popis funkce každého pinu. Významného zlepšení bylo dosaženo laděním motoru a modifikací proporcionálně-integračního regulátoru v řídícím programu. Tyto modifikace mají za následek významné snížení oscilací v okolí nuly. Pro zvýšení využitelnosti a přístupnosti simulátoru byl vytvořen uživatelský manuál a s ním související laboratorní cvičení. Validace funkce implementované řídící jednotky nebyla omezena pouze na jednoduché testovací rutiny, ale rozšířena na testování funkce simulátoru jako celku. Měření na simulátoru byly porovnány a diskutovány s klidovým spirometrickým vyšetřením 20ti probandů. Měření prokázala velkou míru podobnosti mezi simulovaný dýcháním iLung a klidovým lidským dýcháním.

KLÍČOVÁ SLOVA

Lidské dýchání, aktivní mechanická plicní simulace, ladění motoru, cRIO

DECLARATION

I declare that I have written my master's thesis on the theme of "Integration and testing of a real time processing unit for lung simulation" independently, under the guidance of the master's thesis supervisor and using the technical literature and other sources of information which are all quoted in the thesis and detailed in the list of literature at the end of the thesis.

As the author of the master's thesis I furthermore declare that, as regards the creation of this master's thesis, I have not infringed any copyright. In particular, I have not unlawfully encroached on anyone's personal and/or ownership rights and I am fully aware of the consequences in the case of breaking Regulation $\S\,11$ and the following of the Copyright Act No 121/2000 Sb., and of the rights related to intellectual property right and changes in some Acts (Intellectual Property Act) and formulated in later regulations, inclusive of the possible consequences resulting from the provisions of Criminal Act No 40/2009 Sb., Section 2, Head VI, Part 4.

Brno   . . . .
                                                                     (author's signature)

ACKNOWLEDGEMENT

CONTENTS

LIST OF FIGURES

LIST OF TABLES

INTRODUCTION

The cone-shaped lungs are paired organs situated inside the thoracic cavity forming to the great extend lower respiratory tract. The most important functions of lungs include the gas exchange between the alveoli and the pulmonary capillaries via diffusion. Each lung is divided into lobes. The right lung has three lobes and the left lung has two lobes plus a depression, the cardiac notch caused by heart position.

Risk factors such as tobacco smoke, air pollution, dusts, and frequent lower respiratory infections during childhood are among reasons why number of chronic respiratory disease patients continues to grow every year. Chronic respiratory diseases are not curable, however, various forms of treatment that help dilate major air passages and improve shortness of breath can help control symptoms and increase patient's quality of life. Aerosol therapy is widely used form of treatment due to drug precise dosage, sustained localized action and possibility of home therapy.

The use of drug aerosol has been limited by the relative lack of knowledge about the fate of inhaled drugs. Several lung models such as electrical, mechanical and mathematical has been developed in order to approximate behaviour of a human lung with aim of shining a light as to this question. Due to difficulties of simulating a fully functional human lung high effort, either in computational power or in the complexity of the design is needed. One of the most precise and reliable way to simulate a human breathing patterns is to use mechanical lung simulator. The iLung 2.1 is next generation active mechanical lung simulator that offers the possibility to simulate physiological breathing patterns. Latex bags or porcine lung, which structure is similar to human lungs, can be mounted into the simulator. Furthermore, with additional equipment, aerosol measurements are possible.

This Master's Thesis provides compressed overview of human respiratory system and its anatomy. As an integration and testing of a real-time control unit is a main topic of the thesis, all important components of iLung 2.1 are described as they are essential to succeed with the given task. Emphasis was nonetheless given to creating documentation of the entire process for simple repeatability in the future. After real-time control unit implementation and testing question whether the iLung 2.1 active mechanical lung simulator is capable of successfully imitating the human respiratory cycle arose and was answered out of the interest for the topic.

The Master's Thesis is dealt with based on a long-term collaboration between the Brno University of Technology and University of Applied Sciences Technikum Wien.

1 HUMAN RESPIRATORY SYSTEM

Body cells continually use oxygen (O_2) for the metabolic reactions that release energy from nutrient molecules and as a result produce adenosine triphosphate (ATP). These same reactions produce carbon dioxode (CO_2) which is undesirable for a body in higher concentrations. Because excessive amount of CO_2 causes acidity that can be toxic to cells, excess CO_2 must be eliminated quickly and efficiently.[31]

The major function of respiratory system is to supply the body with oxygen and dispose of carbon dioxide. To accomplish this function, at least three processes, collectively called respiration, must occure:

1. **Pulmonary ventilation** (commonly called breathing) is the flow of the air moved into the lungs during inspiration and out of the lungs during expiration. Therefore, gases there are continuously changed and refreshed.
2. **External respiration** is the exchange of gases between the air spaces (alveoli) of the lungs and the blood flowing through the pulmonary capillaries. In this process, pulmonary capillary blood gains O_2 and loses CO_2.
3. **Internal respiration** is the exchange of gases between blood in systemic capillaries and tissue cells. The blood loses O_2 and gains CO_2. The metabolic reactions ongoing within cells, that consume O_2 and give off CO_2 during the production of ATP, is called *cellular respiration* [31, 15].

There is a strong link between the respiratory and circulatory systems. If either system fails, the body's cells begin to die from oxygen starvation.

In addition to its main function *respiration* the respiratory system performs several other functions, including: contributing to the regulation of acid-base balance in the blood, enabling vocalization, participating in defence against pathogens and foreign particles in the airways, providing a route for water and heat losses (via the expiration of air that was moistened and warmed during inspiration).[29]

1.1 Anatomy of the Respiratory Tract

Structurally, the respiratory system consists of two parts:

1. **The upper respiratory system** (upper airways) includes the nose, nasal cavity, pharynx, and associated structures. Occlusion of the upper airways can occur acutely when a person chokes on food or chronically during diseases such as sleep apnoea.
2. **The lower respiratory system** consists of the larynx (voice box), trachea, within lungs bronchus, bronchi (primary, secondary, tertiary), terminal bronchioles, respiratory bronchioles, alveolar duct and alveoli (alveolar sac) [31, 29].

Above mentioned structures can be seen in Fig. 1.1
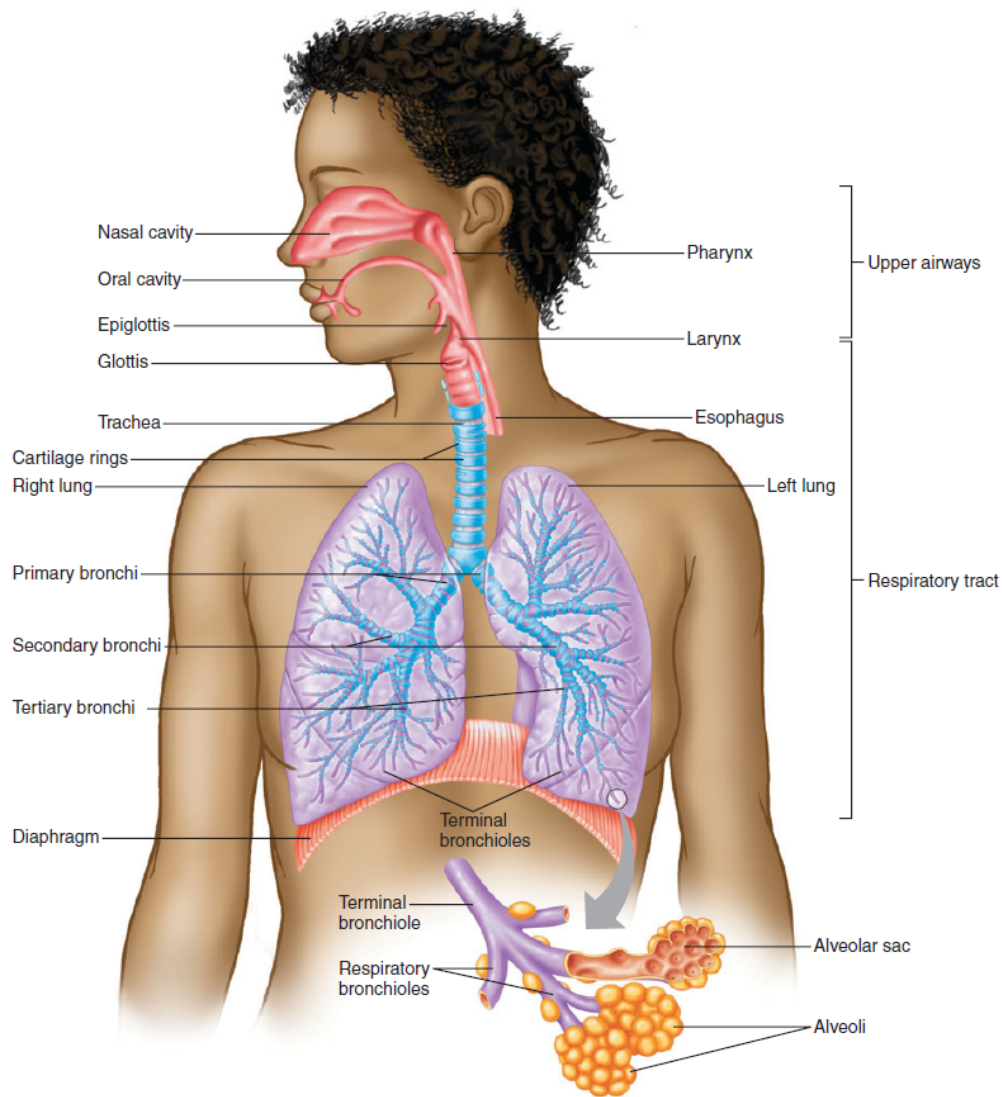
Fig. 1.1: Anatomy of respiratory tract [29]

Functionally, the respiratory system can also be divided into two parts:

- **The conducting zone** includes all other respiratory passageways, which provide fairly rigid conduits for air to reach the gas exchange sites. The conducting zone organs also cleanse, humidify, and warm incoming air. As a result, air reaching the lungs has fewer irritants (dust, bacteria, etc.) than when it entered the body, and it is warm and damp.
- **The respiratory zone** consists of tissues within the lungs where gas exchange occurs between air and blood.[15]

The *chest wall* consists of structures that protect the lungs: the rib cage (12 pairs of ribs), the sternum, the thoracic vertebrae all together with associated muscles and connective tissue. Muscles which are responsible for breathing, include the internal

intercostal, external intercostal (located between the ribs) and the dome-shaped diaphragm. Diaphragm seals off the lower end of the chest wall and separates the thoracic and abdominal cavities [6]. Muscles and connective tissue in the neck close off the chest wall at its upper end. The chest wall forms an protective, airtight, continuous barrier around the lungs.

The interior surface of the chest wall and the exterior surface of the lungs are lined by a membrane called the *pleura*. Each lung is surrounded by a separate pleural sac. The side of the pleural sac attached to the lung tissue is called the *visceral pleura* and the side attached to the chest wall is called the *parietal pleura*. Between the two pleurae is a very narrow compartment called the *intrapleural space*, which is filled with a small volume (approximately 15 ml) of intrapleural fluid. Pleura has an important role in mechanics of respiration [29].

1.2 Physical Aspects of Pulmonary Ventilation

Movement of air into and out of the lungs occurs as a result of pressure differences. Direction of air flow through bronchioles is from higher to lower pressure being directly proportional to the pressure difference and inversely proportional to the frictional resistance to flow. Pulmonary ventilation is influenced by the physical properties of the lungs, including their compliance, elasticity, and surface tension [6].

1.2.1 Pressure Changes in the Thoracic Cavity

Values of respiratory pressures are always described relative to *atmospheric pressure* P_{atm}, which is the pressure exerted by the mixture of atmospheric gases surrounding the body. A negative respiratory pressure in any respiratory area indicates that the pressure in that region is lower than atmospheric pressure. At sea level, atmospheric pressure is 760 mm Hg. This pressure can also be expressed in different units: $P_{atm} = 760$ mm Hg ≈ 1 atm ≈ 101.325 kPa. At altitudes higher than sea level, atmospheric pressure decreases [3]. Remaining primary pressures associated with ventilation are:

- **Intrapulmonary pressure** also called (intra-alveolar) pressure (P_{pul}) is the pressure of air within the alveoli. Intrapulmonary pressure varies during the phases of ventilation. In fact, the difference between intra-alveolar pressure and atmospheric pressure is the pressure gradient that drives ventilation. At rest, it is equal to atmospheric pressure, thus $P_{pul} = 0$ mm Hg.
- **Intrapleural pressure** (P_{ip}) is the negative pressure inside the pleural space. At rest, $P_{pul} = -4$ mm Hg. Although intrapleural pressure varies with the

phase of ventilation, it is always negative during normal breathing (and always less than P_{pul}) because opposing forces exerted by the chest wall and the lungs tend to pull the *parietal pleura* and *visceral pleura* apart. Intrapleural pressure can be positive during forced expiration. Pressure changes will be described in more detail in subsection 1.2.2.

- **Transpulmonary pressure** (P_{tp}) is the difference between the intrapulmonary and intrapleural pressures $P_{tp} = P_{pul} - P_{ip}$. Transpulmonary pressure keeps the lungs from collapsing [29]. Moreover, the size of the transpulmonary pressure determines the size of the lungs at any time. Increase in transpulmonary pressure creates a larger distending pressure across the lungs, which is accompanied by the expansion of the lungs (alveoli) [15].
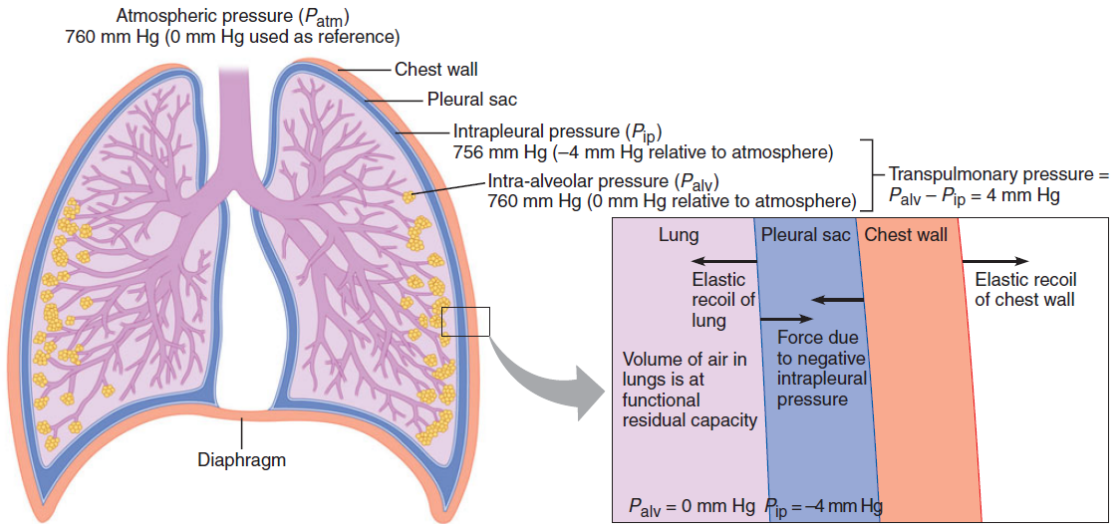
Fig. 1.2: Pleural pressures at rest [29]

When the lungs are at the functional residual capacity (between breaths), as can be seen in Fig. 1.2, the intrapulmonary pressure $P_{pul}=$ atmospheric pressure $= 0$ mm Hg. The lung is distended, and an elastic recoil force tends to collapse it inward. Furthermore, the chest wall is compressed, and an elastic recoil force tends to expand it outward. The net force that these two opposing forces exert on the two sides of the pleural sac creates a negative intrapleural pressure P_{ip}. The entire system is stable because the elastic recoil forces of the lungs and chest wall are in balance, and no net change in size of the lung or chest wall occurs [29, 3].

Negative intrapleural pressure has an important role in normal breathing. The presence of air in the pleural cavity is referred to as a *pneumothorax* which causes lung to collapse due to equalization of intrapreural and atmospheric pressure. Pneumothorax is reversed by drawing air out of the intrapleural space with chest tube. This procedure allows the pleurae to heal and the lung to reinflate and resume

normal function. In general, *Atelectasis* (lung collapse) occurs when a bronchiole becomes plugged (as may follow pneumonia). Affected alveoli then absorb all of their air and collapse. Atelectasis can also occur during pneumothorax as air enters the pleural cavity either through a chest wound or a rupture of the visceral pleura, which allows air from the respiratory tract to enter the pleural cavity [15].

1.2.2   Mechanics of Breathing

Pulmonary ventilation consists of two phases: *inspiration* and *expiration*. Inspiration (inhalation) and expiration (exhalation) are accomplished by alternately increasing and decreasing the volumes of the thorax and lungs. Normal, quiet inspiration results from muscle contraction (active process), and normal expiration from muscle relaxation and elastic recoil (passive).

$$P_1 \cdot V_1 = P_2 \cdot V_2 \tag{1.1}$$

Volume changes lead to pressure changes, and pressure changes lead to the flow of gasses to equalize the pressure. This follows from Boyle's law, Eq.1.1, where P is the pressure of the gas, V is its volume, and subscripts 1 and 2 represent the initial and resulting conditions respectively. Boyle's law states that the pressure of a given quantity of gas is inversely proportional to its volume at constant temperature [15].

Inspiration starts by neural stimulation of the inspiratory muscles. Contraction of the diaphragm causes it to flatten and move downward. Simultaneously, external intercostal muscles oriented obliquely contract, which causes the ribs to move upward and outward, expanding the chest wall. All these actions combined together result in increase of the thoracic cavity volume. Other muscles of the neck (scalene and sternocleidomastoid) and chest region (pectoralis minor) play subsidiary roles in inspiration, and are used especially during forceful inspiration. Pleura that is attached to the chest wall expands outwards, causing the intrapleural pressure to decrease. This decrease in intrapleural pressure leads to an increase in the transpulmonary pressure. An increase in transpulmonary pressure due to a decrease in P_{ip} creates a larger distending pressure across the lungs, so the lungs (alveoli) expand with the chest wall. When the lungs expand, pressure in the alveoli decreases to less than atmospheric pressure, so the air flows into the alveoli. It continues to flow in until the pressure in the alveoli equalize with atmospheric pressure. It is true that stronger contractions of the inspiratory muscles produce a greater expansion of the thoracic cavity, making intrapleural pressure even more negative and creating a greater transpulmonary pressure. As the result lung expansion is greater and volume of air moved into the lungs is larger.

Expiration does not require muscle contraction during quiet breathing (passive process). At the end of an inspiration, the chest wall and lungs are expanded by muscle contraction. Expiration is achieved by simply relaxing these muscles, which occurs when motor neurons to the inspiratory muscles are no longer activated. As consequence the elastic chest wall and lungs recoil to their original (resting) positions. As the chest wall and lungs recoil, the volume of the lungs decreases, causing alveolar pressure to increase to a value greater than atmospheric pressure. Air flows out (expiration) due to the pressure gradient, until the volume in the lungs equals the functional residual capacity (FRC). If it is necessary to rapidly decrease alveolar volume the expiration muscles contracts. Forceful expiration, using the expiration muscles, is called active expiration [29, 32].
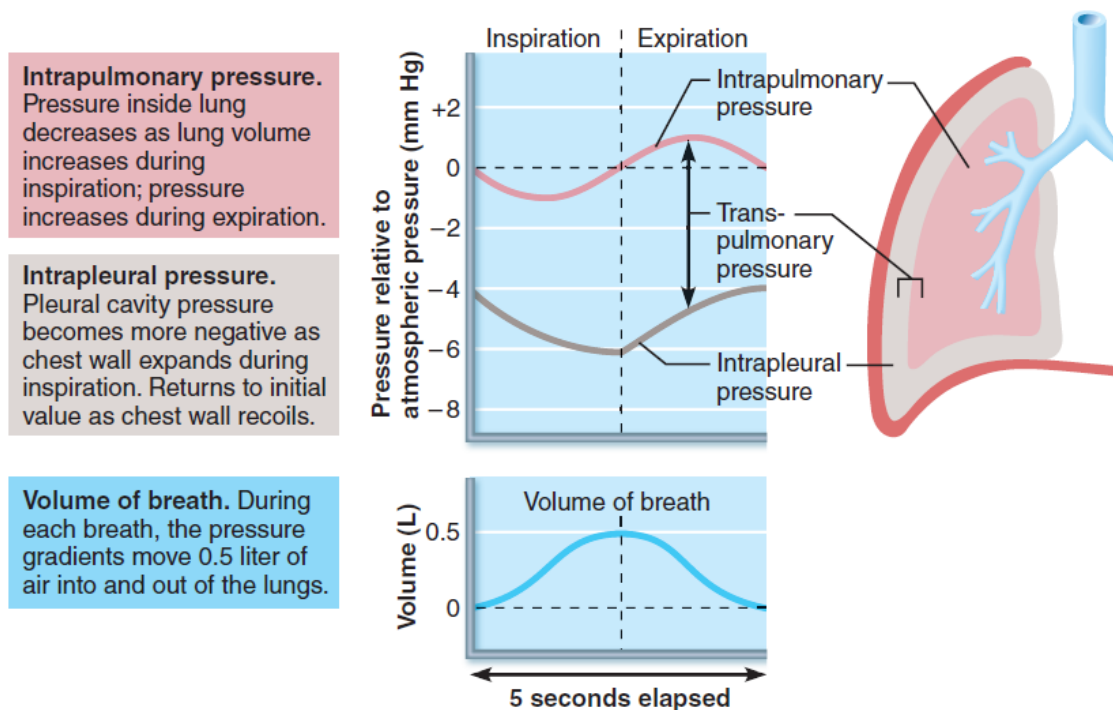
Fig. 1.3: Pressure changes during inspiration and expiration [15]

1.2.3   Physical Properties of the Lungs

Pressure gradients produced by changes in the volume of the lungs drive inspiration and expiration, which is discussed in subsection 1.2.2. In this subsection several factors that affect development of pressure gradients and factors that affect airway resistance are discussed.

Airway Resistance is the resistance of the respiratory tract to airflow during inspiration and expiration, calculated as shown in Eq.1.2. Driving force for air flow

($\dot{V}$) into and out of the lungs is difference between atmospheric and intrapulmonary pressure. Because atmospheric pressure is constant, changes in alveolar pressure determine the direction of air movement. The amount of gas flowing into and out of the alveoli is directly proportional to ΔP [3]. Airway resistance accounts for approximately 80% of the frictional resistance to ventilation. Gas flow decreases as resistance increases. The greatest resistance to gas flow occurs in the medium-sized bronchi. Typical adult resistance values are: $R = 1hPa/l/s - 3$ hPa/l/s [12].

$$R = \frac{\Delta P}{\dot{V}} = \frac{P_{atm} - P_{pul}}{\dot{V}} \tag{1.2}$$

Alveoral Surface Tension occurs at gas-liquid boundary. The molecules of the liquid are more strongly attached to each other than to the gas molecules. As the result of this unequal attraction state of tension is produced at the liquid surface. This *surface tension* causes liquid molecules to be pulled closer together and also reduces their contact with the dissimilar gas molecules. The other effect caused by surface tension is the opposite force to any other, that tends to increase the surface area of the liquid [15]. Major component of the liquid film that lines alveolar wall is water. Due tu its composition of very polar molecules, water has high surface tension. If the film were pure water, the lungs (alveoli) would collapse as water causes the reduction of alveoli to minimum possible size. Complex of lipids and proteins called *surfactant* prevents alveolar collapse. Thanks to surfactant cohesiveness of water molecules decreases and therefore surface tension of alveolar fluid is reduced. As a result, forces needed for lung expansion are lower [32].
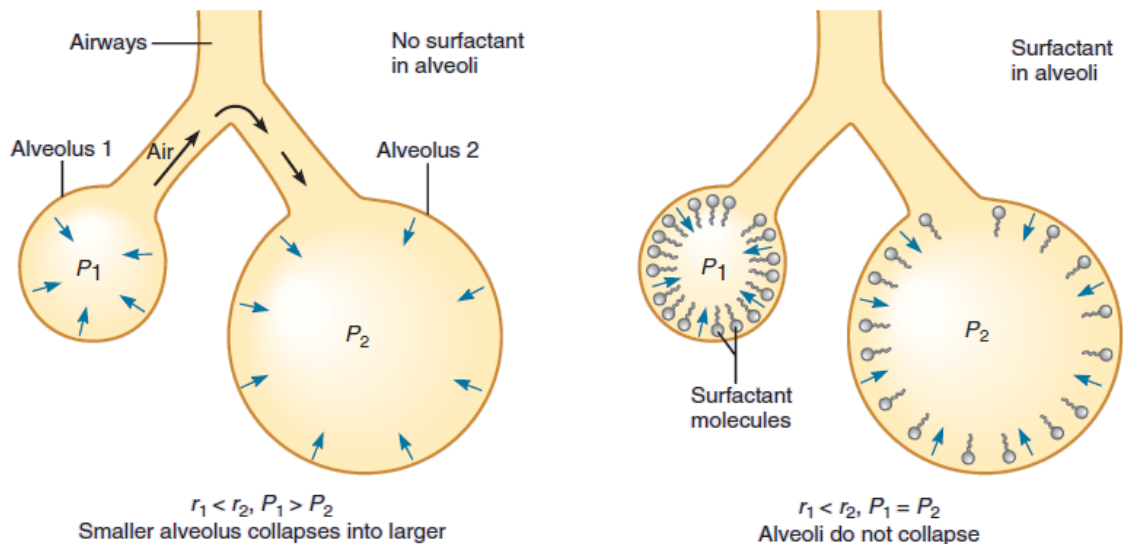
Fig. 1.4: Effect of pulmonary surfactant [29]

According to Laplace's law, Eq.1.3, the air pressure (P) necessary to prevent the collapse of an alveolus (spherical) is directly proportional to the surface tension (T) and inversely proportional to the alveolar radius (r).

$$P = \frac{2 \cdot T}{r} \tag{1.3}$$

At the breathing resting phase, air pressure is the same inside all of the alveoli. The alveoli however are not all the same size. Without surfactant the pressure in larger alveolus is just high enough to prevent it from collapsing, but smaller alveolus should collapse (pressure must be lower). Collapse of smaller alveolus increase its pressure (P_1), making it higher than pressure in larger alveolus (P_2). Air should than follow the pressure gradient from $P1$ to $P2$, as can be seen at Fig. 1.4, at the left side. This effect would culminate in creation of one huge alveolus. In real lung, however, surfactant is present. Due to its higher concentration of surfactant in smaller alveolus, the surface tension there is lower than in large alveolus. Pressure required to keep small alveolus from collapsing is therefore also lower. For this reason, small and large alveoli can both have stable volumes at the same pressure, as shown in Fig. 1.4 at the right side [15].

Lung Compliance is a measure of the lung's ability to stretch and expand. Lung compliance is defined as the change of volume (ΔV) that results from a given change in transpulmonary pressure ΔP, as can be seen in Eq.1.4. If the lung compliance is high, then the smaller change in transpulmonary pressure is needed to bring in a given volume of air. Therefore, higher compliance is advantageous because less work or muscle contraction is required [29]. There are two major factors that determine lung compliance. First is the elasticity of lung tissue and second is the alveolar surface tension, both oppose lung inflation.

$$C = \frac{\Delta V}{\Delta P} = \frac{\Delta V}{P_{pul} - P_{ip}} \tag{1.4}$$

Changes in lung compliance can be cause by pulmonary illnesses. Low compliance indicates a stiff lung for example due to pulmonary fibrosis. Therefore, extra work is required to bring in a normal volume of air. On the other hand, increased compliance results primarily from loss of elastic fibres, which occurs in emphysema. Patients therefore have no problem inflating the lungs but have difficulty exhaling air. Typical adult compliance values are from 70 ml/hPa to 100 ml/hPa [12].

1.3 Lung Volumes and Capacities

The amount of air in the lungs can be subdivided into four volumes and four capacities, as can be seen in Fig. 1.5. Lung capacities are combinations of various lung

volumes, which can be measured directly by spirometer (with exception of residual volume). The typical *respiratory rate* (RR) for a healthy adult at rest is from 12 to 16 breaths per minute (bpm). Total volume of air inhaled and exhaled each minute, called *minute ventilation* (MV), is equal to breathing rate multiplied by tidal volume $MV = 12 \cdot 500 = 6000$ ml [12].

Lung volumes are:

1. **Tidal volume** (TV) is the amount of air that moves into and then out of the lungs during a single, unforced breath. The average resting tidal volume is 500 ml.

2. **Inspiratory reserve volume** (IRV) represents the maximum volume of gas that can be inspired during forced breathing in addition to tidal volume. Average value is 3100 ml.

3. **Expiratory reserve volume** (ERV) is the maximum volume of gas that can be expired during forced breathing in addition to tidal volume. It is in average 1200 ml.

4. **Residual volume** (RV) is the volume of gas remaining in the lungs after a maximum expiration. Average value is 1200 ml.
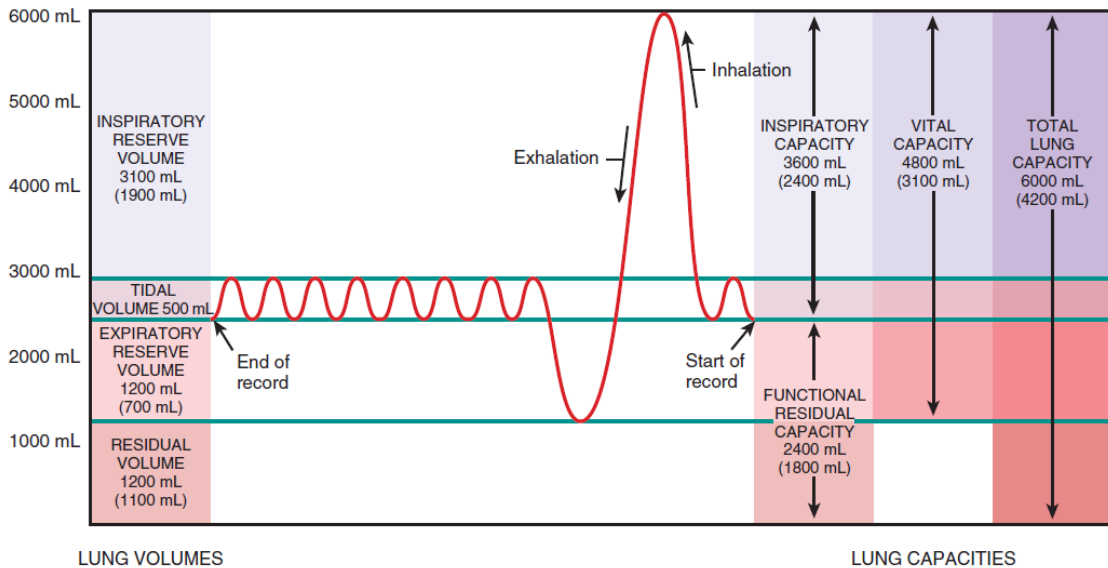
Fig. 1.5: Spirogram - lung volumes and capacities [31]

Lungs capacities are:

1. **Inspiratory capacity** (IC) is the maximum amount of gas that can be inspired after a normal tidal expiration IC = TV + IRV = 3600 ml.

2. **Functional residual capacity** (FRC) is the amount of gas remaining in the lungs after a normal tidal expiration FRC = ERV + RV = 2400 ml.

3. **Vital capacity** (VC) is the maximum amount of gas that can be expired after a maximum inspiration VC = ERV + TV + IRV = 4800 ml.

4. **Total lung capacity** (TLC) is total amount of gas in the lungs after a maximum inspiration TLC = RV + ERV + TV + IRV = 6000 ml. [31]

During the rest breathing not entire tidal volume reaches the alveolar sacs and therefore participates in gas exchange. About 30% (150 ml) remains in the conducting airways of the nose, pharynx, larynx, trachea, bronchi, bronchioles, and terminal bronchioles. Proportion of conducting airways, that does not participate in gas exchange is called *anatomic dead space*. The rest of tidal volume, about 70% (350 ml), participates in gas exchange normally [31].

Pathological conditions of lungs can influence the volume of air contained inside or the rate of air flow into or out of the lungs. Depending upon the nature of particular condition, lung diseases can by classified as restrictive or obstructive [6].

2 ACTIVE MECHANICAL LUNG SIMULATOR

Interdisciplinary biomedical based research project focusing on Advanced Lung research for VEterinary medicine of Particles for Inhalation - Cooperation (AlveoPic), was carried out in collaboration with FH Technikum, ÚAMT FEKT and ÚBMI FEKT [11]. The project deals with different topics like:

- **mobile tissue nutrition**
- **standards based telemetry**
- **aerosol measurements**
- **active lung simulation**

In this chapter one of the project goals, active mechanical lung simulator also called iLung 2.1, will be discussed.

2.1 Simulator Overview

Next generation active mechanical lung simulator enables approximate and save testing of human lung behaviour using a latex bags or a porcine lung. Due to the fact, that a porcine lung has similar internal structure as the human lung, one can achieve precise simulation results. Different lung equivalents are mounted into a thoracic chamber, which is connected to the bellows system and a vacuum pump via a flange. In order to achieve similar conditions, as in a real human lung, the vacuum pump creates constant negative pressure (under pressure), simulating the adhesion of pleural membranes. More details can be found in section 1.2. Movement of the bellows system is used to further simulate lung intrapulmonary pressure changes in vacuum chamber. Ball screw is connected to the bottom side of the bellows and also connected with a motor via threaded connection. The motor rotates the ball screw and because of the threaded connection the bottom of bellows is moved upwards or downwards. Therefore, the pressure changes are induced by bellows movement upwards (compression of bellows) and downwards (extension of bellows). The top side of a bellows system is stationary. Complete functional schematics of the iLung 2.1 can be seen in Fig: 2.1.
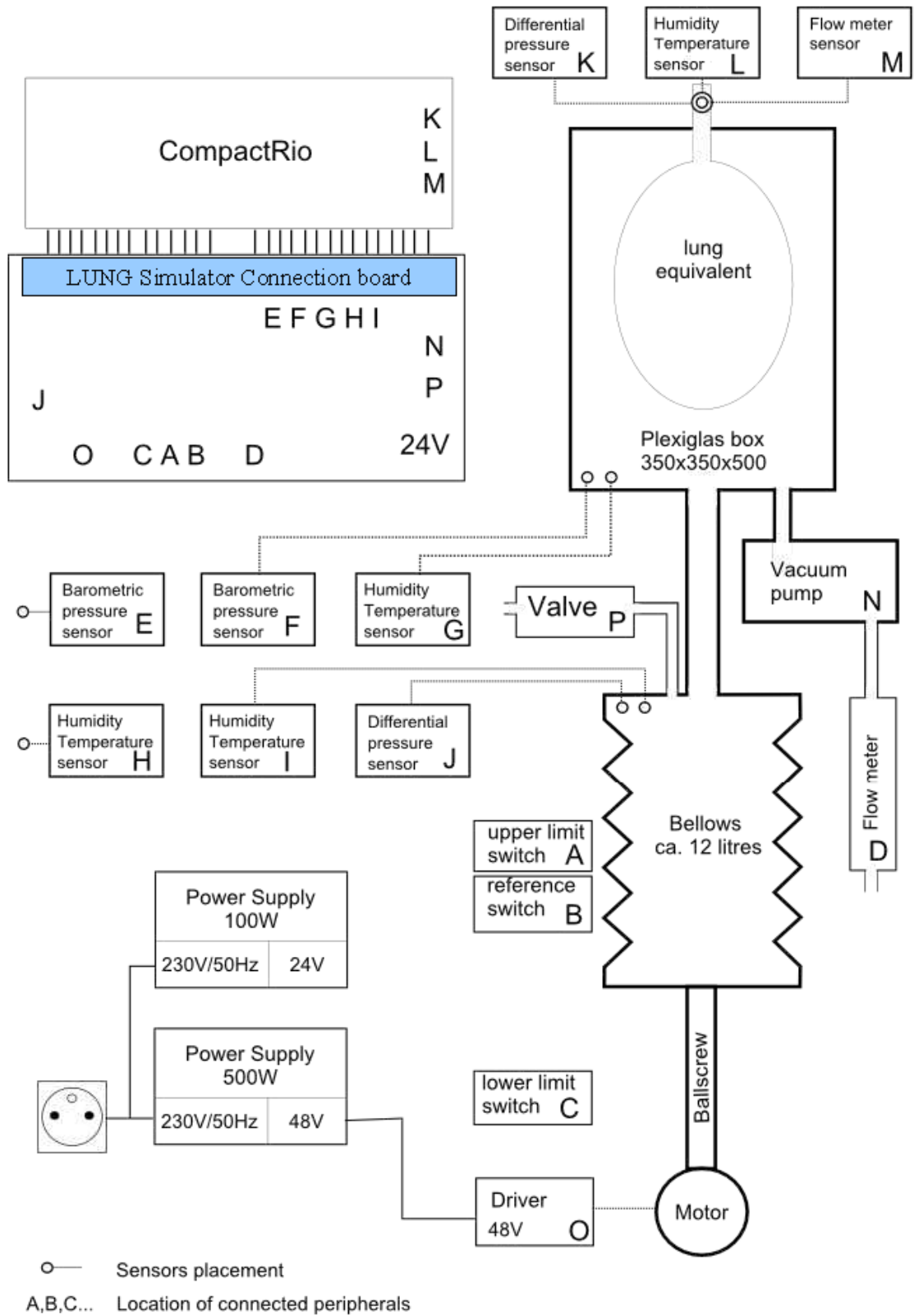
Fig. 2.1: Functional schematics of the Lung model 2.1 [27]

2.2 Mechanical Parts

2.2.1 Respiratory System

Respiratory system consists of bellows, which are moved by motor through rotation of ball screw. Further specifications of all components can be seen in Fig. 2.2.
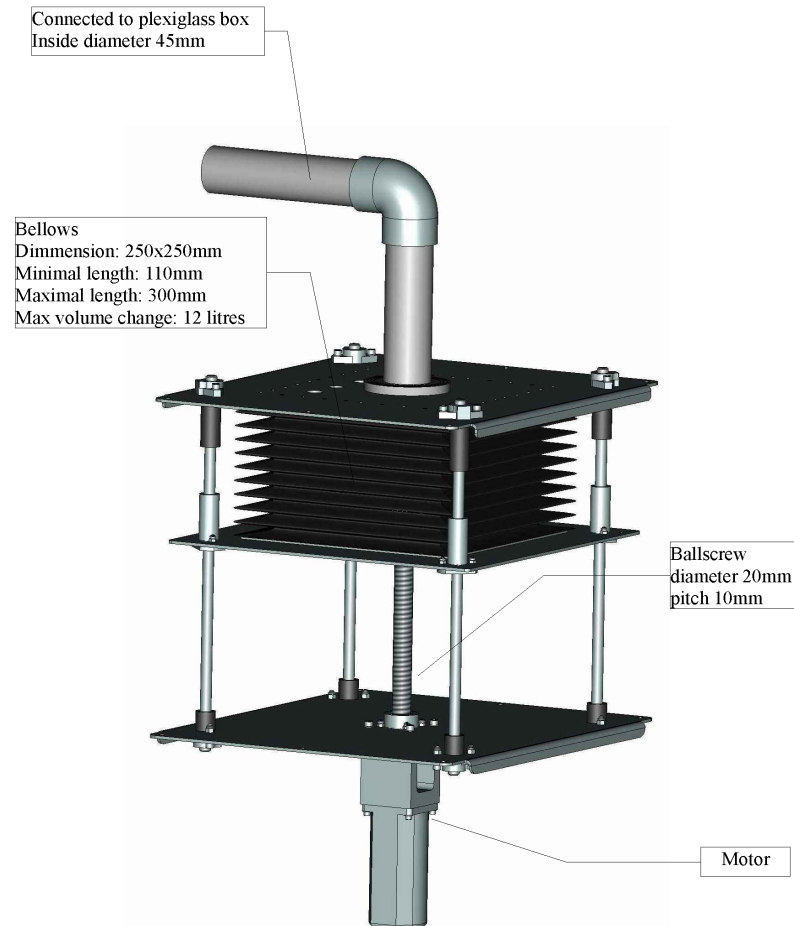
Fig. 2.2: Respiratory system [27]

2.2.2 Polymethylmethacrylate Chamber and Frame

Polymethylmethacrylate (PMMA) box is the core element of simulator, see Fig. 2.3, in which different lung equivalents can be mounted. Inside dimensions are $350 \times 350 \times 500$ mm. The volume of the chamber is approximately 61 l. The four side walls are made of 15 mm thick plexiglass. Top and bottom is thicker made of 20 mm thick plexiglass. In order to reach inside the chamber, the squared shaped lid (240 mm) can be removed. Vertical steel toggle clamps are used to hold a lid and therefore minimize air leakage from the chamber. Frame around the chamber is

constructed using Aluminium Structural Framing 30x30 Series Profile manufactured by Bosch Rexroth.
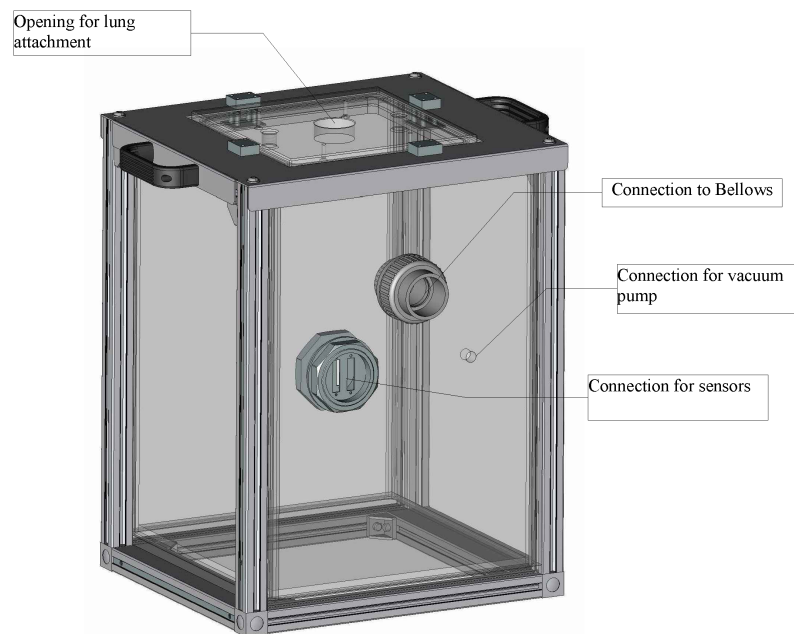
Fig. 2.3: Polymethylmethacrylate chamber [27]

Frame of the lung simulator, see Fig. 2.4, is constructed using Aluminium Structural Framing 30x30 Series Profile manufactured by Bosch Rexroth. Housing is made out of 1.5 mm thick aluminium sheet, called Colour RAL 7035.
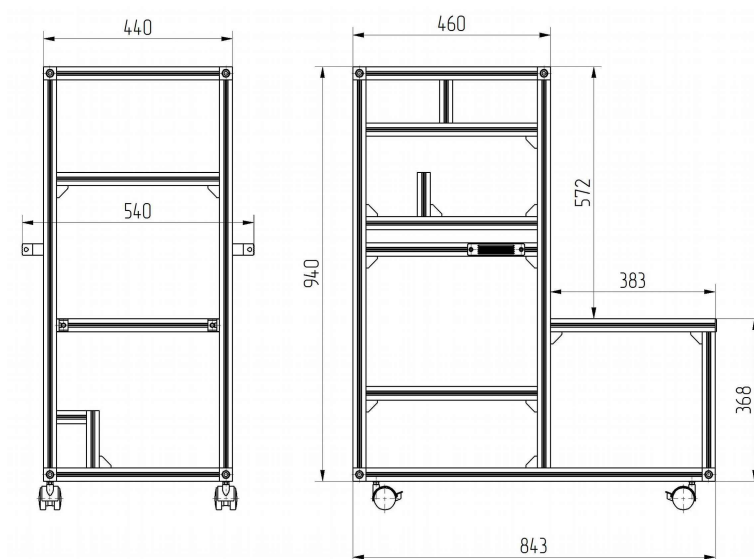
Fig. 2.4: Frame of the lung simulator [27]

2.3 Electronic Parts

Power supply for the lung simulator can be provided from electrical grid 230 V, 50 Hz. Power module is protected by 3 A fuse. Connecting cable used is CEE 7/7 (E/F) angled plug with IEC C13 socket, isolated by PVC in black colour. Complementary socket IEC Appliance Inlet C14 with line switch 2 pole and fuse holder 1 pole, is used on simulator side. For each electronic parts a summary of the parameters is provided. If necessary, additional information can be found in specified datasheets.

2.3.1 Servomotor

Brushless AC servomotor type ACM604 manufactured by Leadshine Technology Co. is used. Most important parameters are: rated power: 400 W, rated torque: 1.27 Nm, peak torque: 3.82 Nm, rated voltage: 60 V, rated speed: 3000 RPM, peak speed: 5000 RPM [14].

2.3.2 Motor Driver

As a servomotor driver ACS806 digital driver is used. Most important parameters are: input: $18 - 80$ VDC, peak current: 18 A, continuous current: 6 A, electronic gear rate: from 1/255 to 255 [13].

2.3.3 Power Supply

Single output power supply type SP-500-48 with PFC[1] function. Most important parameters are: DC voltage 48 V, rated current: 10 A, current range: $0 - 10$ A, rated power: 480 W, voltage tolerance: ± 1 % [16].

Single output switching power supply type GS-100-24. Most important parameters are: DC voltage: 24 V, rated current: 4.5 A, current range: $0 - 4.5$ A, rated power: 108 W [5].

2.3.4 Vacuum Pump

Vacuum pump type 25RNS/T1862 has following parameters: voltage: 24V DC, vacuum flow: 25 l/min, rated pressure: 70 kPa, 0.7 Bar [1].

---

[1]Power Factor Correction reduces the amount of generated reactive power by supplying reactive power of opposite sign.

2.3.5   Valve

Solenoid valve type 21A5KV45 from Stasto Automation company is used. Most important parameters are: switching time: 10 ms - 30 ms, standard voltage: 24VDC, acceptable voltage tolerance: $\pm 10\%$, holding power in W (AC): 8 W. [30]. Valve automatically opens when the pressure reaches -80 mbar to prevent the bellows damage.

2.3.6   Airflow Sensors

Airflow sensor AWN5104VN from manufacturer Honeywell International Inc. is used to measure vacuum pump flow. Most important parameters are: flow range: $0 - 20$ SLPM (standard litre per minute), output voltage: 5 VDC, response time: 60 ms max. Dry gas only. Airflow sensor is not designed to sense liquid flow and will be damaged by liquid flow through the sensor [9].

Airflow sensor AWM720P1 from manufacturer Honeywell International Inc. is used to measure flow going inside and outside of thoracic chamber of iLung 2.1. Two sensors are used, one for each flow direction. Most important parameters are: flow range 200 SLPM, output voltage 10 VDC± 0.01 VDC, power consumption 60 mW, radiometric error ± 0.3 % of VDC, response time 6 ms. Airflow sensor is not designed to sense liquid flow and will be damaged by liquid flow through the sensor [10].

2.3.7   Sensors

Barometric pressure sensor MS5607-02BA03 is a new generation of high resolution sensors. Used sensor has the following parameters: fast conversion time: down to 1 ms, low power consumption: $1\mu A$ (stand by consumption$+ < 0.15$ μA), supply voltage: 1.8 V -3.6 V, integrated digital pressure sensor (24 bit sigma-delta ($\Delta\Sigma$) ADC), operating range: $10 - 1200$ mbar, operating temperature: $-40°C - +85°C$ [18].

Humidity and temperature sensor IC SHT21 is an integrated circuit sensor. Properties: digital output, I^2C interface, low power consumption, fully calibrated, excellent long-term stability, resolution: humidity (12 bit), temperature (14 bit) [28].

Differential pressure sensor type MPXV2010DP manufactured by Freescale semiconductor has the following parameters: temperature compensated: over 0 °C $-+85$ °C, pressure range $0-10$ kPa, Voltage output: 0 mV -25 mV full scale, supply voltage 10 V [7].

2.3.8 Position Switches

Position Limit switches provide protection against bellows and motor damage. There are two limit switches directly connected to the servomotor driver. When bellows reach upper or lower limit position motor stops automatically. In case a bellow is in one of the limit positions, possible travel direction is only the opposite. **Induction reference switch** is used for finding the motor starting (zero) position. All measurements are related to this position.

2.4 Simulator Control Electronics

2.4.1 Connection Board

Connection Board is a printed circuit board (PCB) that focuses connections of all simulator peripherals (inputs and outputs) into one place. Thanks to it, all peripherals can be also connected to CompactRIO (cRIO) while occupying minimal space. All further description of Connection Board in text, refers to the Connection Board orientation in the Fig: 2.5. Connection Board can be divided into three parts where two, three and eight way PCB screw terminal blocks facilitate connections to the iLung 2.1 electronic parts. More information about the PCB terminal block can be found in [24]. Screw PCB terminals at the bottom side of the Connection Board are used for connecting motor driver, up and down limit switches and flow sensor of vacuum pump. Terminals at the right side of the Connection board serves as a power supply outputs for cRIO and Extension of The Connection Board. Finally, terminals at the top side are prepared for connection of driver TTL logic, pressure sensor, vacuum pump and valve to the cRIO I/O modules. All specifications of above mentioned connections can be found in section 2.6. The square in the schematics is always pin 1. Full scale schematics can be found in annex A.

2.4.2 CompactRIO

National Instruments cRIO is an advanced reconfigurable embedded control and acquisition system powered by NI RIO technology for ultrahigh performance, user customization, and reconfigurability. It is designed to perform in the harshest industrial environments. CompactRIO is rated for 50 g shock, and hazardous locations or potentially explosive environments (Class I, Div 2). Most Input/Output (I/O) modules feature up to 2300 V_{rms}[2] isolation (withstand), and 250 V_{rms} isolation (continuous). Each component comes with a variety of international safety,

---

[2]Root Mean Squared Voltage is defined as amount of AC power that produces the same heating effect as an equivalent DC power.
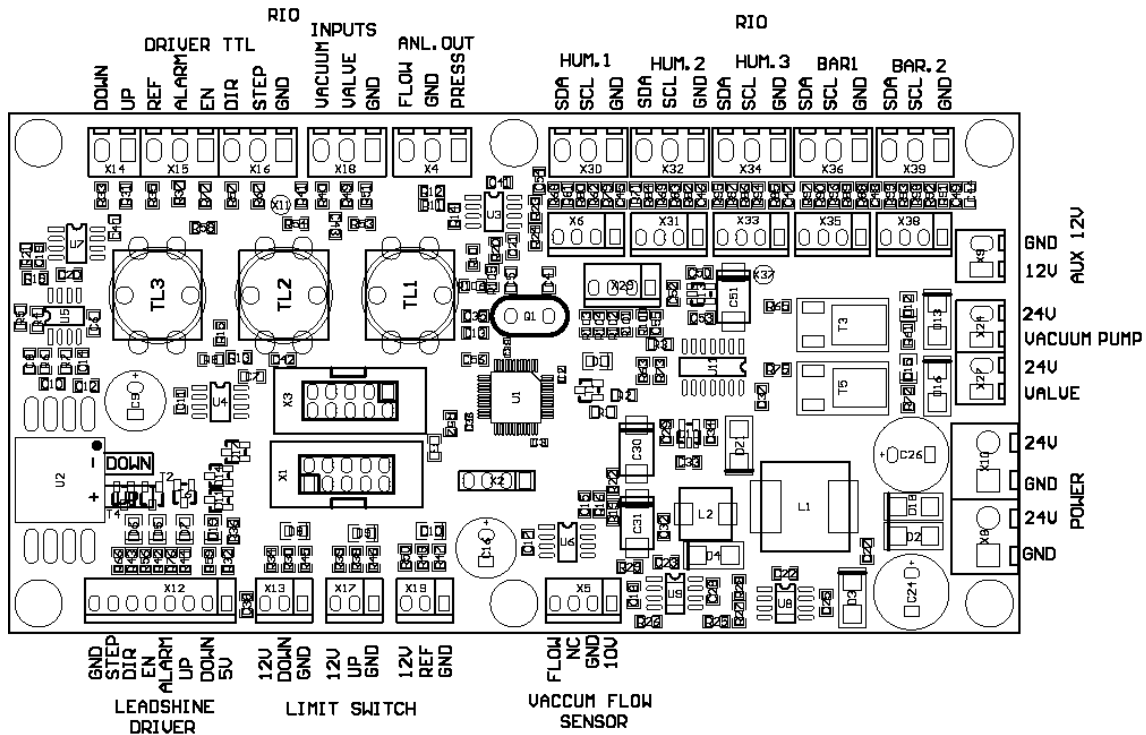
Fig. 2.5: Simulator connection board [26]

electromagnetic compatibility (EMC), and environmental certifications.

cRIO systems consist of an embedded controller for communication and processing, a reconfigurable chassis housing the user-programmable Field Programmable Gate Array (FPGA), hot-swappable I/O modules, and graphical LabVIEW software for rapid real-time, Windows, and FPGA programming. Reconfigurable embedded system architecture can be seen in Fig. 2.6. FPGA based devices were traditionally vendor defined rather than user defined because of the complexity of the electronic design tools. Due to LabVIEW it is possible to create highly optimized reconfigurable control and acquisition systems with no knowledge of specialized hardware design languages such as VHDL [23].

The Real-Time Controller contains a processor that executes LabVIEW Real-Time applications and offers multivariate control, execution tracing, on board data logging, and communication with peripherals. A Real-Time Operating System (RTOS) is able to execute programs with specific timing requirements. General-purpose OS installed (such as Windows) is unacceptable. At any time, the OS might delay execution of a user program for many reasons. Therefore, NI Linux Real-Time OS is used to eliminated these problems as much as possible [20]. In Lung Simulator real-time embedded controller for cRIO 9024 is used. Important parts of the controller can be seen in Fig: 2.7. The cRIO 9024 controller features an industrial 800 MHz real-time Freescale processor, contains 512 MB of DDR2 RAM
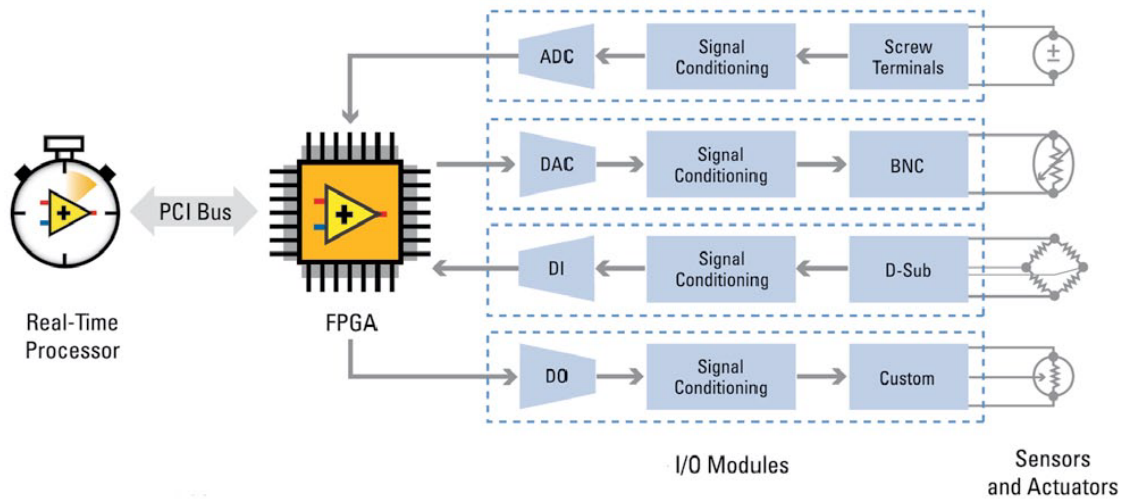
Fig. 2.6: Reconfigurable embedded system architecture [20]

and 4 GB of NVM[3] storage for holding programs and logging data. Other parameters are: operating temperature range: $-20\,°C$ to $55\,°C$, input voltage range: 6 VDC to 35 VDC, isolated dual power supply output for chassis/modules in voltage range: 9 VDC to 35 VDC, two Ethernet ports, 10/100 and 10/100/1000, that can be used to conduct programmatic communication over the network and built-in web and file servers. C Series I/O modules are compatible. Additional storage can be provided through Hi-Speed USB host port by means of flash drives and hard drives. In addition, the controller features a fault-tolerant file system.

Reconfigurable FPGA Chassis is the center of the embedded system architecture, for overview see Fig 2.6. Each I/O module is connected directly, therefore there is almost no control latency for system response compared to other controller architectures. Programs on a real-time controller can access I/O modules with less than 500 ns of jitter between loops. Furthermore, modules timing, triggering, and synchronization is also precise. Additionally, because the FPGA runs all code in hardware, it provides high reliability [20]. The NI cRIO 9118 embedded chassis is used in the Lung Simulator. Chassis contains eight module slots and user-programmable Xilinx Virtex 5 FPGA.

Input/Output Modules contain isolation, conversion circuitry, signal conditioning, and built-in connectivity for direct connection to industrial sensors. Space and wiring costs are reduced by integrating the connector junction box into the modules. There is more than 100 NI C Series I/O modules for cRIO fulfilling wide variate of function. Specific information about modules and their function can be found in [23]. It is also possible to build custom modules to meet application specific

---

[3]Non-Volatile Memory can retrieve stored information even after having been power cycled

31

1	LEDs	6	Reset Button
2	Power Connector	7	DIP Switches
3	RS-232 Serial Port	8	RJ-45 Ethernet Port 1
4	USB Port	9	RJ-45 Ethernet Port 2
5	USB Retention Standoff		
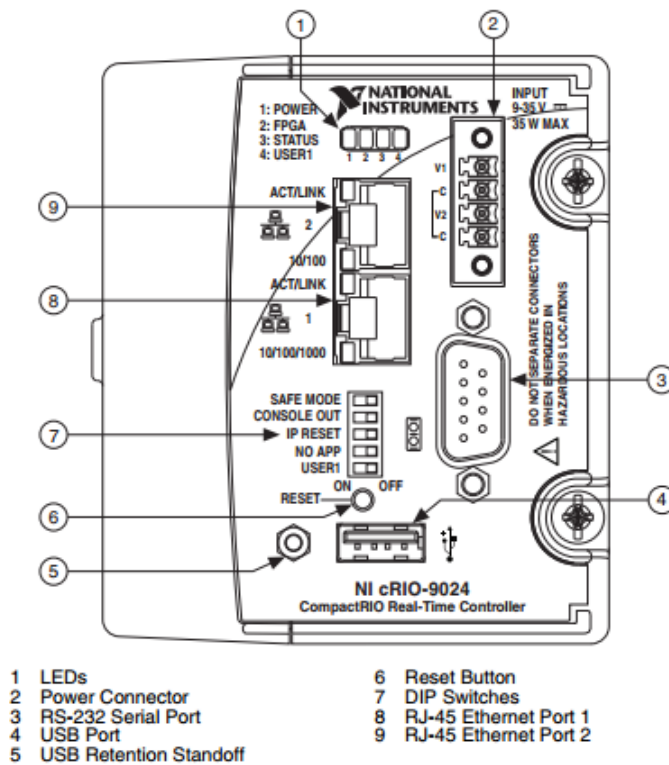
Fig. 2.7: Controller for cRIO version 9024 [19]

needs.

Input/Output modules used in iLung 2.1

- **I/O module NI 9403** is a 32 channel, 7 μs bidirectional digital I/O module compatible with any Chassis. Direction of each digital line can be configured for input or output. Further module parameters are: 5 V/TTL signals, transient isolation between the I/O channels and the backplane: 1000 V_{rms}, overvoltage protection: ± 30 V, output current for channel: 2 mA [22].

- **I/O module NI 9205** is a 32 single ended or 16 differential analogue input C Series module. Further module parameters are: maximum sampling rate: 250 kS/s, 16 bit resolution, overvoltage protection: 1000 V_{rms}, input channels to common channel protection: 60 V, channel to ground double isolation barrier, noise reduction, and high common mode voltage range. Each channel has programmable input ranges of ± 200 mV, ± 1 V, ± 5 V, and ± 10 V [21].

2.5 Simulator Control Software

The simulator control software was created during Alveopic project. Author of this thesis adapted the software so that its functions meet the requirements set by FH Technikum Wien. Most important change is the motor tuning, which is described in subsection 3.4.2.

This section shortly describes simulator control software. More detailed explanation of the software functions and usability can be found in created user manual in annex H.

LabVIEW based software for iLung consists of two parts:

1. **Real-time program** is running on cRIO and can, with the FPGA program, function as standalone embedded system. Sequence running on the controller can be customised within the LabVIEW user interface. LabVIEW user interface is running on the PC, that is connected to the cRIO via Ethernet cable. This setup provides possibilities of changing lung simulation settings. Program consists of two modes: Calibration & Initialization mode and Run mode. Calibration allows the possibility to set flowmeters and pressure sensor offset before actual measurements. Therefore, increasing precision of the recorded values. Starting piston position and pressure inside thoracic chamber can be set during initialization according to requirements of the experimenter. Run mode window offers possibility of choosing the piston movement type. There are four different types of movement called: Gener sin, PI sin, PI breath and Manual. Setting for each type of movement can be modified. Manually control of the pump and the valve can be also turned on. Graphs of airflow and pressure recorded during simulation can be saved into Microsoft Excel spreadsheet. Additional optimization and safety options such as the PI controller setting, maximum negative pressure check and compensation of deflation are also available.

2. **FPGA program** is compiled and flashed directly on cRIO system. FPGA program evaluates, sets and passes data concerning iLung peripherals status between Real-time program and Connection board. For example, it handles pressure sensor output voltage values and calculates pressure values in bar, calculates revolution, position and therefore speed of the motor according to the values given from the motor encoder etc. Due to the hardware implementation precise timing in real time is possible.

Integration of a software as well as relations between iLung 2.1 parts can be seen on block diagram Fig. 3.1 on page 38.

2.6   Connection of Electronic Parts

Previous sections dealt with the description of electronic parts, section 2.3, and control electronic, section 2.4, used in iLung 2.1. In this chapter mutual connections between electronics parts and Connection Board, which have been wide by iLung manufacturer, are specified in form of tables. Header of each table consists of the name of electronic part, pin number which is a number of pin situated on Connection board, see Fig. 2.5, pin setting which states whether analogue or digital input or output value is to be expected on corresponding pin and finally brief description of function. Following symbols are used in tables below: Connection Board (CB), Digital Input (DI), Digital Output (DO), Analog Input (AI), Analog Output (AO), SCL (Synchronous Clock), SDA (Synchronous Data).Barometric Pressure Sensor (BPS), Humidity and Temperature Sensor (HTS). Differential pressure sensor is located directly on the Connection Board. Connections of Electronic parts include motor driver, vacuum pump, valve, limit switches and sensor. More specifications can be found in Tab. 2.1.

Tab. 2.1: Connection of Electronic Parts to Connection board

Pin number	Function	Pin number	Function
X12	Motor Driver	X5	Flow meter
X24	Vacuum Pump	X6	Ambient BPS
X27	Valve	X31	Ambient HTS
X13	Limit Switch Down	X33	Bellows HTS
X19	Limit Switch Up	X35	PMMA Box BPS
X19	Induction Reference Switch	X38	PMMA Box HTS

2.6.1   Connection to Sensors

There are two types of digital sensors used in the iLung 2.1: barometric pressure sensor and humidity and temperature sensor. Idea behind this, is to measure pressure, temperature and humidity in ambient air, inside thoracic (PMMA) box and inside bellows. Sensors are not connected to cRIO so far as problems with attaching them inside smooth thoracic box occurred. It has been decided by supervisor to connect sensor in a future and rather concentrate efforts on simulator validation measurements. Differential pressure sensor measures pressure data inside thoracic box and is connected to cRIO, see specifications in section 3.3.

Barometric pressure sensor connections to specific pin numbers can be found in Tab. 2.2 for ambient sensor and Tab. 2.3 for PMMA box sensor. Further

specification can be found in subsection 2.3.7.

Tab. 2.2: Ambient barometric pressure sensor

Ambient barometric pressure sensor		
Pin number	Pin setting	Function
X30.1	GND	Ground
X30.2	SCL	I^{2}C clock line
X30.3	SDA	I^{2}C data line

Tab. 2.3: PMMA box barometric pressure sensor

PMMA box barometric pressure sensor		
Pin number	Pin setting	Function
X36.1	GND	Ground
X36.2	SCL	I^{2}C clock line
X36.3	SDA	I^{2}C data line

Humidity and Temperature Sensor connections to specific pin numbers for ambient conditions can be found in Tab. 2.4, for bellows sensor in Tab. 2.5 and for PMMA box sensor in Tab. 2.6. For further specification can be found subsection 2.3.7.

Tab. 2.4: Ambient humidity and temperature sensor

Ambient humidity and temperature sensor		
Pin number	Pin setting	Function
X32.1	GND	Ground
X32.2	SCL	I^{2}C clock line
X32.3	SDA	I^{2}C data line

Tab. 2.5: Bellows humidity and temperature sensor

Bellows humidity and temperature sensor		
Pin number	Pin setting	Function
X34.1	GND	Ground
X34.2	SCL	I^{2}C clock line
X34.3	SDA	I^{2}C data line

Tab. 2.6: PMMA box humidity and temperature sensor

PMMA box humidity and temperature sensor		
Pin number	Pin setting	Function
X39.1	GND	Ground
X39.2	SCL	I^2C clock line
X39.3	SDA	I^2C data line

2.6.2 Connection to Power Distribution

Simulator is plugged into 233 V/ 50 Hz distribution network that powers all electronic parts after being transformed desired voltage value by power supply sources, see subsection 2.6.2 for specifications. Connection Board operational input voltage is 24 V. Available output power voltage is 12 V, which can be used to power external electronic, with max current rate 0.5 A and 24 V output, is used to power cRIO.

Tab. 2.7: Connection to power distribution

Power distribution		
Pin number	Pin setting	Function
X8.1	GND	Ground
X8.2	24V Input	CB power supply
X9.1	12V Output	External electronic power supply
X9.2	GND	Ground
X10.1	GND	Ground
X10.2	24V Output	Power supply to CRIO

2.7 Motor Driver Protection Functions

Servomotor driver, for more information see subsection 2.3.2, features built-in protection functions to further prevent damage to the device. Information about the type of error is visualized by means of flashing red LED. Specific error can be determined from the number of times in which the red LED is turned on during the period of 5 seconds. As there is one red LED, only the highest priority error is displayed when multiple occur simultaneously. Protections are sorted by priority from highest priority to lowest priority in following text. Description of error is included into Master's Thesis because it was necessary to use it during iLung 2.1 technical failure.

Overcurrent protection is activated when continuous current exceeds 24 A. It is first protection priority error and red LED is turned on once within each 5 second period.

Overvoltage protection occurs when power supply voltage exceeds 90 VDC. It is second protection priority error and red LED is turned on twice within each 5 second period.

Undervoltage protection indication means that power supply voltage is lower than 18 VDC. It is third protection priority error and red LED is turned on three times within each 5 second period.

Phase error protection is activated when servomotor power lines are wrongly connected or not connected at all. Other possibility is that encoder or hall sensor feedback signals is wrongly connected. In this cases the red LED is turned on four times within each 5 second period and it is fourth protection priority error.

Encoder of hall error protection occurs when there is no encoder feedback signals or wrong encoder/hall sensor feedback signals. It is fifth protection priority error and red LED is turned on five times within each 5 second period.

Limit error connection is activated when there is positive or negative limit input in FL or RL pin. It is sixth protection priority error and red LED is turned on six times within each 5 second period.

Position following error protection indicates, that the Position Following Error Limit parameter in the servomotor driver is reached. It is seventh protection priority error and red LED is turned on seven times within each 5 second period. Wrong motor connection also causes this error protection indication. It is important to check motor connection at the start up as there is no protection against power leads polarity reversal. Failure to do so may result in destruction of servomotor driver. [13]

3 IMPLEMENTATION OF SIMULATOR CONTROL UNIT

As the iLung 2.1 control unit cRIO has been selected mainly due to the ability of processing data in real time. Information flow and physical connections between the iLung 2.1 units are shown on Fig. 3.1. The Real time program is running on standalone computer and offers the possibility of changing simulation parameters through graphical user interface (GUI). Communication between computer and cRIO is established via standard Ethernet cable (Cat-5). Connection Board (CB) and Extension of Connection Board (EoCB) are PCBs that gather connections of all iLung 2.1 electronic parts into one place. CB and EoCB have a common ground, but EoCB is connected to cRIO also separately and not only through CB. Practical work on hardware (soldering, connecting, purchasing) described in this chapter was done by the author of this theses if not stated otherwise.
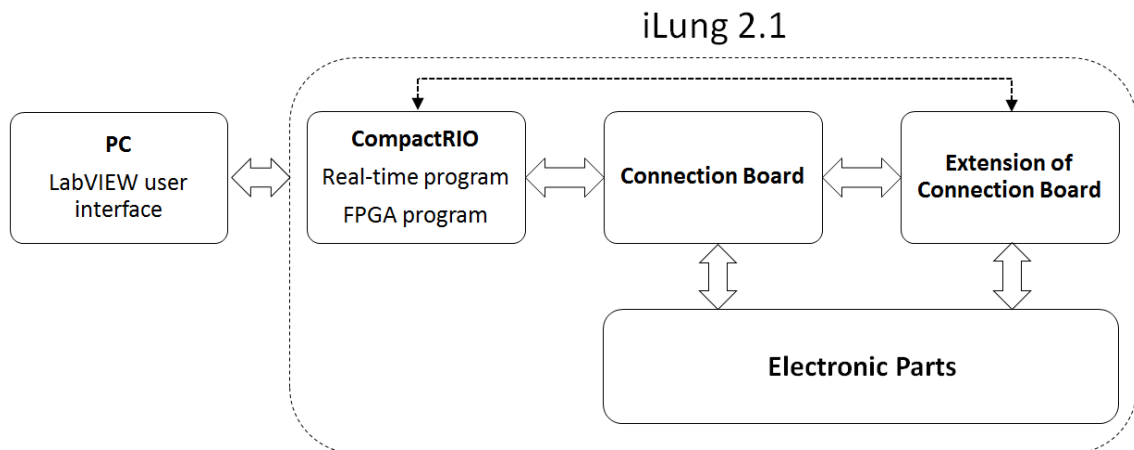
Fig. 3.1: Connections of iLung 2.1 Electronic Parts

Implementation starting point

When being introduced into the topic, connections were established only between iLung 2.1 electronic parts and the CB/EoCB respectively. The cRIO was not a part of iLung 2.1 in that time. There was no documentation available for the EoCB, as the PCB was created additionally after official simulator documentation release. Therefore the task was to implement the cRIO as the simulator control unit. To be more specific connections between the cRIO and the PC/CB/PC respectively had to be arrange using available hardware and software. Emphasis on extending, updating and completing of the iLung 2.1 documentation was also made by FH Technikum

Wien so that it is possible to replicate all connections and settings in the future. Implementation process can be divided into several parts: measurements and description of the Extension of Connection Board, Honeywell AWM720P1 flowmeters connection, implementation of the cRIO and the LabVIEW software installation, adaptation and documentation.

3.1 Extension of The Connection Board

Extension of The Connection Board is a PCB, created by company RW etc. s.r.o., that allows connections of the Honeywell AWM720P1 flowmeters and a motor encoder to the cRIO control unit. Documentation for the EoCB was created based on pin by pin experimental measurements. To provide example, procedure was as following. First flow sensor was connected to the EoCB and expected output voltage values were determined from datasheet. Consequently, pin by pin measurement were conducted and output pin with corresponding voltage values found and identified. Initial conditions were changed until function of all pins was identified. Created schematics, based on assembly drawings, with description of function for each pin are results of the measurements and care shown on Fig. 3.2. In all schematics square is always pin 1. Full scale schematics can be found in annex B.1.

Cannon 9 pole male connector, that is soldered on EoCB, allows a possibility of connecting Honeywell AWM720P1 flowmeters. The EoCB provides power supply for the flowmeters and receives output voltage proportionate to airflow. Pin specifications can be found in Tab. 3.1. Incremental rotary encoder of ACM 640 motor is also connected, specifications are stated in Tab. 3.2, as input into the EoCB. Encoder and hall sensor provide information of the motor shaft position and rotor magnetic field orientation. The output signals from the hall sensor have absolute phase information which is used at motor start up. Connections from the EoCB to the cRIO are stated in separate section 3.3

3.2 Connection of flowmeters

As a measurement sensors of airflow, that is flowing inside and outside the thoracic box, Honeywell flowmeters AWM720P1 were chosen because of low response time and high precision. Sensors specification can be found in subsection 2.3.6. Two sensors were used, each one measuring different direction of the airflow. Flowmeters are placed at the top of iLung 2.1 simulated trachea and connected to the simulator side panel. Due to the fact, that each flowmeter needs three contacts to work
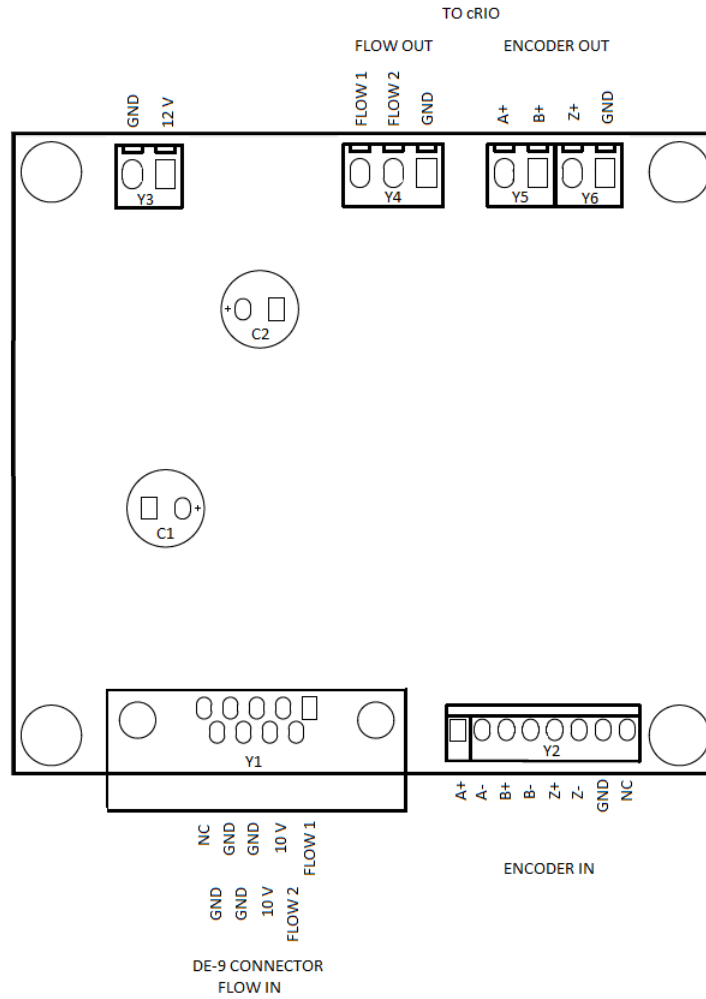
Fig. 3.2: Created labels for Extension of The Connection Board from assembly drawings

properly [10], six pole DIN[1] male connector MAS 6100 [8] with locking screw was selected to facilitate both flowmeters. Male connector can be plugged into the six pole DIN female connector MAB 45322 [25] which was integrated into the iLung 2.1 side panel. Therefore, it is easily possible to connect/disconnect flowmeters when it is necessary, for example during simulator transport. Specific connections to the side panel can be found in Tab. 3.3, where number on the first position in pin number of flowmeters column indicates first or second flowmeter.

To further establish connection inside the iLung 2.1, between the simulator side panel and EoCB, cabel terminated with standard cannon 9 pole female connector was chosen. Therefore, it can be plugged into cannon 9 pole male connector, that was already soldered on the EoCB by manufacturer. Connections between the simulator

---

[1]A DIN connector is an electrical connector that was originally standardized by the Deutsches Institut für Normung (DIN), the German national standards organization.

Tab. 3.1: Connections of flowmeters to Extension of The Connection Board, results of 3.1

Honeywell flowmeters AWM720P1		
Pin Number	Pin Setting	Function
Y1.1	AI	Flowmeter 1 output
Y1.2	AO	Power supply to flowmeter 1
Y1.3	GND	Ground
Y1.4	GND	Ground
Y1.5	NC	Not connected
Y1.6	AI	Flowmeter 2 output
Y1.7	AO	Power supply to flowmeter 2
Y1.8	GND	Ground
Y1.9	GND	Ground

Tab. 3.2: Connections of motor encoder to Extension of The Connection Board, results of 3.1

ACM 604 motor incremental rotary encoder		
Pin number	Pin setting	Function
Y2.1	AI	A+
Y2.2	AI	A−
Y2.3	AI	B+
Y2.4	AI	B−
Y2.5	AI	Z+
Y2.6	AI	Z−
Y2.7	GND	Ground
Y2.8	NC	Not connected

side panel and EoCB are specified in Tab. 3.4. All pin numbers used in Tab. 3.3 and Tab. 3.4 correspond with pin numbers listed in relevant product datasheets. More information can be found in [10] for flowmeters, [8] for male 6 pin DIN connector pole, [25] for female 6 pin DIN connector pole and [4] for used cannon 9 pole standard pinout.

3.3   Connections to the CompactRIO

In order to implement cRIO as a iLung 2.1 simulator control unit connections between CB, EoCB and cRIO I/O modules had to be established. Original simulator

Tab. 3.3: Connections of flowmeters to the simulator side panel, results of 3.2

Connections of flowemeters to 6-DIN male connector		
Pin number of flowmeters	Pin number of DIN	Function
1.3	1	+ 10 V to flowmeter 1
1.4	2	V_{OUT1} of flowmeter 1
1.2	3	Ground to flowmeter 1
2.3	4	+ 10 V to flowmeter 2
2.4	5	V_{OUT2} of flowmeter 2
2.2	6	Ground to flowmeter 2

Tab. 3.4: Connection between 6 pin DIN pole female and cannon 9 pole female connector

Connections between the simulator side panel and EoCB		
Pin number of DIN	Pin number of cannon 9	Function
1	2	+ 10 V
2	1	V_{OUT1}
3	3	Ground
4	7	+ 10 V
5	6	V_{OUT2}
6	8	Ground

control software (real time program and FPGA program), which has been developed during Alveopic project, served as a reference. After studying and understanding the principle of the FPGA program, set up of I/O modules has been changed according to original program. Goal was to adjust setting of cRIO hardware as much as possible, so that the FPGA program could be used with minimal changes. Therefore, all program inputs and outputs were noted and according to them physical wiring was done between corresponding pins of CB, EoCB and cRIO I/O module channel. To be more specific procedure will be shown on connection of upper limit switch. From CB was known, that digital output on pin X14.1 is high, when piston position reaches upper position. According to FPGA program CB and cRIO module 9403 channel DI/O 1 was connected by wire. This procedure was repeated for every used electronic parts.

Ground pins of the I/O modules are connected to the common chasis ground screw and also to the ground of each electronic part. CB and EoCB have a common ground. Connections of all electronic parts used for iLung 2.1 control are organised in form of tables. Following symbols are used: Digital Input (DI), Digital Output

(DO), Analog Input (AI), Analog Output (AO). In tables dash is used in cases when direct control of electronic part is not necessary for simulations. These parts are therefore not connected to cRIO I/O modules, but can be in the future.

Motor driver pin connections can be found in Tab. 3.5. Further specification can be found in subsection 2.3.2. Motor driver controls the function of the motor, turning it on and off an also in terms of movement speed (rotations per second), movement direction and piston position. Limit switches are not connected to the cRIO but directly to the motor driver from manufacturer.

Tab. 3.5: Connection of motor driver, results of 3.3

Motor driver			
Connection Board		cRIO module 9403	Electronic part
Pin number	Pin setting	Pin number	Function
X14.1	DO	-	Limit switch up
X14.2	DO	-	Limit switch down
X15.1	DI	DIO4	DI Enable
X15.2	DO	-	Motor driver alarm
X15.3	DI	DIO5	Reference switch
X16.1	GND	COM	Ground
X16.2	DI	DIO0	Step
X16.3	DI	DIO1	Direction

Differential Pressure and Vacuum pump flow Meter pin connections can be found in Tab. 3.6. Further specification can be found in subsection 2.3.7 and subsection 2.3.6. Pressure sensor provides the information about pressure values inside thoracic box. Voltage values are recalculated to pressure values using real time math script in LabVIEW software. Sensor is calibrated and temperature compensated with linear voltage output directly proportional to the applied pressure. Vacuum pump flowmeter is not connected to cRIO as flow value is not necessary for simulator control. It can be added in the future if necessary.

Vacuum pump and Valve pin connections can be found in Tab. 3.7. Further specification can be found in subsection 2.3.4 and subsection 2.3.5. Valve opens automatically at the start of the program as atmospheric pressure is necessary inside the thoracic box during pressure sensor calibration. After simulation ends valve is also opened to equalize pressure with atmospheric pressure so that the lung equivalent can be fully deflated. Valve can be also operated manually if the pressure value exceeds acceptable limit. Vacuum pump is used to compensate leakages, which are caused due to thoracic chamber not being completely airtight. In feedback con-

Tab. 3.6: Connection of differential pressure sensor, results of 3.3

Differential pressure sensor			
Connection Board		cRIO module 9205	Electronic part
Pin number	Pin setting	Pin number	Function
X4.1	AO	AI0	Pressure
X4.2	GND	AI8	Ground
X4.3	AI	-	Vacuum pump flow meter

trolled mode vacuum pump is turned on and off according to the values set during initialization with aim of maintaining constant pressure across all cycles. Vacuum pump can be also operated manually.

Tab. 3.7: Connection of vacuum pump and valve, results of 3.3

Vacuum pump and valve			
Connection Board		cRIO module 9403	Electronic part
Pin number	Pin setting	Pin number	Function
X18.1	GND	COM	Ground
X18.2	DI	DIO3	Valve ON/OFF
X18.3	DI	DIO2	Vacuum pump ON/OFF

AWM720P1 flowmeter pin connections can be found in Tab. 3.8. Further specification can be found in subsection 2.3.6 and section 3.2. Flowmeters voltage output is not directly proportional to flow and is recalculated to liters per minute by using real time math script in LabVIEW software. Relationship between voltage and flow variables can be found in product datasheet [10]. In feedback controlled mode flowmeters are used to regulate movement of the piston according to shape of required curve.

Tab. 3.8: Connection of AWM720P1 flowmeters, results of 3.3

AWM720P1 flowmeters and encoder			
Extension of the Connection Board		cRIO module 9403	Electronic part
Pin number	Pin setting	Pin number	Function
Y4.1	GND	AI9, AI10	Ground
Y4.2	AO	AI2	FLOW1
Y4.3	AO	AI3	FLOW2

Motor encoder pin connections can be found in Tab. 3.9. Further specification can be found in subsection 3.1.Encoder and hall sensor provide information of the

motor shaft position and rotor magnetic field orientation. The output signals from the hall sensor have absolute phase information which is used at motor start up. Position of the piston is obtained by the number of tick in the LabVIEW software. At the start of the calibration, piston position is identified by reference hall sensor (most upper position) and every movement is therefore calculated from this starting position.

Tab. 3.9: Connection of encoder, results of 3.3

Incremental rotary encoder			
Extension of the Connection Board		cRIO module 9205	Electronic part
Pin number	Pin setting	Pin number	Function
Y6.1	GND	COM	Ground
Y6.2	DO	-	Z+
Y5.1	DO	DIO7	B+
Y5.2	DO	DIO6	A+

3.4   Implementation of The Simulator Software

The simulator control software, more information can be obtained in section 2.5 and user manual in annex H , is a LabVIEW based software that consists of two parts: Real-time program and FPGA program. In this section steps that are necessary to follow for the software proper function are stated, together with adaptation changes made to the software and the software documentation.

3.4.1   The software installation procedure

Software installation procedure is described because as oppose to normal basic cRIO software setting, simulator software requires installation of several specialised modules, drivers and setting changes. Description of software installation was also one of a task assigned by second supervisor, therefore in a future installation can be repeated without problems, that occurred during software initial installation. Problems were related to software and driver versions compatibility.

The following basic LabVIEW software components are required for simulator proper function:

- **Full Development System 15.0.1** enables a possibility of programming in fully integrated graphical mode.
- **Real-Time Module 15.0** for developing real time applications.

- **FPGA Module 15.0** for programming FPGA modules.
- **FPGA Xilinx Compilation Tools for ISE 14.7** used for compilation of FPGA code.
- **MathScript RT Module** mediates conversion of the sensors output voltage values to flow and pressure units.
- **Measurement & Automation Explorer (MAX)** provides access to cRIO. Therefore, it is possible to configure hardware and software installed. It is recommended to use static internet protocol (IP) address.

Step by step guideline for setting cRIO hardware and software can be found on National Instruments (NI) official website in section getting started [23]. However, guideline describes software installation process in general. Therefore, version of the software does not have to be compatible with modules or processor architecture of used cRIO. For that reason, summary of required software versions is available in this chapter. Full list of installed software can be used can be found in annex C.1.

Comparability of iLung 2.1 control software is guaranteed only with software mentioned above. However, it is possible, that the other even older product versions, will also successfully work. Software was tested on Microsoft Windows 7 Premium 64 bit operation system.

3.4.2 Servomotor tuning

One of the most important adaptation of iLung 2.1 software is optimization of motor movement. After the initial measurements it became clear, that the servomotor is not preforming as expected with factory settings. Discrepancies between the required flow curve and actual airflow during the simulations were significant. Especially in feedback controlled mode, when simulator uses measured values of flow from Honeywell AWM720P1 flowmeters and adapts movement of the piston accordingly to fit required flow curve. Due to the fact, that the control of the motor is not linear at low motor revolutions, a oscillations of piston occurred around zero flow region, shown on Fig. 3.4. Polarity of motor supply voltage determines the direction of motor movement. In the transition from negative to positive direction (or vice versa) regulator has to switch and integrates position error. At the completion of the integration the position error is high (it also increases during integration) and as a result motor tries to compensate the error. High voltage impulse causes motor to move quickly and overcompensate calculate error. In an effort to eliminate the error high voltage impulse of opposite polarity is applied. Whole process repeats around zero flow region until required flow value are by far greater or lower than zero.

In order to minimize the oscillation error servomotor tuning was carried out. Professional tuning tool developed for all Leadshine digital drives, ProTuner has

been used to configure the servo driver settings. ProTuner offers the numeric method for tuning position-loop parameters (K_p, K_i, K_d) and give a visualization result synchronously for users to evaluate the performance of the system. Instruction from the ACS806 datasheet [13] were followed while tuning the system. Motor tuning is a multi-step process that requires a lot of time and effort. The aim of tuning was to reduce oscillation to acceptable level. Special RS232 cable is necessary for communication between PC and motor driver. One end of the cable is a RJ-11 connector and the other end is a cannon 9 pole connector. Connection was solved by using adapters for RJ-11 and RS232.

Motor was tuned by changing the (K_p, K_i, K_d) parameters in position tuning mode. Position loop tuning is dependent on the mechanical load, and therefore will change with any mechanical system changes. Position loop tuning was performed with the motor installed in the system. System response to present trapezoid impuls was evaluated and parameters changed until reasonable result was achieved. Final parameters, system response (blue curve) to a trapezoid impuls (green curve) and taken current (red curve) are shown on Fig. 3.3, figure was taken from Pro Turner GUI. Parameters for best measured performance are set as following: $K_p = 500$, $K_i = 60$, $K_d = 4$ and Encoder Line = 10000.
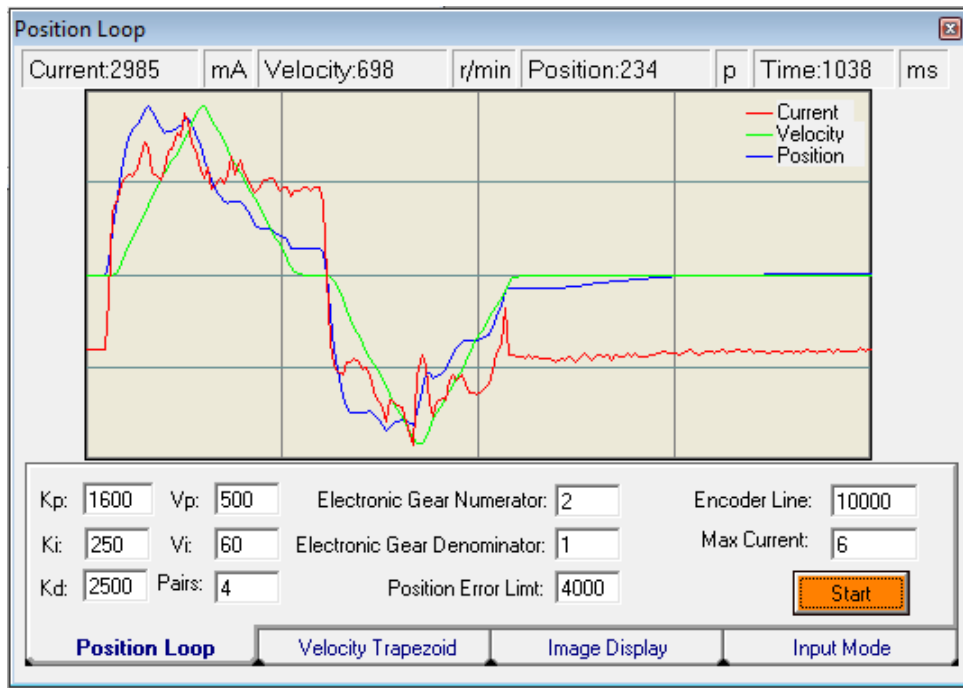
Fig. 3.3: System response to a trapezoid impulse after tuning

Tuning of the proportional-integral controller

In order to additionally increase precision of regulation and therefore further minimize the piston oscillations, proportional-integral (PI) controller, that is a part of original LabVIEW software, was also tuned. Main advantage in comparison to P controller is that integral action enables PI controllers to eliminate offset. PI controllers provide a balance of complexity and capability that makes them by far the most widely used algorithm in process control applications. Tuning was done empirically by changing values of controller proportional-integral gain (K_p, K_i) in accordance to the magnitude of the error signal. The result of the tuning process are shown on Fig. 3.4. The airflow during the PI breath mode simulation is measured with Honeywell AWM720P1 flowmeters. A green solid line represents required flow curve, a red dashed line show airflow before motor was tuned and finally blue dash-dot line shows airflow after the motor was tuned. Tuned values for PI breath mode and latex bags are $K_p = 0.03$ and $K_i = 0.7$.

3.5 Development of an introductory user manual and laboratory experiment

The user manual familiarizes user with legal information and possible risks at the beginning. Afterwards instructions are given in case of first use of the iLung 2.1. Manual continues with step by step guide describing advised measurement setup and control software. Particular attention is given to software description usage, specifically to real-time program. Due to the fact that normal user, without deep understanding of iLung 2.1 function, will not in any case modify the FPGA program, only brief overview of this software par is given. The FPGA program is compiled, flashed and running on the cRIO. Real-time program is also running on the cRIO and can be modified by means of the LabVIEW user interface. LabVIEW user interface is running on the standalone PC, that is connected to the cRIO via Ethernet cable. This setup provides possibilities of changing lung simulation settings User Manual can be found in annex H due to its extent.

Laboratory experiment presents students with assignments, that has to be practically performed with the use of the i Lung 2.1 simulator. It provides theoretical overview of simulation problematic, present necessary tools to conduct the measurements and leads students in step by step instructions. After completing all assignments, evaluating measurements and answering theoretical question students should have decent understanding of iLung 2.1 function. Complete laboratory experiment can be found in annex I
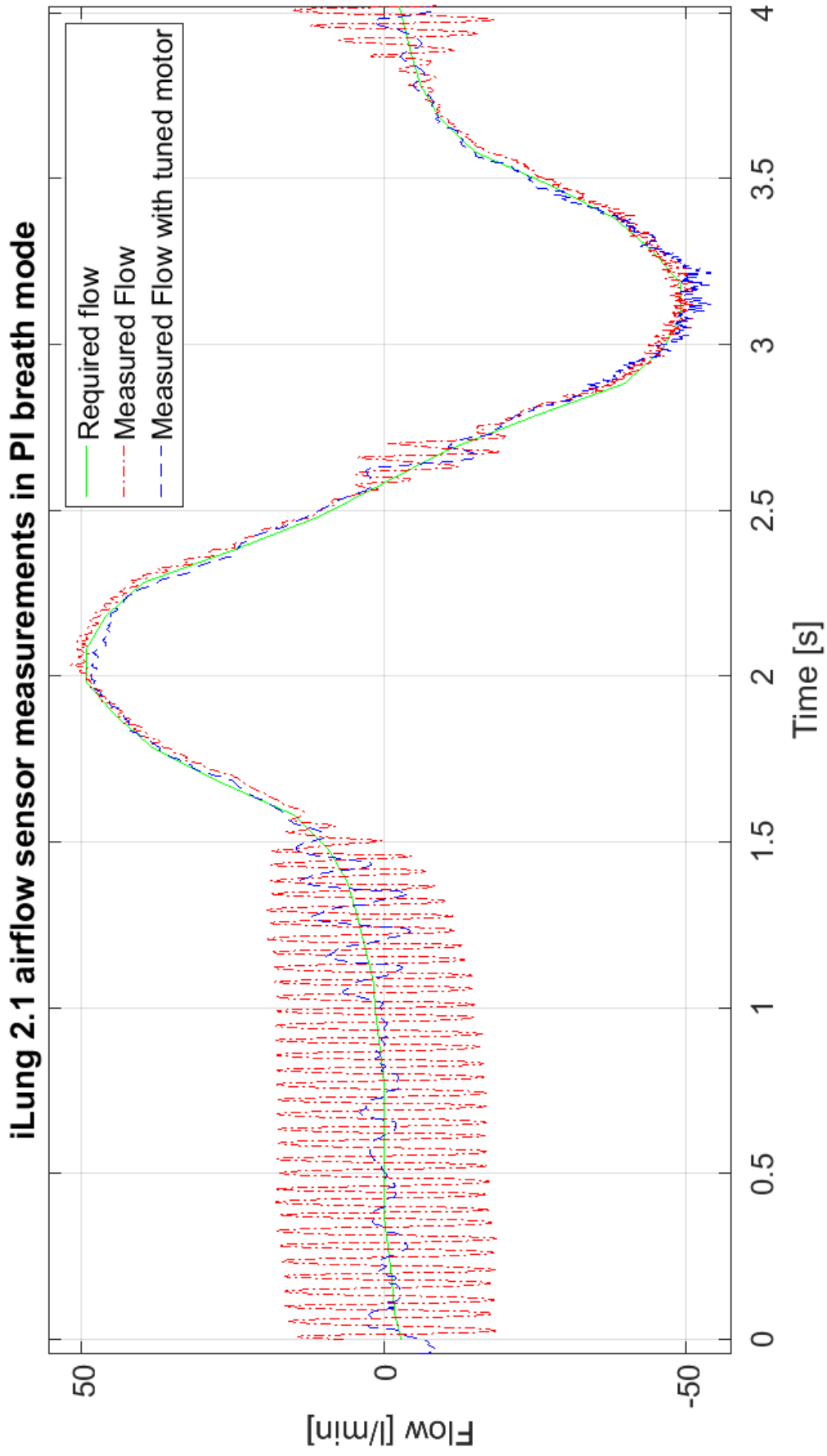
Fig. 3.4: Airflow measured during PI breath mode simulation: a) green solid line - required flow curve b) red dashed line - airflow before motor was tuned c) blue das-dot line - airflow after motor was tuned

4 MEASUREMENTS FOR SIMULATOR VALIDATION

In order to validate a function of implemented cRIO and more importantly, iLung 2.1 simulator function as a standalone unit, measurements were made. Measurement process consists of two parts. Firstly, spirometry based measurements of subjects was conducted using certificated medical spirometer. Secondly, iLung 2.1 simulator spirometry measurements were taken during simulations using the same medical spirometer and two different lung equivalents, 2.3l latex bags and primed porcine lungs. Both datasets were evaluated and compared with each other.

4.1 Medical measurement device

The device used during measurements is correctly called pneumotachograph. Unlike a spirometer, wherein the basic measured quantity is volume V [l], the pneumotachograph measures volumetric flow rate $\dot{V}$ [l · s^{-1}]. The volume is determined by integrating the volume flow over time. When working with a pneumotachograph the patient is breathing fresh air constantly, which enables unlimited length of measurement. However, to be consistent with documentation designation spirometer will be used in following text.

During both measurements the Spirobank II Advanced spirometer was used. Spirobank II Advanced meets the criteria of the European Safety Standards EN 601−1 and guarantees the EMC requirements within the limits laid down in the European Standard EN 60601 − 1 − 2. Product also conforms to the established security levels and quality standards laid down by the Council Directive 93/42/EEC for medical devices.

The Spirobank II Advance is a pocket spirometer in which a flow and volume measurement sensor is a digital turbine. Measurement are based on the infrared interruption principal. This principal ensures the accuracy and the reproducibility of the measurements, without requiring a periodic calibration. During measurements spirometer was connected to a personal computer (PC) via universal serial bus (USB). The single-use disposable turbines with a pre-connected mouthpiece, that are individually factory calibrated and packaged were used in order to ensure precision and hygiene of the measurements [17].

4.2 Processing of measurements from spirometer

Measured data from Spirobank II Advanced spirometer contains slow direct current (DC) drift, that prevents further quantitative data analysis by shifting of zero isoline. In order to eliminate DC drift and preserve signal properties finite impulse response (FIR) high pass (HP) filter was designed using the MATLAB software. More specifically an equiripple FIR filter using the Parks-McClellan algorithm was designed because equiripple filters have a frequency response that minimizes the maximum ripple magnitude over all bands. As filtering of signal is concerned zero-phase distortion digital filtering by processing the input data in both the forward and reverse directions was performed. Cut off frequency $f_c = 37$ mHz was determined empirically as a lowest frequency that eliminated slow DC drift for all measured signals. Detail of magnitude response of the designed filter used for filtering DC drift can be found on Fig. 4.1.
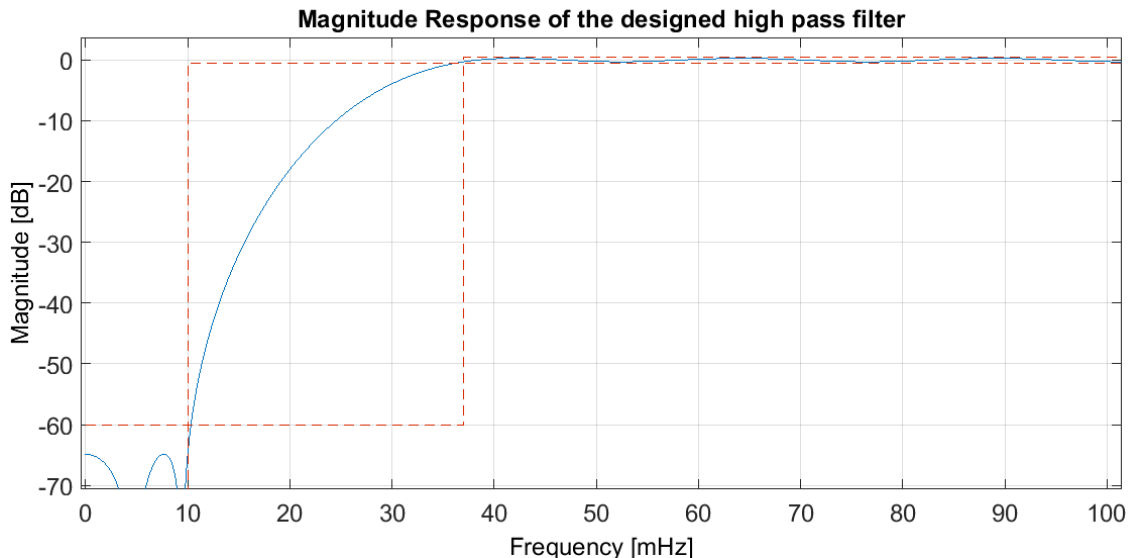
Fig. 4.1: Magnitude response of designed high pass filter

Comparison of spirometry measurements after and before filtration for volunteer 06M9175N can be seen on Fig. 4.2 where blue line shows original spirometry measurement and red dash dot line shows resulting signal after high pass filtration.

Time normalization for repetition cycles

Aim of the data analysis was to compare human breathing patterns at rest with data collected from iLung 2.1 during rest breathing pattern simulations. First approach was to calculate average breathing pattern of both, simulator and human by aligning measured curves and calculating average. However, due to natural variability within
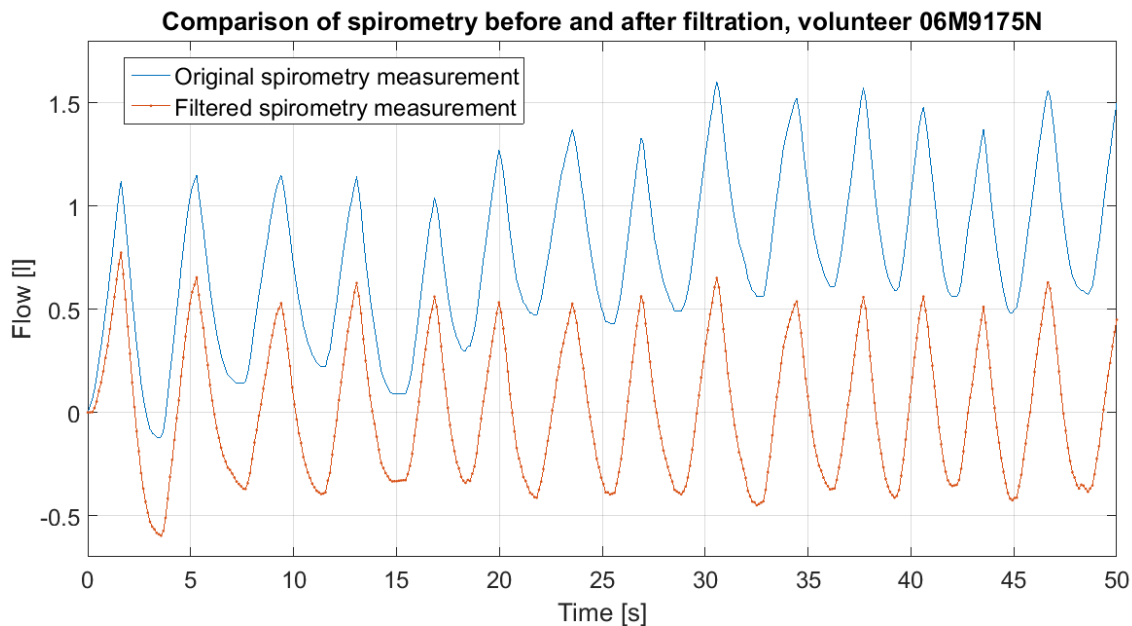
Fig. 4.2: Spirometry measurements: a) blue line - original measurement b) red dash dot line - signal after high pass filtration

human breathing (RR, TV), information about shape and amplitude of the curve was lost after averaging. Therefore, more appropriate approach of time normalization for each breathing cycle was implemented.

Time normalization for repetition cycles consists of isolation of each breathing cycle by finding corresponding intersections of analysed breathing signal with zero level. The original second time scale is converted to percent of cycle ranging from 0 to 100% for each breathing cycle. In case that number of sample in given breathing cycle is lower than 100 samples, cubic spline interpolation is done to ensure same amount of sample over each cycle (1 data point at each 1% step). After time normalization mean value and standard deviation for each measurement is calculated and also represented graphically.

Time normalization for repetition cycles is done for all measured spirometry data and therefore calculated values and shape of the resulting curve allows comparison between human spirometry and iLung 2.1 measurements.

4.3 Measurement of subjects

Spirometry measurements at rest were taken following the Guidelines for spirometry, see subsection 4.3.1. Guidelines were created particularly for the measurement of subjects so that the relevant data can be obtained and repeatability of measurements is secured. Guidelines are based on Spirobank II Advanced documentation [17]

and the Spirometry in Practice booklet created by British Thoracic Society [2]. Clinical study was non conducted and the result provide only proximate comparison. Personal data of all subjects were anonymized. Unique identifier consists of: number of the volunteer, gender - male (M) / female(F), last two numbers of year of birth, weight of the volunteer and smoking habits - Yes (Y) / No (N).

Overall 26 subjects were measured and have been informed about the measurement procedure and tasks. All subjects have been informed and gave informed oral consent regarding the measurements and use of data.

4.3.1 Guidelines for spirometry measurements

Due to the fact that the iLung 2.1 can simulate human breathing patterns at rest, subjects were asked to perform simple breathing exercise. For 50 seconds volunteer was relaxed and asked to breath at rest, while remain seated. Guidelines were created in cooperation with group of students, that were performing spirometry measurements for study project. The steps of the measurement procedure can be summarized as follows:

1. Collect personal data of the volunteer (i.e. gender, age, weight, height, smoking habits, health status).

2. Add to the spirometer a disposable part with which the individual will have direct mouth contact. Ensure that the mouthpiece is locked properly in the spirometer aperture.

3. Explain the exercise clearly and inform the volunteer about the duration of the measurement as well as the breathing technique that should be performed.

4. Fit the nose clip onto the nose of the subject to ensure that air cannot escape through the nostrils. This step is fundamental in order to ensure a correct set of data. In absence of the clip, the breathing curve will be subjected to a drift.

5. Hold spirometer at either end by one hand. The display should be facing the user.

6. Insert the mouthpiece well into the mouth beyond the teeth. Ensure that the mouthpiece is being used correctly. For an optimal result, the perimeter of the outer surface of the disposable part should be completely enclosed in the volunteer's mouth.

7. Provide volunteer with an input signal that denoted the beginning of the measurement. Measurement always stars with inhalation.

8. Save the collected spirometry measurements for further evaluation.

9. Repeat steps 4 to 7 with the aim of collecting acceptable data, it is advised to perform at least 2 trials 5 minutes apart for each volunteer. Moreover, during the second trial the individual will already have familiarized with the

measurement procedure and is therefore more likely to perform better.

4.3.2 Spirometry results of subjects

Measured spirometry data were analysed in terms of respiratory rate (RR), estimated tidal volume (ETV), average tidal volume (TV) and complemented by graphical representation of average berating pattern from all measurements. For each volunteer spirometry trial with correctly executed breathing exercise was selected. Spirometry trial with correctly executed breathing exercise is defined as not containing extreme volume changes (higher than double TV), swallowing, air leakages and sudden changes of breathing frequency. The results calculated from the measurements are summarized in Tab. 4.1.

Tab. 4.1: Spirometry data taken from non-smoking subjects

Spirometry data of non-smoking subjects				
Volunteer identifier [-]	Respiratory rate [bpm]	Estimated tidal volume [ml]	Average tidal volume [ml]	Standard deviation [ml]
01M9186N	16	602	573	127
02M9190N	10	630	859	59
03M9274N	18	518	1151	194
04M9160N	4	420	2767	293
05M9199N	12	693	2387	217
06M9175N	16	525	991	124
07M9182N	12	574	542	217
08M9290N	13	630	721	132
09M9381N	11	567	427	226
10M9372N	13	504	1382	316
11M9285N	12	595	2004	231
12M9288N	8	616	1046	188
13F9253N	15	371	537	62
14F9166N	15	462	512	96
15F9155N	18	385	554	53
16F9285N	16	595	591	104
17F9167N	16	469	543	73
18F9165N	10	455	539	76
19F9460N	13	420	1620	210
20F9170N	12	490	316	129

Due to the fact, that tidal volume varied during conducted measurements, its value was determined in each breathing cycle (inspiration and expiration). The average value of tidal volume for each volunteer was calculated as the sum of tidal volume values divided by the number of breathing cycles (RR). Estimated tidal volume was also calculated using volunteer weight and average physiological value of TV (7 ml/kg) [15].

Following time normalization for repetition cycles procedure normalized breathing pattern was calculated for each one of 20 subjects. Normalized average breathing pattern at rest from subject 01M9186N can be seen on Fig. 4.3. Subject was chosen because variability in breathing pattern is in this case clearly visible. Normalized average breathing pattern at rest, calculated form one trial, for each of 20 subjects can be found in annex D due to its extend.
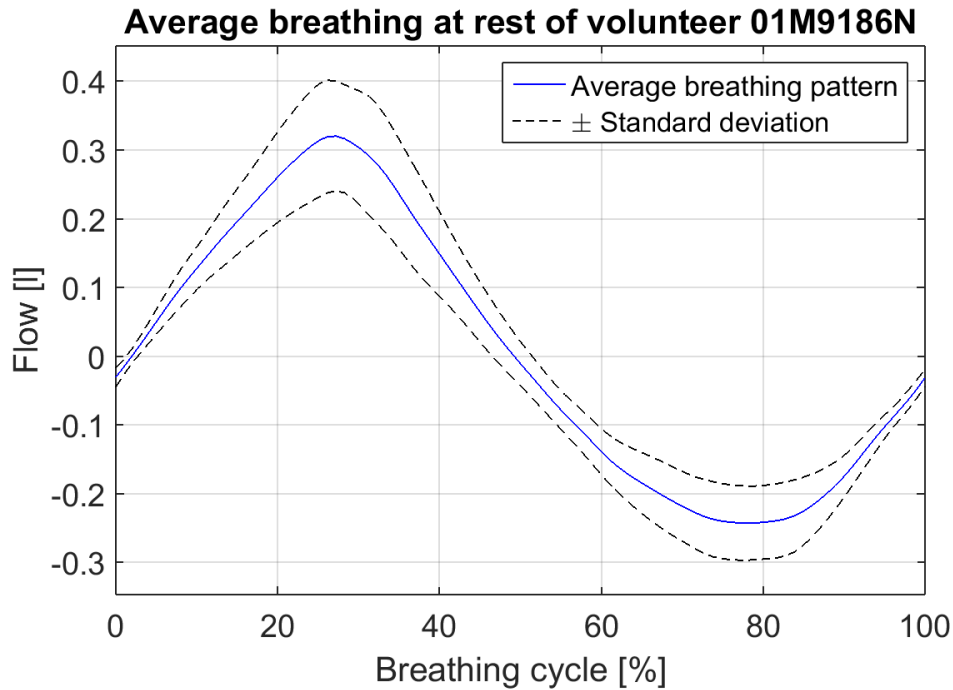
Fig. 4.3: Normalized average breathing pattern at rest for volunteer 01M9186N

In sum 26 subjects have been measured. From all measured subjects 10 were female and 16 were male. Because of different measurement setup and exclusion of smokers 7 subjects had to be rejected. Additionally, even after repeated measurements some subjects had tidal volume more than three times the physiological tidal volume (500 ml). Because measured breathing activity clearly was not breathing at rest 4 subjects were removed from further processing. From 26 measured subjects 16 non-smokers, age 24 ± 0.875, 9 male, 7 female, were finally included into evaluation.

In order to create reference breathing pattern at rest, which will be compared to iLung 2.1 breathing simulation curve, average of 12 cycles per person in one trial was averaged from all 16 measured subjects. In the following text, this method will be called average of average. Resulting average of average breathing pattern from 16 measured subjects is shown on Fig. 4.4.

Average of average breathing pattern of 16 volunteers
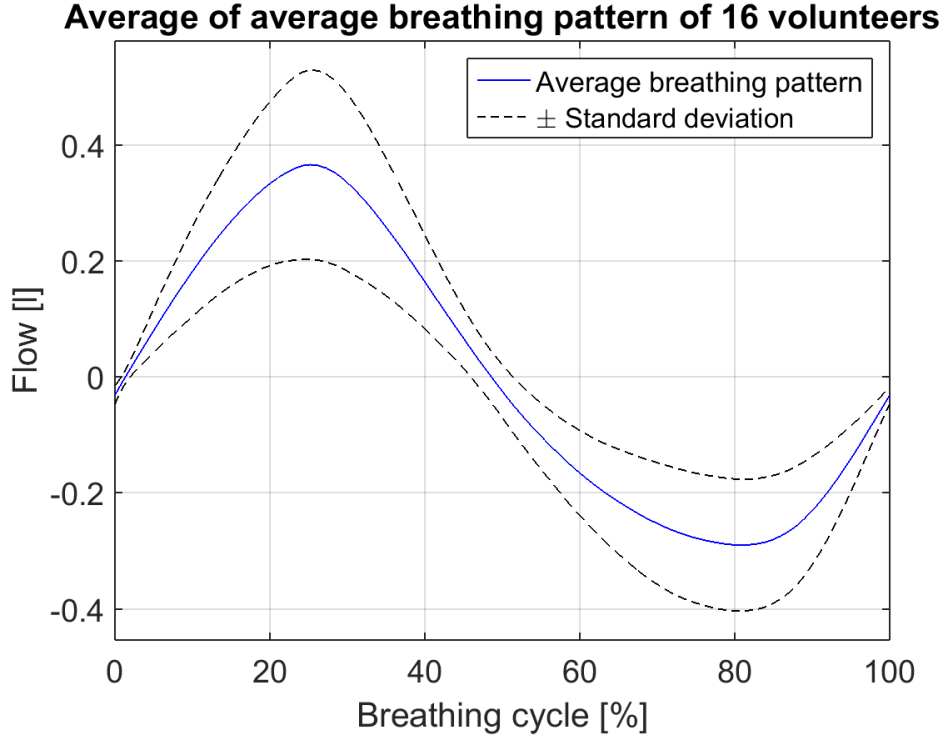
Fig. 4.4: Average of average breathing pattern from 16 measured subjects

4.4   Measurements of iLung 2.1 simulator

Preformed measurements of iLung 2.1 followed the same procedure. Lung equivalent (latex bags or primed porcine lungs) was attached inside thoracic box and sealed. The Spirobank II Advance pocket spirometer was placed at the top of iLung 2.1 simulated trachea. By using the same spirometer comparability with human spirometry data was ensured. In each mode (PI sin and PI breath) measurements were recorded for 50 s and repeated 10 times. Measured iLung 2.1 data were always analyzed the same way as human spirometry data to allow later comparison. More information about used measurement setup contains the User manual, which can be found in annex H.

4.4.1 Measurements with 2.3 l latex bags

Measurements in PI sin mode f = 0.2 Hz, TV = 650 ml

Measurements in PI sin mode with 2.3 l latex bags was carried out with setting of f = 0.2 Hz, amplitude = 30 l/min, that according to certified medical spirometer represents TV = 650 ml and under pressure in range -30 mBar to -20 mBar (inspiration / expiration). Calculated RR, average TV and its standard deviation for each measurement trial is stated in Tab. 4.2. Normalized average simulation breathing curve, calculated form one trial, for each of 10 measurement trials can be found in annex E. Average of average breathing curve of iLung 2.1 in PI sin mode using 2.5 l latex bags was calculated from all 10 trials. Resulting curve can be found on Fig. 4.5.

Tab. 4.2: iLung 2.1 measurements in PI sin mode f = 0.2 Hz, amplitude representing TV = 650 ml

Spirometry of iLung 2.1 in PI sin mode using 2.3l latex bags			
Measurement [#]	Respiratory rate [bpm]	Average tidal volume [ml]	Standard deviation [ml]
1	12	670	27
2	12	642	84
3	12	627	36
4	12	671	45
5	12	584	123
6	12	602	85
7	12	618	75
8	12	619	71
9	12	630	80
10	12	645	40

Measurements in PI breath mode f = 0.25 Hz, TV = 700 ml

Measurements in PI breath mode with 2.3 l latex bags was carried out with setting of f = 0.25 Hz, amplitude = 30 l/min, that according to certified medical spirometer represents TV = 700 ml and under pressure in range from -30 mBar to -20 mBar (inspiration/expiration). As mentioned before difference between PI sin mode and PI breath mode is, that in PI sin mode simulator breathing curve is sinusoid however in PI breath mode simulator breathing curve is physiological human breathing curve at rest taken from literature.
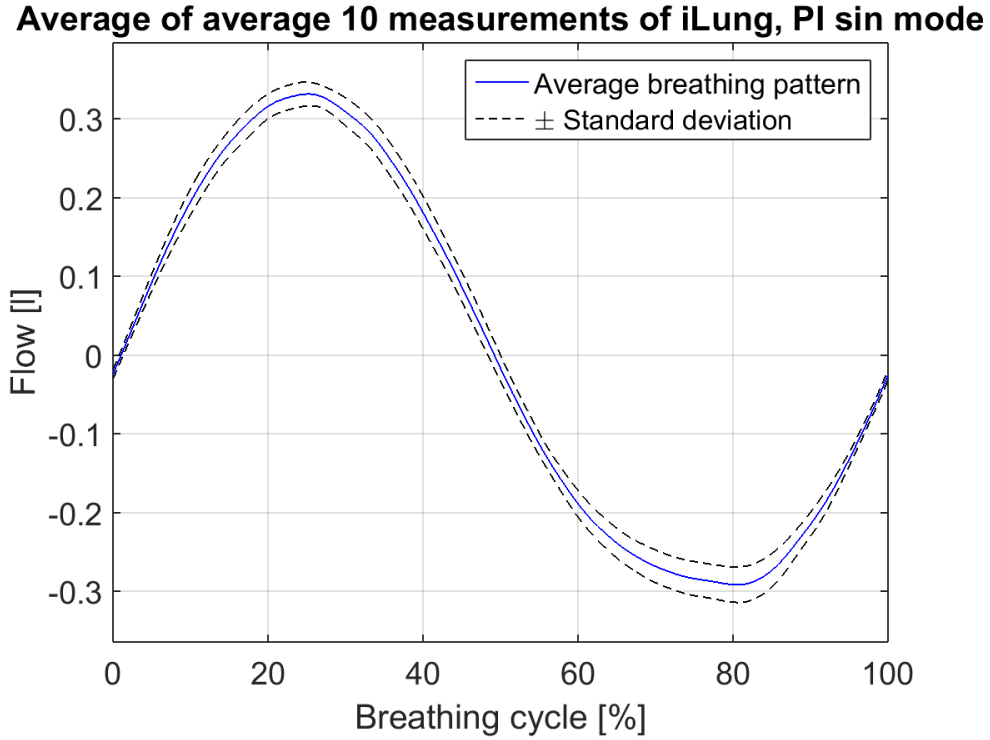
Fig. 4.5: Average of average curve of iLung 2.1 in PI sin mode from 10 trials

PI breath mode has preset values of frequency f = 0.25 and tidal volume TV = 700 ml. Calculated RR, average TV and its standard deviation for each measurement trial is stated in Tab. 4.3. Normalized average simulation breathing curve, calculated form one trial, for each of 10 measurement trials can be found in annex F. Average of average breathing curve of iLung 2.1 in PI sin mode using 2.5 l latex bags was calculated from all 10 trials. Resulting curve can be found on Fig. 4.6.

4.4.2 Measurements with primed porcine lungs

Primed porcine lungs provides an internal structure which is very similar to the human lung. For the measurements porcine lungs were imported from USA. Porcine lungs suffered damage above the first bifurcation during transportation and due to the air leakage it was not possible to measure all simulation modes. However, Gener sine mode with settings: f = 0.2 Hz manual control of a pump was measured successfully. Measurements in Gener sin mode with primed porcine lungs were carried out with following settings: f= 0.2 Hz, amplitude = 2rps that corresponds to TV ≈ 1000 ml and under pressure in range from -5 mbar to -15 mbar (inspiration/expiration).

Calculated RR, average TV and its standard deviation for each measurement trial is stated in Tab. 4.4. Normalized average simulation breathing curve, calculated form one trial, for each of 10 measurement trials can be found in annex G. Average of

Tab. 4.3: iLung 2.1 measurements in PI sin mode f = 0.2 Hz, TV = 650 ml

Spirometry of iLung 2.1 in PI breath mode using 2.3 l latex bags			
Measurement [#]	Respiratory rate [bpm]	Average tidal volume [ml]	Standard deviation [ml]
1	15	730	59
2	15	704	33
3	15	720	55
4	15	702	35
5	15	728	58
6	15	719	42
7	15	729	51
8	15	727	46
9	15	731	52
10	15	727	56
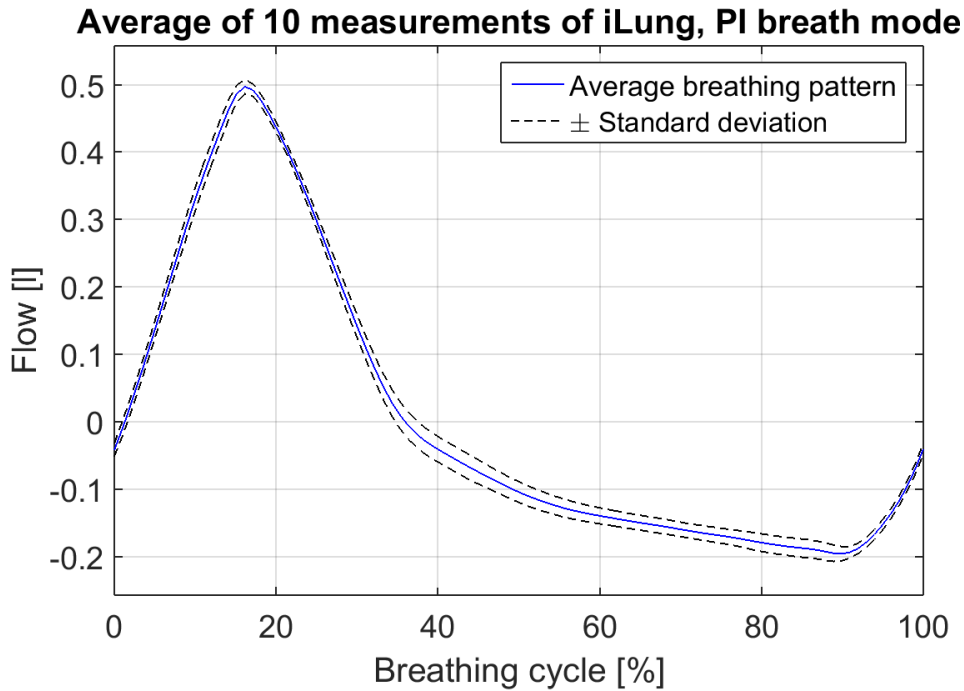
Fig. 4.6: Average of average curve of iLung 2.1 in PI breath mode from 10 trials

average breathing curve of iLung 2.1 in Sin mode using porcine lungs was calculated from all 10 trials. Resulting curve can be found on Fig. 4.7. In Gener sin mode amplitude of a breathing curve is represented in rpm (rotations per minute), where 2 rpm are approximate to tidal volume of 1 l .

Tab. 4.4:   iLung 2.1 measurements in Sin mode f = 0.2 Hz, amplitude representing TV ≈ 1000 ml

Spirometry of iLung 2.1 in sin mode using primed porcine lungs			
Measurement [#]	Respiratory rate [bps]	Average tidal volume [ml]	Standard deviation [ml]
1	12	961	156
2	12	1148	50
3	12	1059	80
4	12	983	139
5	12	1029	172
6	12	1014	162
7	12	987	80
8	12	979	77
9	12	1016	58
10	12	1040	52
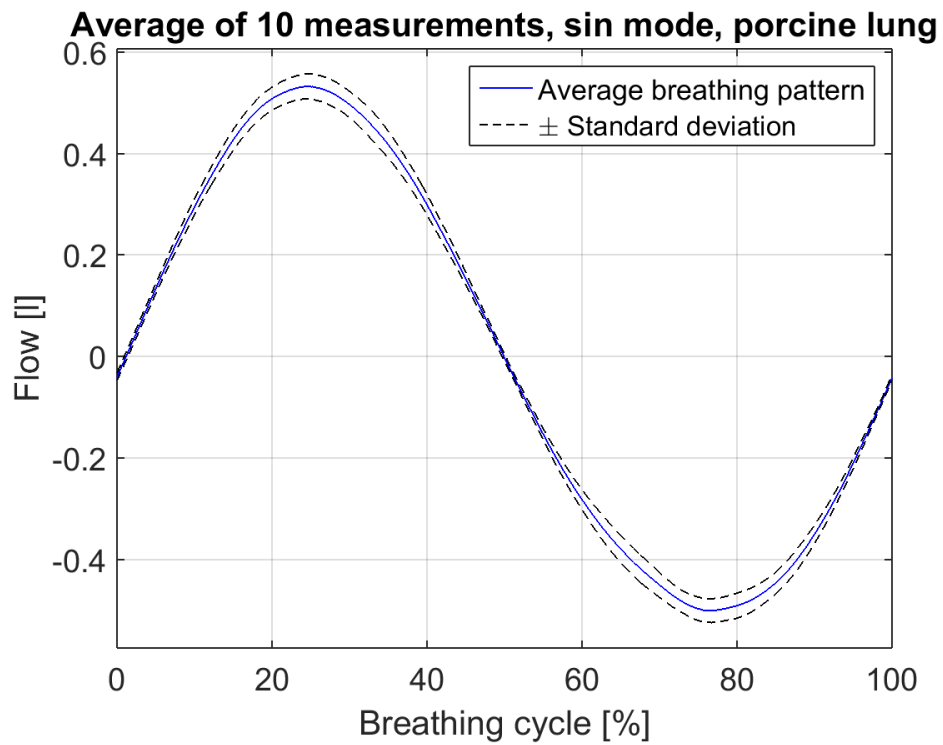
Fig. 4.7: Average of average curve of iLung 2.1 in sin mode from 10 trials

5 DISCUSSION

5.1 Spirometry measurements overview

During the spirometry measurements it became clear, that changes in surrounding environment significantly affect performance of volunteers. Large number of people in the room where the measurement was performed, lead to distraction, stress and anxiety reflecting in higher respiratory rate and tidal volume. Same phenomena were observed, when volunteer could see, even if partially, recorded spirometry curve. In order to ensure data validity all measurement were repeated in quite environment, without additional people in the examination room and with volunteer facing opposite to measurement computer screen. Only non-smoking subjects were participating in the experiment. Therefore, the obtained set of data is comparable to the one provided by the iLung 2.1 simulator. Individuals who have had smoking habits for a longer period of time, have reduced the performance of their lungs significantly and could not be objectively comparable to iLung 2.1.

An effort was made to balance the number of subjects of both sexes equally despite the fact that measured quantities in conducted experiment does not vary with respect to gender. Spirometry measurements of subjects exhibit high variability in both respiratory rate and tidal volume.

Majority of subjects had tidal volume higher than was estimated from their weight. The cause of this phenomenon lies in the subconsciously increased efforts also known as white coat syndrome. Even though the measurements were not conducted in doctor's office, subjects paid close attention to their breathing. Inspiration to expiration ratio is closer to 1:1 than to the physiological 1:2 when breathing at rest. This is clearly visible from measurements of volunteer number 1, 8, 7 and 11. Because of exceeding physiological values of tidal volume more than three times 4 subjects were excluded from average breathing pattern analysis. These subjects were not able to perform exercise of breathing at rest even after several trials and remained heavily focused on their breathing.

Respiratory rate is also higher than was expected from physiological values due to the principle described above. Variance in tidal volume corresponds with variance in frequency. For example, volunteer number 4 had abnormally high tidal volume and also significantly lower respiratory rate. A possible explanation is that subject is actively involved in regular sport activities (diving, ruining etc.).

However, after excluding 4 subjects with outline measurements average measured values provide a good reference for comparison with the iLung 2.1 simulator as they fall within the physiological range.

5.2 iLung 2.1 evaluation and comparison to spirometry

Measurements with 2.3 l latex bags in PI sin mode exhibit steady respiration rate of 12 bpm over all trials, which is in direct correlation to frequency settings of f = 0.2 Hz within the simulator control software. Airflow amplitude, that is in software calculated from Honeywell AWM720P1 flowmeter, was in the control software set to 30 l/min. This value corresponds to TV = 500 ml. However, value of TV was determined to be 650 ml by certified spirometer. Real time math script converting Honeywell AWM720P1 flowmeter voltage output to airflow for all measurement modes have to be therefore modified. However, this change will effect only amplitude coefficients as time evolution of the measured signal is consistent with certified spirometer.

Concerning the measurements conducted by spirometer, average tidal volume for each measured trial varies around set value of 650 ml with exception of measurement number 5, where average TV = 584 ml and is therefore only value under 600 ml. This could be caused by piston reaching the end limit mechanical switch. Piston motion range is in this case limited by the end limit switch and consequently the value of tidal volume is slightly lower than demanded. PI breath mode exhibits steady respiratory rate of 15 bpm that corresponds to values f = 0.25 set in control software. Respiratory rate in this mode is fixed, taken from the literature values of breathing at rest and cannot be modified. As a real-time script calculates the values of airflow for all modes amplitude setting also do not match the measured value from certified spirometer, that was determined as TV = 700 ml. Measured and calculated average values of TV are close to the desired one without any outline measurements.

Vacuum pump created required under pressure from -30 mbar to -20 mbar (inspiration/expiration) without difficulties in both PI sin and PI breath mode. Latex bags were therefore fully inflated during all measurement trials. Due to the motor tuning there are no detectable motor oscillations. The applicability of PI breath mode was therefore significant increase in comparison to the state before tuning, when the measured values around zero were uninterpretable due to the significant motor oscillations.

Primed porcine lungs were measured in Gener sine mode, without the feedback control from the Honeywell AWM720P1 flowmeters due to significant tissue defects before the first bifurcation and several other small defects on various locations. When measuring in PI sin or PI breath mode, the vacuum pump was not able to created sufficient under pressure (-30 mbar) required by this modes and piston

movement therefore tried to compensate this insufficiency by moving in one direction. Due to the significant leakages, the piston soon reached the end limit switch and stopped the simulation. However, in Gener sinus mode feedback control is not active. The primed porcine lungs were measured with following setting f = 0.2 Hz, amplitude = 2 rmp which corresponds to TV ≈ 1000 ml and vacuum pump turned on manually creating under pressure in range from −5 mbar to −15 mbar (inspiration/expiration). Measured frequency 12 bpm matches the setting in the control software as well as TV measurements with only trial number 2 exceeding value of 1100 ml

Measurements with both latex bags and prime porcine lungs exhibit a high degree of repeatability in given settings for both RR and TV. In comparison to human spirometry where variability in breathing cycles are clearly visible iLung can replicate the same pattern without significant deviations. Human respiration is influenced by complicated cascade of reactions dependent not only on the physical condition of the individual but also his state of mind. Therefore, higher variability in human respiration is understandable in comparison to mechanical simulator.

5.3 Breathing pattern comparison

Measured breathing curves of subjects show an inspiration to expiration ratio close to 1:1. Therefore the PI breath mode with a fixed 1:2 ratio is not comparable to acquired measurements of subjects. For that reasons PI breath mode was excluded from further comparison. Comparison of human breathing pattern with curves recorded during iLung 2.1 PI sin simulation with latex bags and Gener sin simulations with prime porcine lungs can be seen on Fig. 5.1. In comparison to Gener sin mode with porcine lungs human respiration shows steeper onset (inhalation) followed by gradual decrease (exhalation). Maximum inhalation occurs for both waveforms at very close point (25% of the cycle) however there is clearly noticeable discrepancy in exhalation. Minimum for human breathing occurs at 80% of the cycle and for Gener sin mode in 76%

In second case PI sin mod exhibits high similarity with measured breathing of subjects. Maximum inhalation and minimum exhalation occurs for both waveforms almost in identical points. Additionally, inspiration to expiration ratio is for both slightly higher than 1:1. PI sin mode shows promising results in comparison to human breathing and should be further tested with porcine lungs.

Due to the fact that iLung 2.1 at FH Technikum Wien had a technical breakdown during the middle of the experiments, measurements were conducted on the identical simulator at Brno University of Technology (BUT). Latex bags, primed

porcine lungs, spirometer and all other essential measurement equipment including the adapted software with the tuned motor controller, was moved to BUT for ensuring the same measurement setup. Part of a work was also determining the cause of a problem. After a week of trials, osciloscope measurements, control software reinitialisation and consultation with iLung 2.1 manufacturer the cause of a problem was determined to be a faulty motor encoder. Replacement of the motor is therefore necessary.
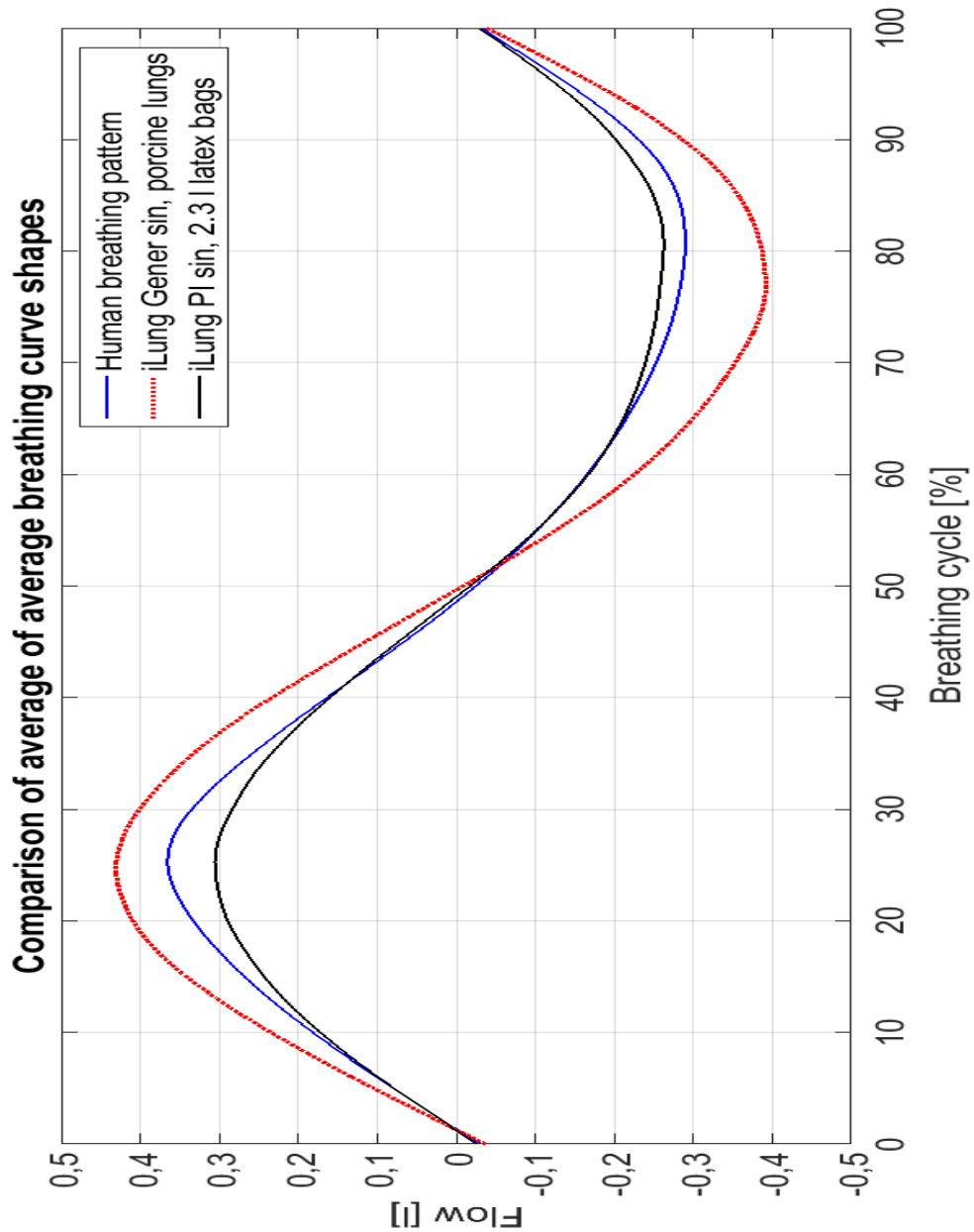
Fig. 5.1: Comparison of average breathing curve shapes for subjects in PI sin and Gener sin mode

CONCLUSION

This Master's Thesis deals with the topic of integration and testing of a real-time control unit into the iLung 2.1 active mechanical lung simulator. As a simulator control unit cRIO was used. The integration process was documented through tables that summarize the connection between electrical parts of the simulator and cRIO. To provide easy usability user manual was created, describing basic operational settings and measurement setup. Furthermore, laboratory experiment that familiarizes students with simulator basic principle throughout practical work was also created. Laboratory experiment will be used in the teaching of the Master's course named Biomedical Engineering in Respiration and was already tested by a group of volunteer students and modified in accordance to theirs remarks.

LabVIEW based simulator control software was developed prior to this Master's Thesis within the Alveopic project. Simulator cRIO was therefore implemented in a way that ensured usability of the software. However, changes have been made to the software according to tasks given by supervisor at FH Technikum Wien. Most influential change involves simulator motor tuning. Prior to motor tuning it was not possible to interpret the measured flow curves near zero values in PI breath simulation mode due to the significant motor oscillations. Overall recorded values were therefore devaluated. After motor tuning, the preciously detected oscillations in PI breath mode, are very small and undetectable by medically certified spirometer.

Various measurements of iLung in Gener sin, PI sin and PI breath mode using latex bags and porcine lungs as human lungs equivalent were performed. All conducted measurements support the conclusion, that iLung 2.1 is capable of simulating human breathing patterns, given the correct settings.

The final tasks of this Master's Thesis were complicated to be accomplished, due to iLung 2.1 servomotor breakdown during the final measurements. Due to that fact measurements were redone on identical machine, under equivalent laboratory conditions on a short notice.

Further studies should be conducted in future using primed porcine lungs to ensure maximal similarities with human lungs. Aerosol measurements to test drugs or quality of air in the surrounding environment should be also involved. Simulator function can be further improved by adding additional modes simulating pathological breathing and calibrating Honeywell AWM720P1 flowmeters to fit flow values from medically certified spirometer.

It can be concluded, that all Master's Thesis assignments were fulfilled.

BIBLIOGRAPHY

[1] ALITA INDUSTRIES, INC. *Linear compressors and vacuum pumps: General Catalog* [online]. 2002 [cit. 2015-12-13]. Available from: `http://www.alita.com/literature/AlitaLinearPumpCatalog.pdf`.

[2] BELLAMY, David. BRITISH THORACIC SOCIETY. *Spirometry In Practice: A Practical Guide To Using Spirometry In Primary Care.* 2nd. London, 2005.

[3] CALLENTINE, Lainna. *The breathtaking respiratory system: God's Wondrous Machine.* 1st edition. New York: New Leaf Publishing Group, 2015. ISBN 978-089-0518-625.

[4] PINOUTSRU. *D-sub 9 Connector Pinout* [online]. 1999 [cit. 2016-04-21]. Available from: `http://connector.pinoutsguide.com/9_pin_D-SUB_female/`

[5] ENSTICK. *Switching mode power supply* [online]. 2005 [cit. 2015-12-12]. Available from: `http://www.tme.eu/en/Document/012474e1bbeb1192420243c1264ad92c/GS100E.pdf`.

[6] FOX, Stuart. *Human Physiology.* 12th edition. New York: McGraw-Hill, 2011. ISBN 978–0–07–337811–4.

[7] FREESCALE SEMICONDUCTOR. *Temperature compensated and calibrated silicon pressure sensors: MPX2010* [online]. 2008 [cit. 2015-12-13]. Available from: `http://www.mouser.com/ds/2/161/MPX2010-256329.pdf`.

[8] HIRSCHMANN. *MAS 6100 grey: Product information* [online]. 2000. Germany [cit. 2016-4-19]. Avaliable from: `http://docs-europe.electrocomponents.com/webdocs/13ed/0900766b813ed1af.pdf`.

[9] HONEYWELL INTERNATIONAL INC. *Airflow Sensors: Line guide* [online]. 2014 [cit. 2015-12-13]. Available from: `http://sensing.honeywell.com/honeywell-sensing-airflow-sensors-line-guide-008150-7-en2.pdf?name=AWM5104VN`.

[10] HONEYWELL INTERNATIONAL INC. *Airflow Sensors: AWM700 Series* [online]. 2015 [cit. 2016-4-19]. Available from: `http://sensing.honeywell.com/honeywell-sensing-airflow-sensors-awm700-series-datasheet-32301627-b-en.pd?name=AWM720P1`.

[11] FH TECHNIKUM WIEN. *Healthy interoperability: Advanced Lung research for VEterinary medicine Of Particles for Inhalation - Cooperation: AlveoPic* [online]. 2005 [cit. 2015-12-12]. Available from: `http://healthy-interoperability.at/alveopic`.

[12] KACMAREK, Robert, James STOLLER a Albert HEUER. *Egan's fundamentals of respiratory care.* 10th ed. St. Louis, Mo: Elsevier, 2013, xvii, 1401 s. ISBN 978-0-323-08203-7.

[13] LEADSHINE TECHNOLOGY CO., LTD. *Digital AC Servo Drive: ACS806* [online]. 2009 [cit. 2015-12-12]. Available from: `http://leadshine.com/UploadFile/Down/ACS806m.pdf`.

[14] LEADSHINE TECHNOLOGY CO., LTD. *Servo motors: ACM604/60V* [online]. 2012 [cit. 2015-12-12]. Available from: `http://leadshine.com/UploadFile/Down/Leadshine_ServoMotors_Catalog_20130507_1P.pdf.`.

[15] MARIEB, Elaine a Katja HOEHN. *Human Anatomy and Physiology.* 9th edition. United States of America: Pearson Education, Inc, 2013. ISBN 978-0-321-74326-8.

[16] MEAN WELL. *Single output with PFC function: SP-500 series* [online]. 2012 [cit. 2015-12-12]. Available from: `http://www.mouser.com/ds/2/260/mean%20well_sp-500-spec-342993.pdf`.

[17] MEDICAL INTERNATIONAL RESEARCH. *Spirobank II: User Manual* [online]. 2015 [cit. 2016-04-07]. Available from: `http://www.spirometry.com/ENG/Products/SpiroBank2.asp`

[18] MEASUREMENT SPECIALITIES. *Barometric pressure sensor* [online]. 2012 [cit. 2015-12-13]. Available from: `http://www.mouser.com/ds/2/418/MS5607-02BA03-710181.pdf`.

[19] NATIONAL INSTRUMENTS. *Operating Instructions and Specifications: NI cRIO-9024* [online]. 2009 [cit. 2015-12-21]. Available from: `http://www.ni.com/pdf/manuals/375233c.pdf`.

[20] NATIONAL INSTRUMENTS. *CompactRIO Developers Guide: Architectures and Development Practices for Control and Monitoring Applications.* 2012 [cit. 2015-12-21].

[21] NATIONAL INSTRUMENTS. *Operating Instructions and Specifications: NI 9205* [online]. 2007 [cit. 2015-12-22]. Available from: `http://www.ni.com/pdf/manuals/374188d.pdf`.

[22] NATIONAL INSTRUMENTS. *Operating Instructions and Specifications: NI 9403* [online]. 2007 [cit. 2015-12-22]. Available from: `http://www.ni.com/pdf/manuals/374069e.pdf`.

[23] NATIONAL INSTRUMNETS. *NI CompactRIO* [online]. 2015 [cit. 2015-12-21]. Available from: `http://www.ni.com/compactrio/`.

[24] Phoenix Contact: PCB terminal block [online]. Blomberg, 2014 [cit. 2016-04-15]. Available from: `www.phoenixcontact.com/online/portal/gb?uri=pxc-oc-itemdetail:pid=1725656&library=gben&tab=1`.

[25] RS ELECTRONIC. *MAB 45322: Product information* [online]. 2000 [cit. 2016-4-19]. Avaliable from: `http://docs-europe.electrocomponents.com/webdocs/1409/0900766b814098cc.pdf`.

[26] RWETC. S.R.O. *Electronics schematic: Assembly drawings* [online]. Revision 2.1. Jihlava, 2014 [cit. 2015-12-15].

[27] RWETC. S.R.O. *Lung model 2.1 simulator: Documentation Revision 1.1.* Jihlava, 2014 [cit. 2015-12-12].

[28] SENSIRION. *Datasheet SHT21: Humidity and temperature sensor IC* [online]. 2014 [cit. 2015-12-13]. Available from: `http://bit.do/sensirion-SHT21`.

[29] STANFIELD, Cindy. *Principles of Human Physiology.* 5th edition. San Francisco: Pearson Education, 2013. ISBN 978-0-321-81934-5.

[30] STASTO AUTOMATION. *Solenoid valve series 21A* [online]. 2013 [cit. 2015-12-13]. Available from: `https://www.stasto.eu/crmablage/oc/data/datenblaetter/21A3KV20_EN.pdf`.

[31] TORTORA, Gerard and Bryan DERRICKSON. *Introduction to the human body: the essentials of anatomy and physiology.* 9th edition. Hoboken, NJ: John Wiley, 2012. ISBN 978-111-8129-197.

[32] WARD, Jeremy, Jane WARD and Charles WIENER. *The Respiratory System at a Glance.* London: Blackwell Publishing, 2013. 3rd edition. ISBN 978-1-4051-9919-3.

[33] WINDMAIER, Eric, Hershelf RAFF and Kevin STRANG. *Vander's human physiology: The Mechanisms of Body Function.* 13th edition. New York: McGraw-Hill, 2014. ISBN 978–0–07–337830–5.

LIST OF SYMBOLS, PHYSICAL CONSTANTS AND ABBREVIATIONS

ATP — Adenosine triphosphate

CB — Connection board

EoCB — Extension of connection board

ETV — Estimated tidal volume

FIR — Finite impulse response

FPGA — Field programmable gate array

PCB — Printed circuit board

PMMA — Polymethylmethacrylate

RR — Respiratory rate

TV — Tidal volume

A   LUNG SIMULATOR CONNECTION BOARD

Fig. A.1: Original schematics of Lung simulator connection board

B   EXTENSION OF THE CONNECTION BOARD
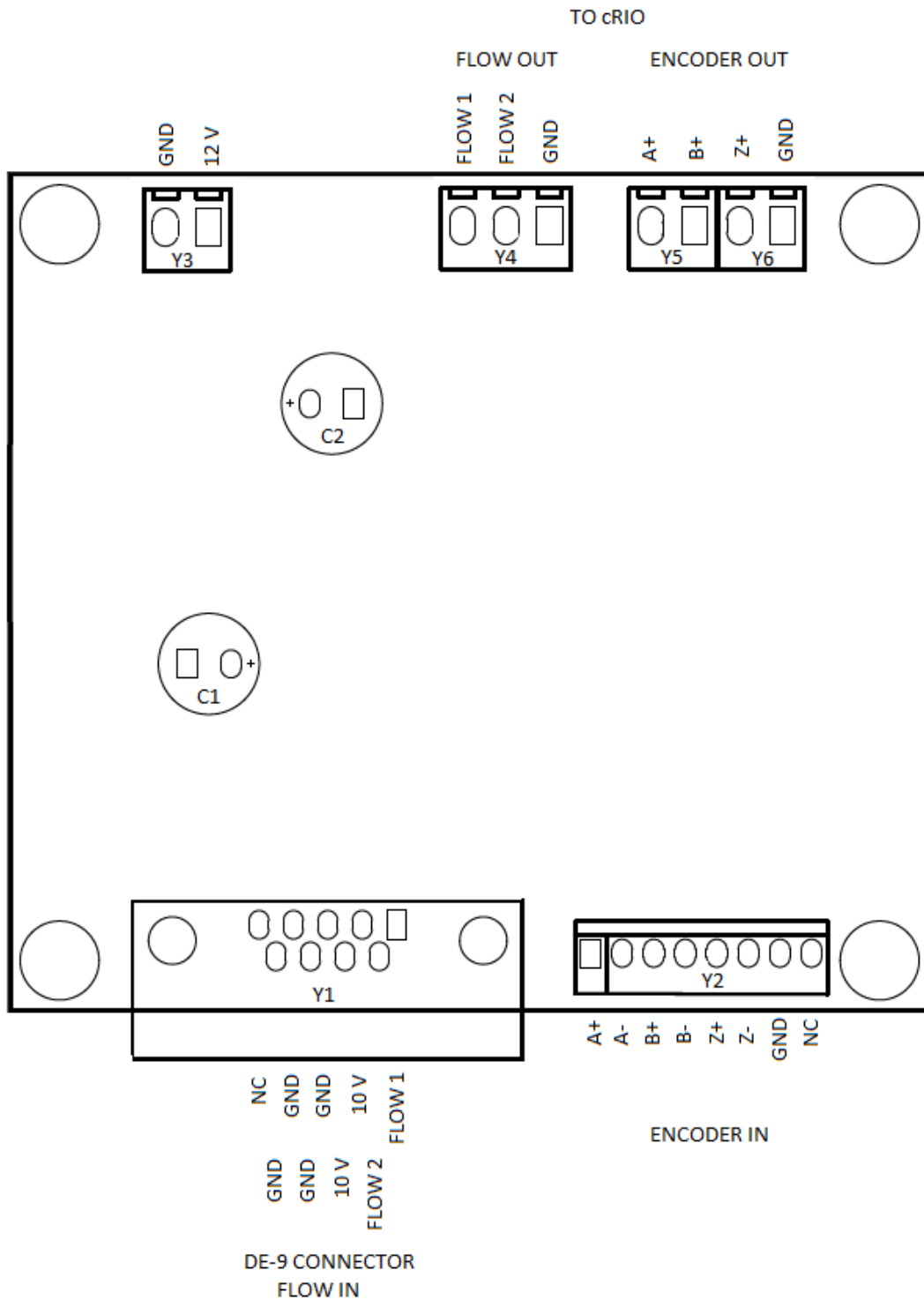
Fig. B.1: Schematics of Extension of The Connection Board based on assembly drawings labelled according to results - Top side view

C RECOMMENDED LABVIEW SOFTWARE
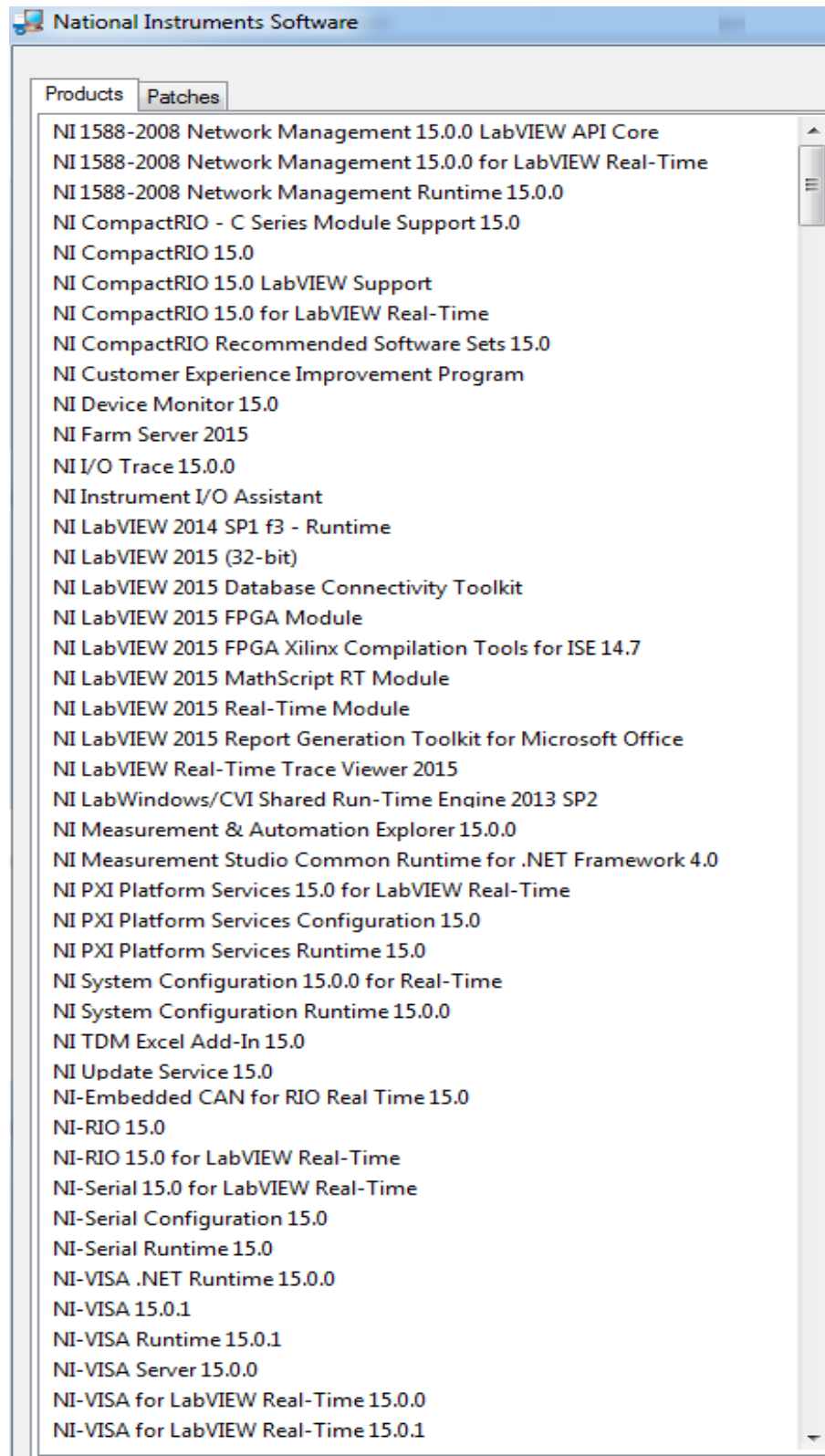
Fig. C.1: Recommended and tested LabVIEW software modules for iLung 2.1

D HUMAN SPIROMETRY
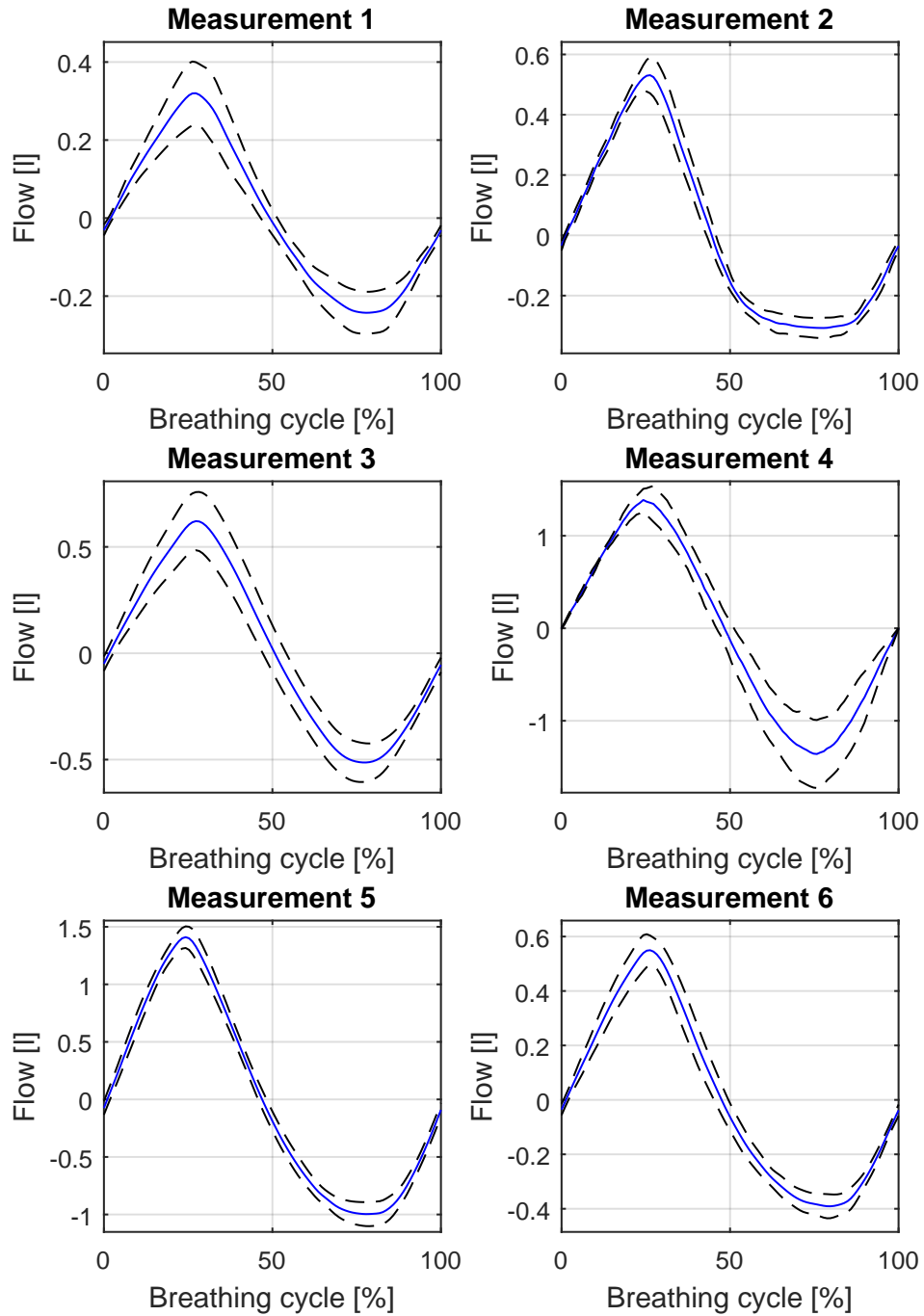
Fig. D.1: Measurements of subjects 1 - 6: a) solid blue line - normalized average breathing pattern of subject calculated from 12 breathing cycles b) black dash line - ± standard deviation
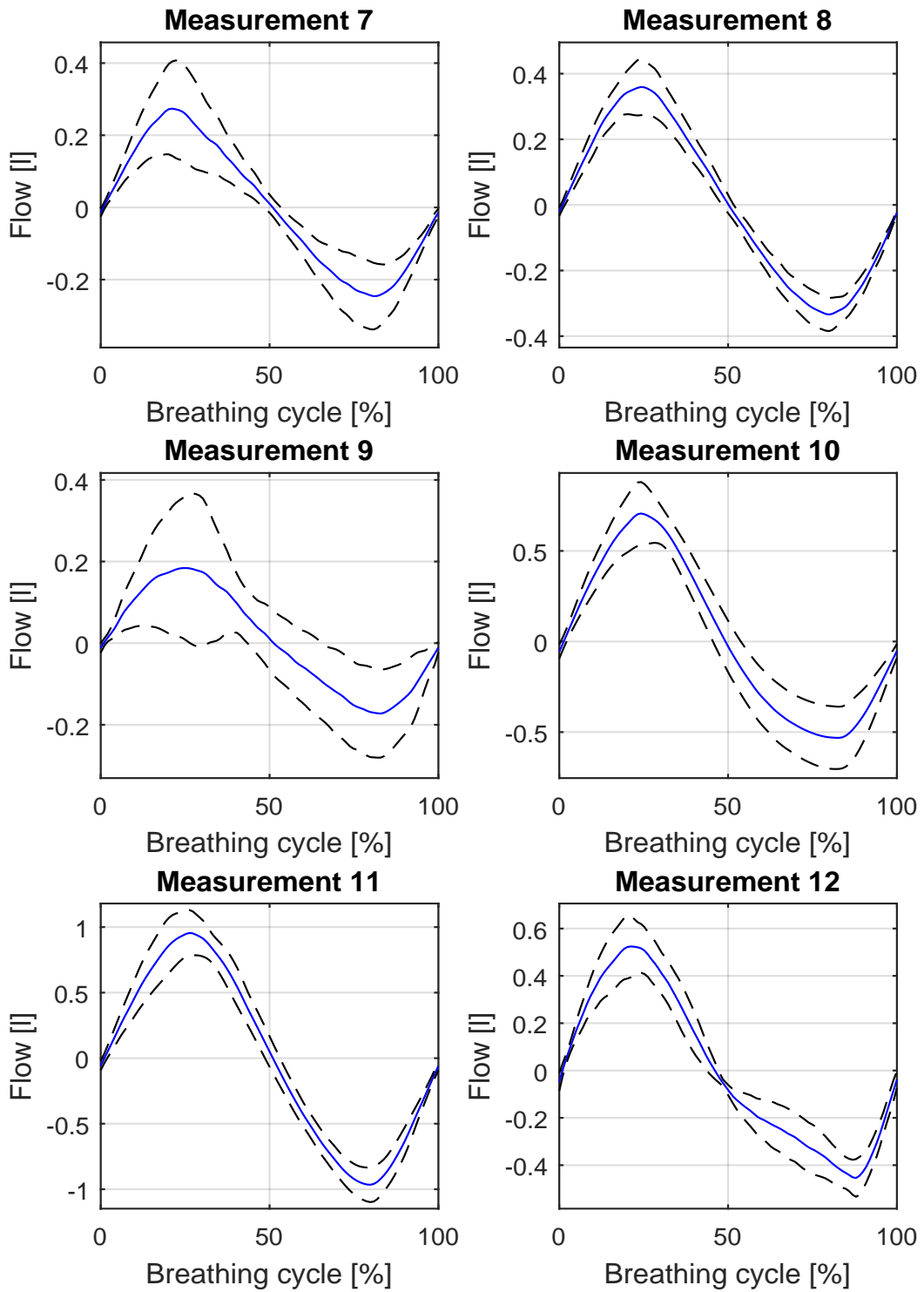
Fig. D.2: Measurements of subjects 7 - 12: a) solid blue line - normalized average breathing pattern of subject calculated from 12 breathing cycles b) black dash line - ± standard deviation

74
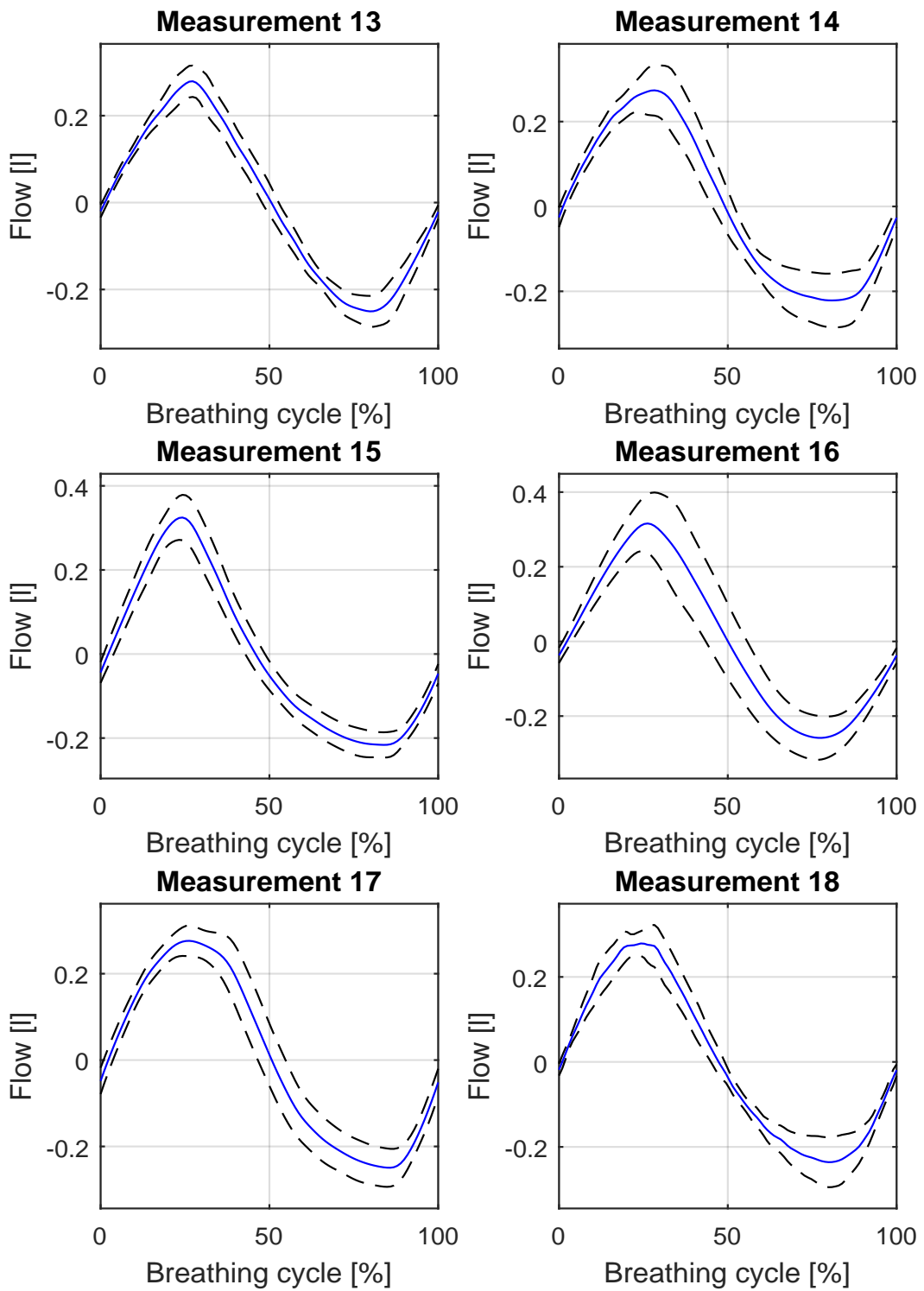
Fig. D.3: Measurements of subjects 13 - 18: a) solid blue line - normalized average breathing pattern of subject calculated from 12 breathing cycles b) black dash line - ± standard deviation
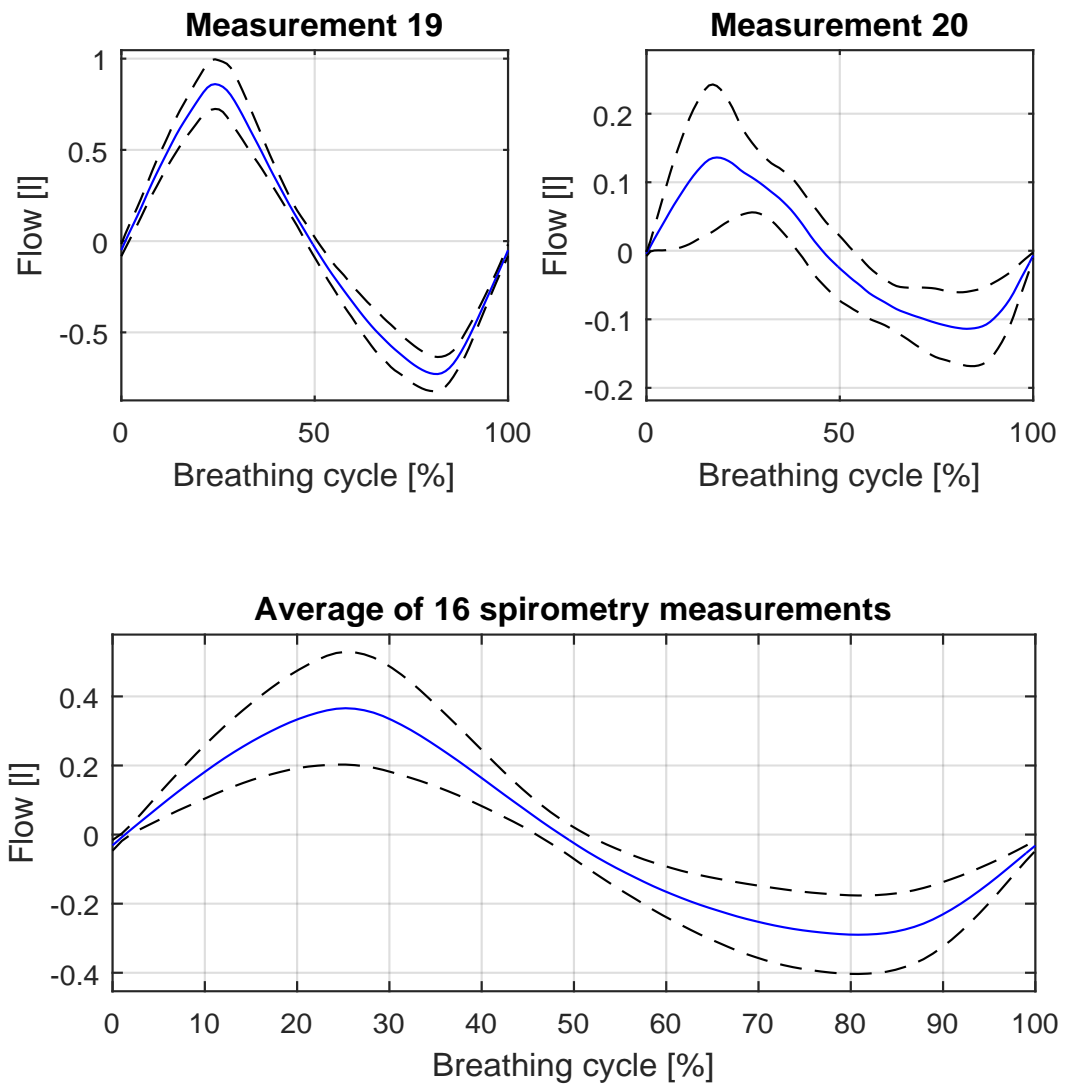
Fig. D.4: Measurements of subjects 19 - 20 and average of 16 subjects: a) solid blue line - normalized average breathing pattern of subject calculated from 12 breathing cycles b) black dash line - ± standard deviation

E   ILUNG PI SIN MODE 2.3 L LATEX BAGS
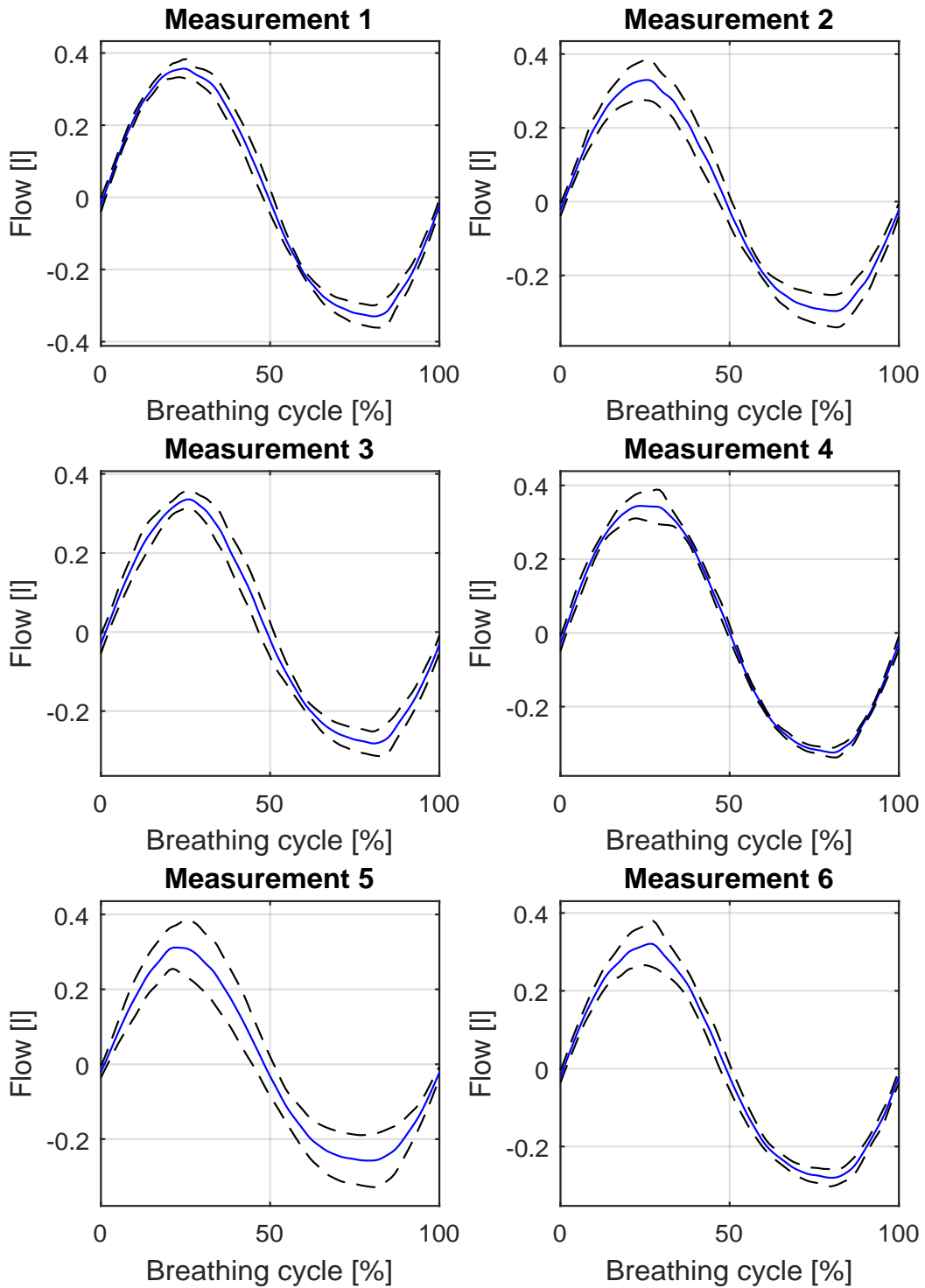
Fig. E.1: Measurements of iLung in PI sin mode using 2.3l latex bags, trial 1 - 6: a) solid blue line - normalized average breathing curve of trial calculated from 12 breathing cycles b) black dash line - ± standard deviation
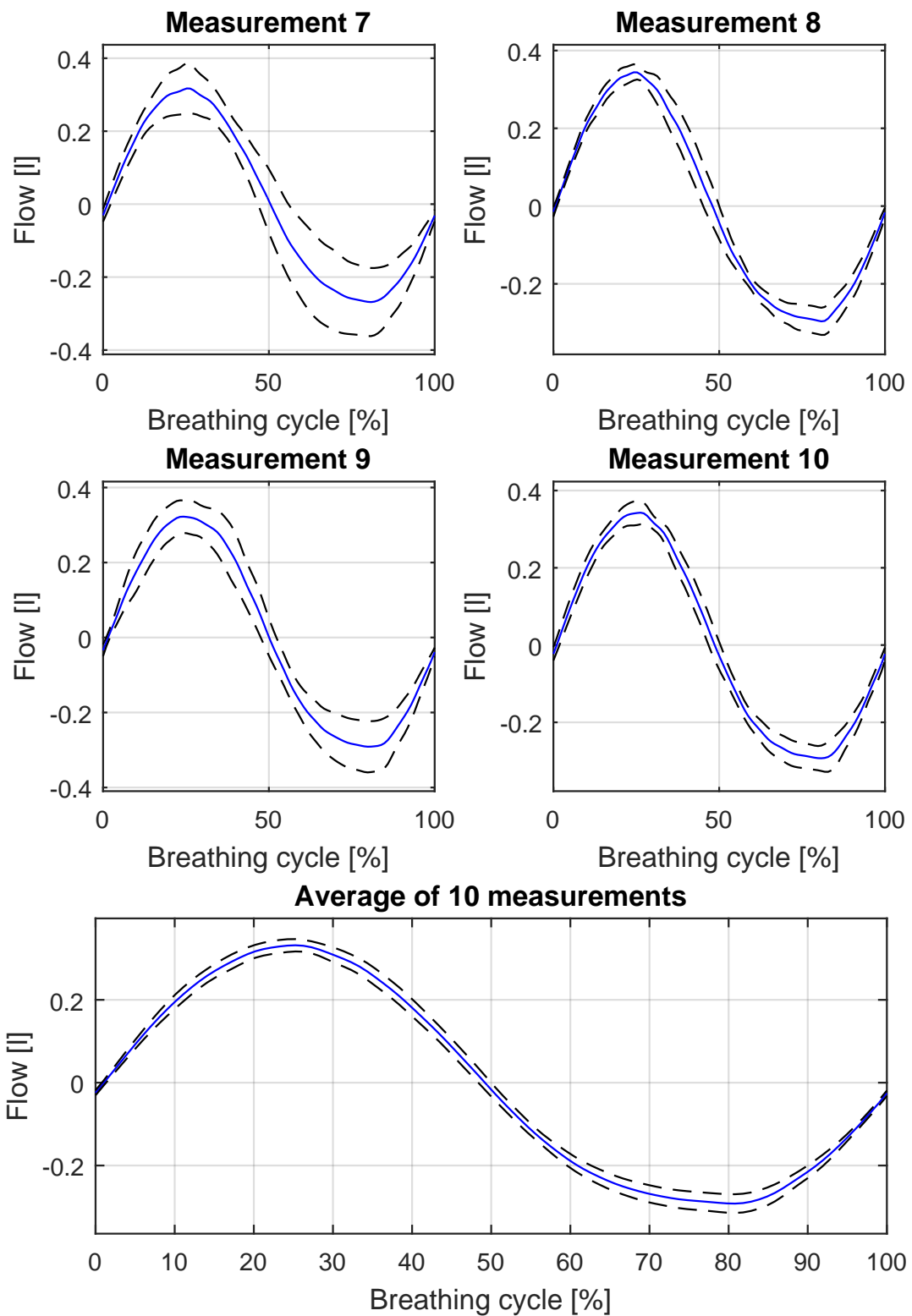
Fig. E.2: Measurements of iLung in PI sin mode using 2.3l latex bags, trial 7 - 10 and average breathing curve of 10 trials: a) solid blue line - normalized average breathing curve of trial calculated from 12 breathing cycles b) black dash line - $\pm$ standard deviation

F ILUNG PI BREATH MODE 2.3 L LATEX BAGS
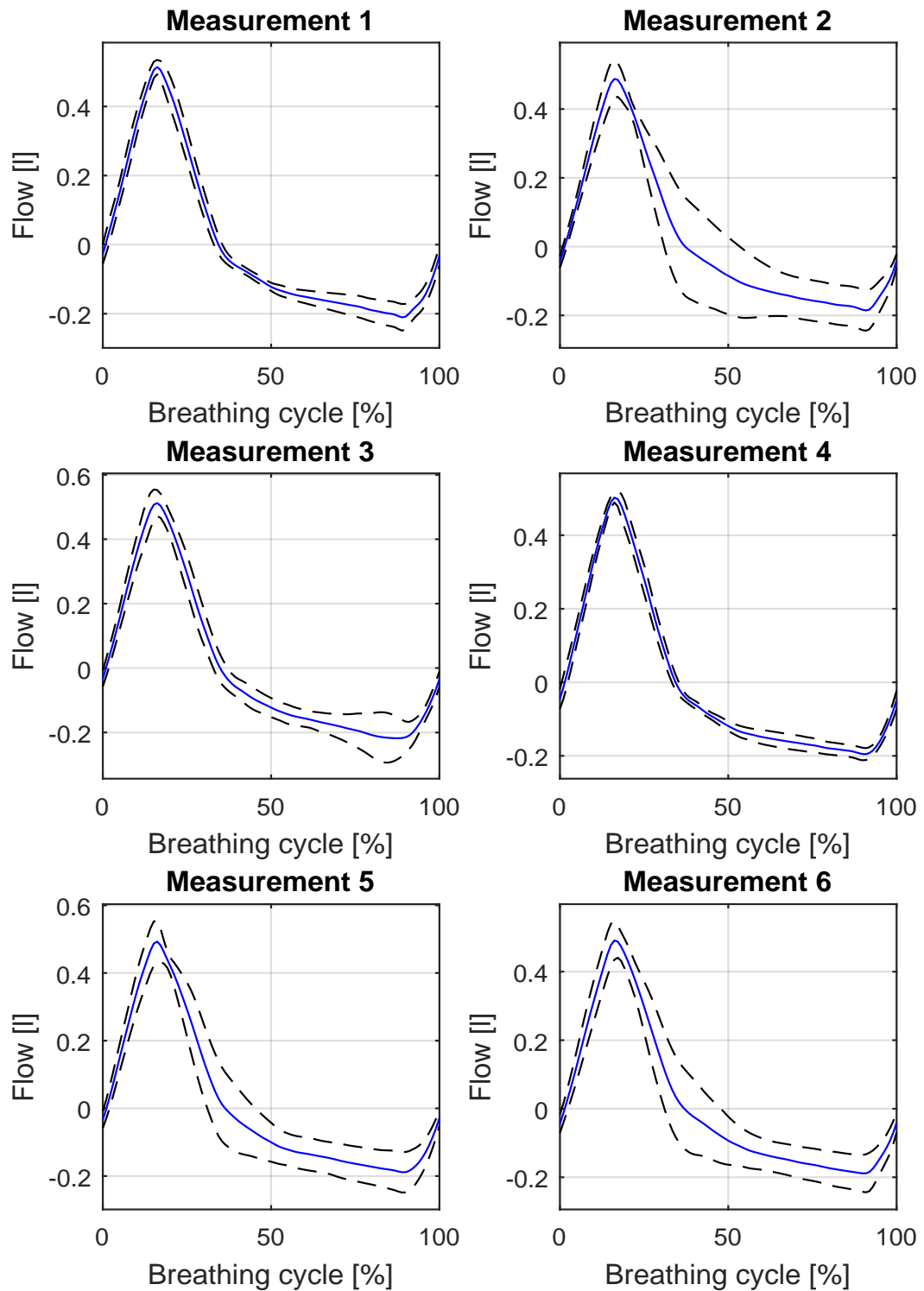
Fig. F.1: Measurements of iLung in PI breath mode using 2.3l latex bags, trial 1 - 6: a) solid blue line - normalized average breathing curve of trial calculated from 12 breathing cycles b) black dash line - ± standard deviation
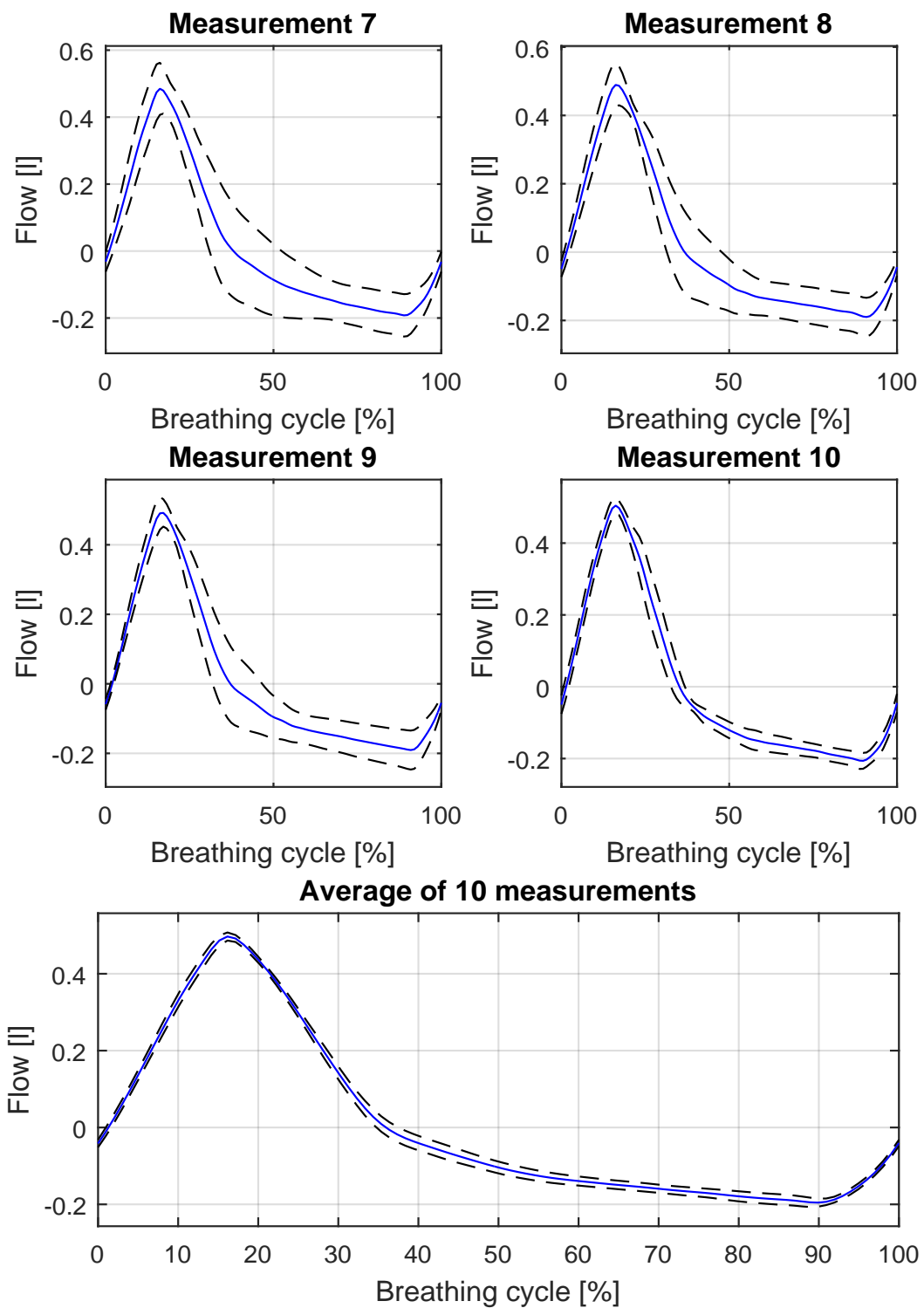
Fig. F.2: Measurements of iLung in PI sin mode using 2.3l latex bags, trial 7 - 10 and average breathing curve of 10 trials: a) solid blue line - normalized average breathing curve of trial calculated from 12 breathing cycles b) black dash line - ± standard deviation

G ILUNG SIN MODE USING PORCINE LUNG
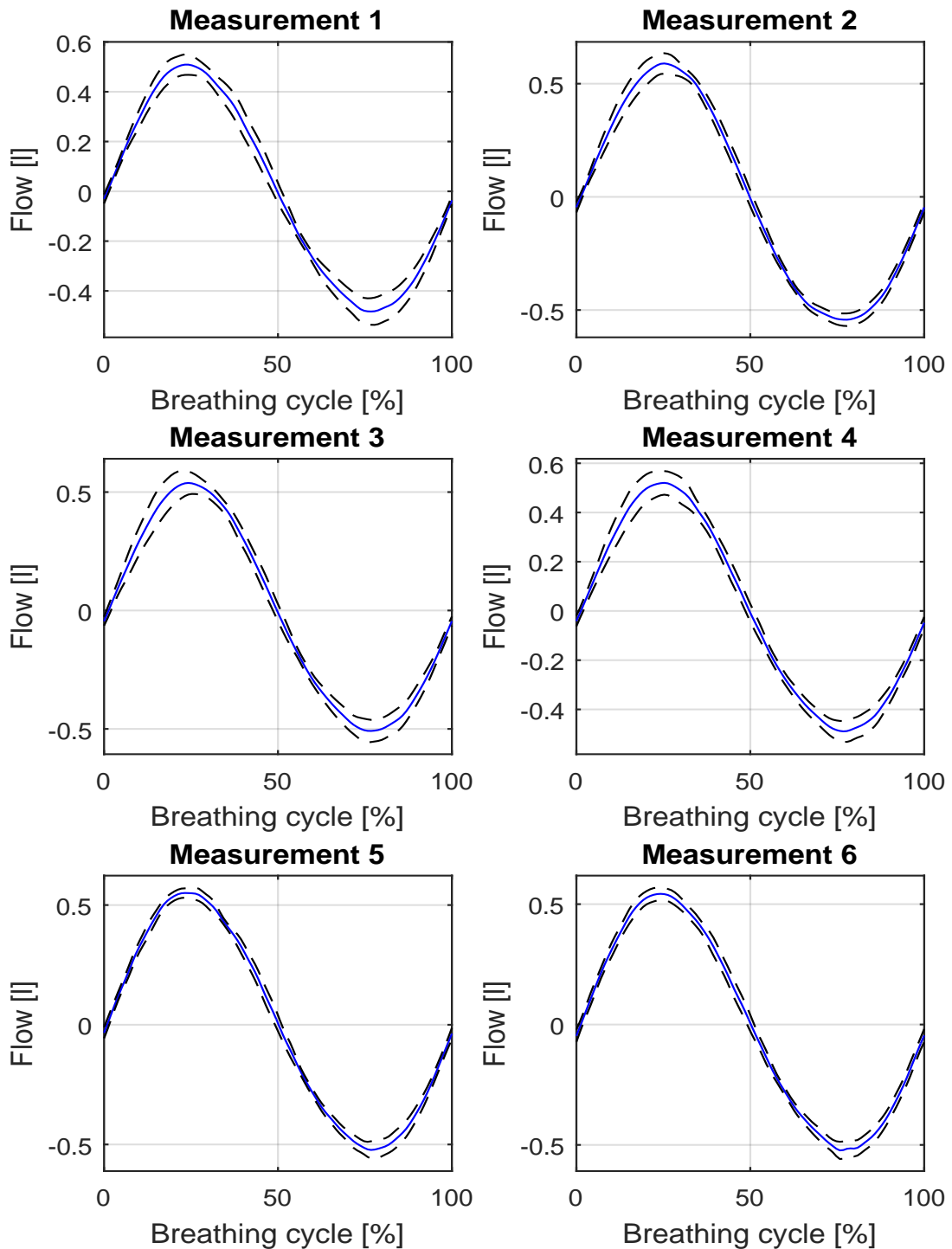
Fig. G.1: Measurements of iLung in Gener sin mode using 2.3l porcine lung, trial 1 - 6: a) solid blue line - normalized average breathing curve of trial calculated from 12 breathing cycles b) black dash line - ± standard deviation
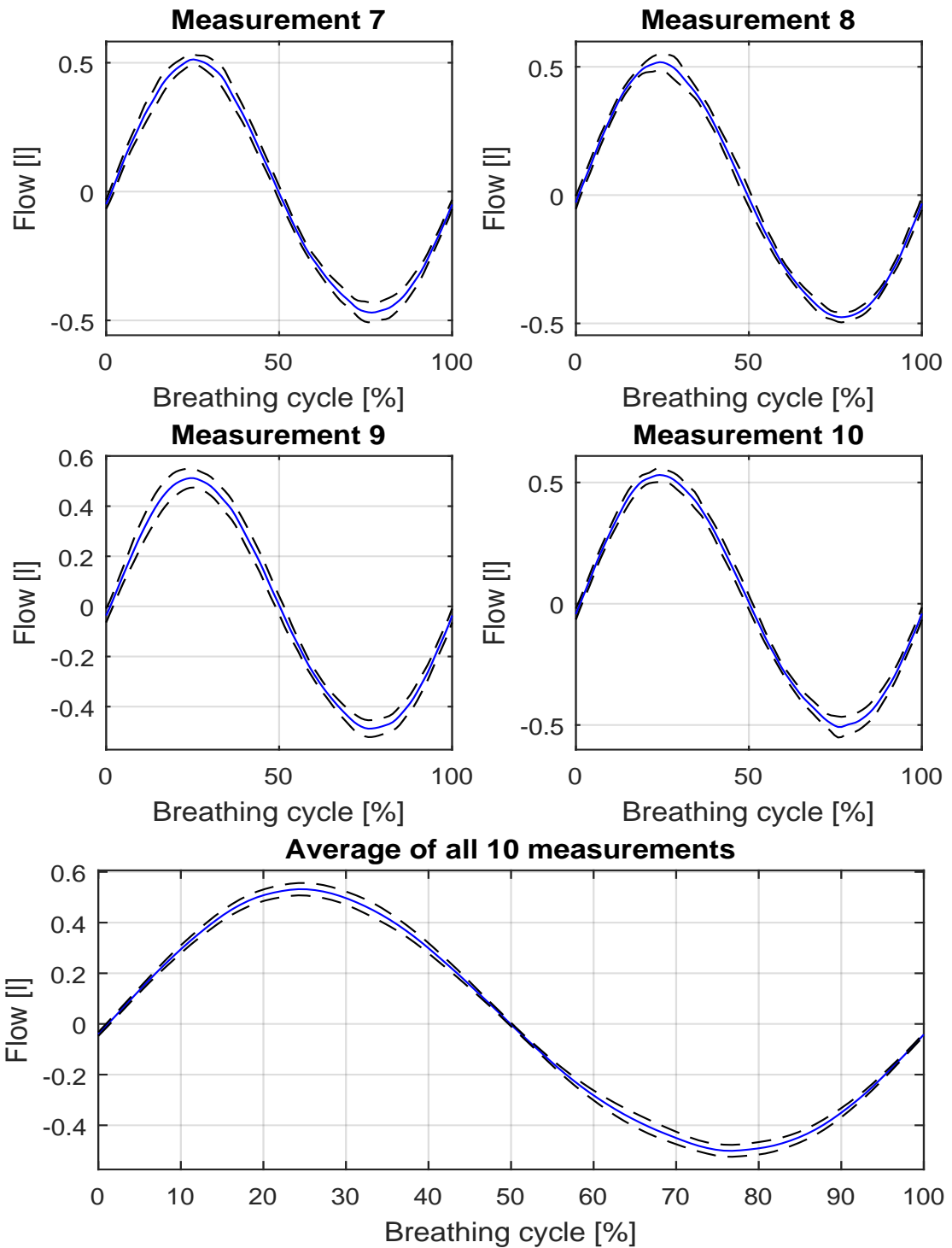
Fig. G.2: Measurements of iLung in PI sin mode using porcine lung, trial 7 - 10 and average breathing curve of 10 trials: a) solid blue line - normalized average breathing curve of trial calculated from 12 breathing cycles b) black dash line - ± standard deviation

H   USER MANUAL

BRNO UNIVERSITY OF TECHNOLOGY

&

UNIVERSITY OF APPLIED SCIENCES VIENNA

User Manual

Active Mechanical Lung Simulator
iLung 2.1

User manual Rev 1.0

Issued on: 8.4.2016

LEGAL INFORMATION

This manual contains notices you have to observe in order to ensure your personal safety, as well as to prevent damage to the device and property. The notices referring to your personal safety are highlighted in the manual by a safety alert symbol, notices referring only to property damage have no safety alert symbol. If more than one degree of danger is present, the warning notice representing the highest degree of danger will be used. A notice warning of injury to persons with a safety alert symbol may also include a warning relating to property damage.

Device usage

The product/system described in this documentation may be operated only by personnel qualified for the specific task in accordance with the relevant documentation, in particular its warning notices and safety instructions. Qualified personnel are those who, based on their training and experience, are capable of identifying risks and avoiding potential hazards when working with these products/systems. Students can operate the device under the direct supervision of an lecturer.

Disclaimer of Liability

Content of this manual has been reviewed to ensure consistency with the hardware and software described. Since variance cannot be precluded entirely full consistency cannot be guarantee. However, the information in this publication is reviewed regularly and any necessary corrections are included in subsequent editions.

Safety information

The following notices are intended to ensure both your personal safety and to prevent damage occurring to the products described or any connected devices and machines

WARNING ⚠

> - **Repairs to devices must be carried by manufacturer**
> - **When replacing parts or components, only use those parts that are included in the spare parts list.**
> - **Before opening the device, always disconnect the power supply.**
> - **Before the machine transport always remove the plexiglass chamber and disconnect all cables**

> - **Note that due to printing limitations the screenshots shown in this manual may differ from the display of the machine and/or from the keyboard icons. Copying this manual is forbidden.**
>
> -

> - **The manufacturer cannot be held responsible for any damage caused by the user of the device failing to follow the instructions and warnings contained in this manual.**

TABLE OF CONTENT

1 Before Using iLUNG 2.1

- Read this manual carefully, plus all labels and other product information supplied.
- Additional information can be obtained at a dedicated workplace in the Respiration Laboratory or will be provided by lecturer on demand.

This User Manual contains compressed information about iLung 2.1 most important operational setup and software usage description. Further information about simulator working principle together with electrical and mechanical parts specifications can be found in manufacturer documentation.

2 Basic measurement setup

1. Mount two 3l Latex bags as a lung equivalent into simulator thoracic chamber (plexiglass box) and seal it. As a lung equivalent 3l latex bags or porcine lung can be used.
2. Place Honeywell AWM720P1 flowmeters at the top of simulated trachea of the iLung. Marked side of the Honeywell AWM720P1 flowmeters must face downwards.
3. Connect Honeywell AWM720P1 flowmeters into the simulator front panel.
4. Connect dedicated PC at the experiment workplace and the simulator front panel via ethernet cable.
5. If not already plugged in, connect the power cable into a power socket situated on a back side of a device. Do no switch on the device before setup is approved by lecturer or laboratory assistant.
6. Power on the device.
7. Start LabVIEW software and run the Real-time program subchapter 0. called: iLung 2.1 Real time program.

3 Control software for iLung 2.1

LabVIEW based software for iLung consists of two parts. First part, the real time program, is running on standalone computer and provides the possibility of changing lung simulation settings. Second part, FPGA program, is flashed directly on CompactRIO system. Data concerning iLung peripherals status are obtained from printed circuit board called Connection Board and transferred to CompactRIO for processing and evaluation by described software.

3.1 FPGA program

Reconfigurable FPGA Chassis is the center of the embedded system architecture. Each I/O module is connected directly, therefore there is almost no control latency for system response compared to other controller architectures. Programs on a real-time controller can access I/O modules with less than 500 ns of jitter between loops. Additionally, because the FPGA runs all code in hardware, it provides high reliability. The NI cRIO 9118 embedded chassis is used in the Lung Simulator. Chassis contains eight module slots and user-programmable Xilinx Virtex 5 FPGA.

FPGA program is compiled and flashed directly on cRIO system. FPGA program evaluates, sets and passes data concerning iLung peripherals status between Real-time program and Connection board. For example, it handles pressure sensor output voltage values and calculates pressure values in bar, calculates revolution, position and therefore speed of the motor according to the values given

from the motor encoder etc. Due to the hardware implementation precise timing in real time is possible.

3.2 Real-time program

Real-time program is running on cRIO and can, with the FPGA program, function as standalone embedded system. Sequence running on the controller can be customised within the LabVIEW user interface. LabVIEW user interface is running on the PC, that is connected to the cRIO via ethernet cabel. This setup provides possibilities of changing lung simulation settings. Program consists of two modes: Calibration \& Initialization mode and Run mode. Calibration allows the possibility to set flowmeters and pressure sensor offset before actual measurements. Therefore, increasing precision of the recorded values. Starting piston position and pressure inside thoracic chamber can be set during initialization according to requirements of the experimenter.

Run mode window offers possibility of choosing the piston movement type. There are four different types of movement called: Gener sin, PI sin, PI breath and Manual. Setting for each type of movement can be modified. Manually control of the pump and the valve can be also turned on. Graphs of airflow and pressure recorded during simulation can be saved into Microsoft Excel spreadsheet. Additional optimization and safety options such as the PI controller setting, maximum negative pressure check and compensation of deflation are also available. It consists of two modes: Calibration & Initialization mode and Run mode.

Calibration & Initialization

After the start of LabVIEW program calibration and initialization window is opened. This window is divided into two parts. The left side is used for calibration of flow and pressure sensors and the right side is used to set the initial conditions for start of the simulation, see Fig. 1.
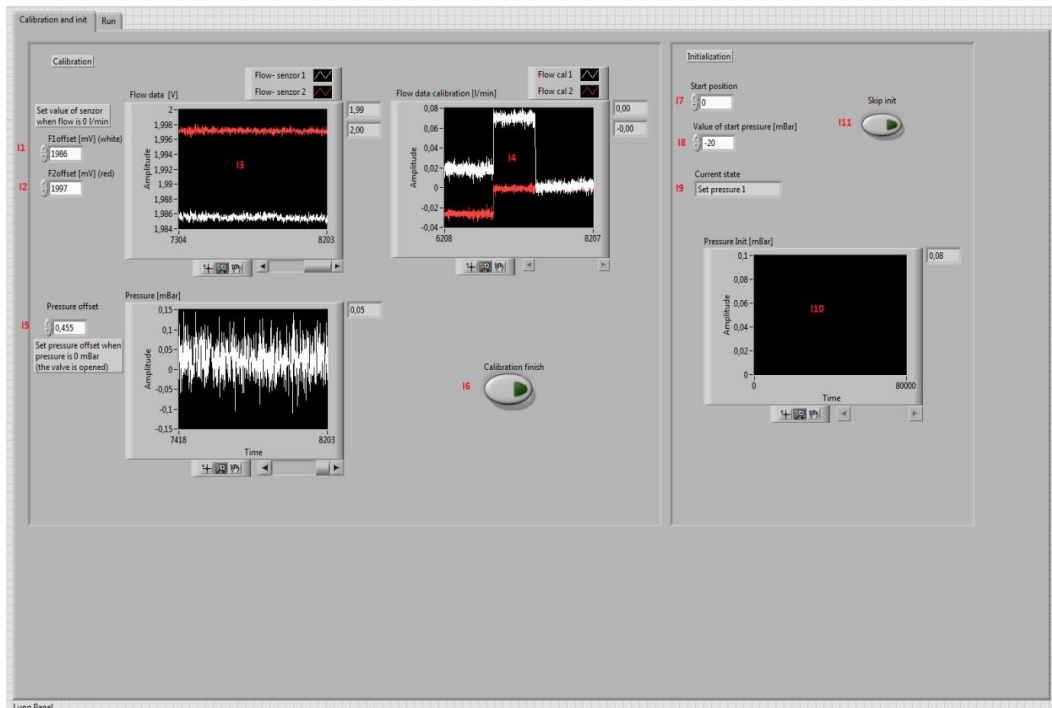
Fig. 1 Calibration and inicialization window

Calibration

As the precision of calibration setting significantly affect measurement results, its necessary to devote enough time into the task [5].

Prior to actual measurements, sensors offset has to be set [mV]. Ensure zero flow throughout the sensors and after you do so set measured sensor values into corresponding boxes situated on the top of the Lung Panel, see Fig. 1. There is one box for each Honeywell AWM720P1flowmeter distinguished by colour of the curve (*I1-F1offset, I2- F2offset*). Ideally both curves in *Flow data calibration [l/min]* graph will be very close to zero, example can be seen on graph I4, after you do so. The values of offsets are taken from graph *I3- Flow data [V]*

The calibration of pressure is based on iterative setting. The offset of pressure must be set (*I5- Pressure offset*) when pressure in the box is equal to atmospheric pressure. Therefore, pressure calibration requires valve to be opened.

%opravit I v programu!! Calibration and ini.. button

The button I6- *Calibration finish* must be push to finish the calibration and then program will continue with initialization. The values of initialization must be set before to press this button.

1. Initialization

Purpose of initialization is to set starting value of piston position and pressure inside thoracic box. The maximum value of piston position is 104000 (piston is the lowest point) and minimum is -104000 (piston is the highest point) *Start position*. Zero position is recommended for the test. The value of piston position is inserted into box *I7*. Second initial condition is the initial pressure value inside the thoracic box. Negative value in mBar is inserted into box *I8- Value of start pressure*.

Current operation of initialization is shown in box *I9- Current state.* Under this box is the graph *I10*, which shows value of pressure during *Set pressure 1* state. Initialization can be skipped by pressing button *I11- Skip init*.

After initialization is completed, program automatically switches into *Run mode*.

Run mode

Run mode window can be divided into three parts, see Fig. 2, from which each serves different purpose. Control elements situated on the top side offer possibility of choosing the piston movement type. Setting for each type of movement can be modified by typing desired value into corresponding box. Middle part of the run mode window presents option to manually control pump and valve. Most importantly graphs of airflow and pressure recorded during simulation are shown. Bottom side provides additional optimization and safety options such as the PI controller setting, maximum negative pressure check and compensation of deflation.
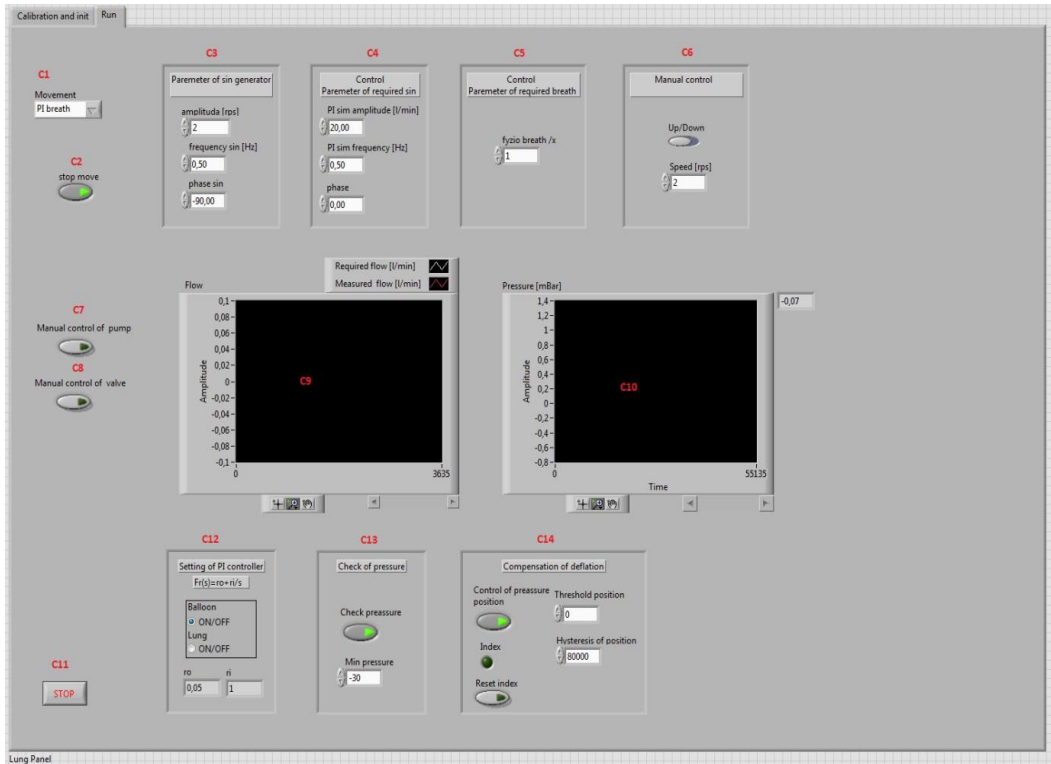
Fig. 2 Run mode window

1. Movement

Various types of piston movement can be chosen from the selection box *C1- Movement*, see Fig. 3.There are four different types of movement called: *Gener sin*, *PI sin, PI breath, Manual.*

Movement parameters are set in boxes *C3, C4, C5, C6* and activated by button *C2-stop move*. When button *C2* is activated, green light is on, the piston does not move.
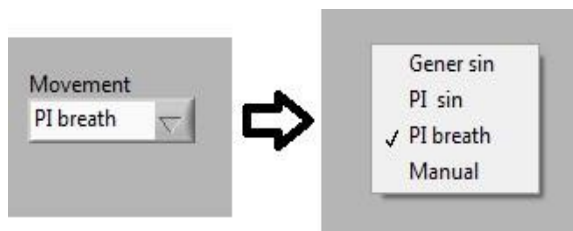
Fig. 3 Possible choices of piston movement

Gener sin

First mode generates sine movement of a piston without feedback control. Shape of the resulting flow curve can vary in correlation to different properties of used lung equivalent.

Sine wave is generated from LabVIEW Sine Generator. Generator parameters are: amplitude of sin wave in revolutions per second [rps], frequency [Hz] and phase [°]. Value of each parameter can be changed in box *C3 -Parameter of sin generator.* Default values are: amplitude 2 rps, frequency 0.5 Hz and phase -90°.

89

PI sin

Second mode uses controller (control loop feedback mechanism) to achieve required flow curve as precisely as possible. Required flow curve is sinus wave. Actual airflow during simulation is measured by Lung 2.1 Honeywell AWM720P flow sensors. PI controller compares measured and required value of flow and adjust piston movement accordingly to the calculated difference.

Parameters of required sinus shape are set in box *C4 - Control Parameter of required sin*. Contrary to previous mode unit of amplitude is liter per minute [l/min] because the values are recounted in LabVIEW real time script thanks to values from flow sensors. Default values are: amplitude 20 l/min, frequency 0.5 Hz and phase 0°.

PI breath

Third mode approximates physiological breathing pattern of human lung. Feedback control is also used but the required flow curve is predefined physiological breathing cycle taken from literature. Tidal volume (gain of the signal) can be changed in the box *C5- Control Parameter of required breath*. Predefined breathing cycle can be seen on Fig. 4 with frequency 0.25 Hz.
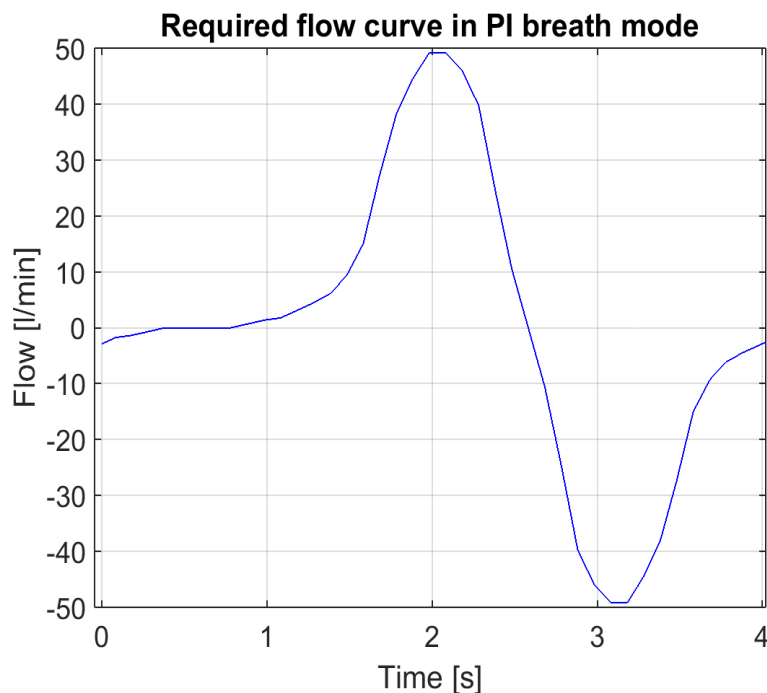
Fig. 4 Predefined flow curve in PI breath mode

Example: Maximum breathing cycle amplitude is 50 l/min. When value *fyzio breath/x* in box C5 will be 0.5 the maximum amplitude will be 25 l/min.

Predefined physiological breathing pattern can be change directly in the program code. String constant *Breath generator* is used for curve setting in first window of flat sequence, see Fig. 5. Breath generator periodically generates new signal where each value in string variable corresponds to 1ms on time axis. Number of values is not limited, however first value should start from zero and also integration over one period must be zero to achieve constant volume of air in the lung.

90
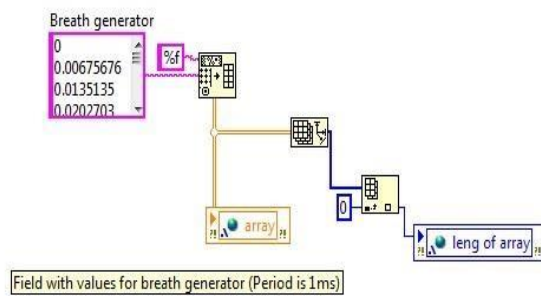
Fig. 5 Generation of physiological breathing cycle in LabVIEW

Manual

Piston movement can be manually controlled by user in this mode. Movement parameters are set in box *C6 – Manual control*. Direction of movement and speed in revolution per second [rps] can be modified. Default values are: direction UP, speed 2 rps.

2. Display of measurements

Graphical representation of measured data is being displayed at graph *C9* and *C10* in real time First graph *C9* shows current flow measured by iLung 2.1 Honeywell AWM720P1 sensors. In modes where controller is used for simulation control required curve of flow is also visible. Second graph *C10* shows currently measured value of pressure inside the thoracic box.

Measured variables are shown in two graphs. First one shows required shape of the airflow and second actual measured one.

Manual control of pump & manual control of valve

In case that currently measured pressure values does not meet user requirements manual control is possible. Vacuum pump can be turn on/off by button *C7,* assuming negative pressure did not reach value required by experimenter. Similarly, valve can be opened/closed by button *C8* in case the pressure inside thoracic chamber is too high.

3. Optimization and safety options

Additional optimization and safety options such as the PI controller setting, maximum negative pressure check and compensation of deflation are described in this section.

PI controller setting

Due to different transfer functions of balloon and lung tested and optimized settings of PI controller are used for better accuracy. Type of the used lung equivalent can be chosen in box *C12*.

Check of the pressure

In case that button in a box *C13 – Check pressure* is activated, the program compares currently measured pressure value inside the thoracic box with set value *Min pressure.* If the pressure value

exceeds set limit piston movement is stopped immediately and the vacuum pump is switched off. Pressure limit is obtained experimentally before simulation and depends on properties of the selected lung model (size, compliance, material, etc.). Minimal value of pressure corresponds with state when lung equivalent is most bloated. Exceeding this limit can permanently damage the lung equivalent.

Compensation of deflation

Active mechanical lung simulator is not completely airtight and during simulations pressure slowly raises due to leakages. Assuming the PI controller is active, piston would try to compensate the leakage by moving downwards. In that case the piston movement would only be in one direction (down) and the simulation would stop after reaching downwards limit position. Therefore, to prevent this from happening, vacuum pump, that creates under pressure, is switched on. As a result of pump function, piston moves upwards to keep steady pressure inside the thoracic chamber After reaching upward position limit the pump is switched off and the whole process repeats itself. Due to that mechanism, simulation can continue without interruption.

4 Known Bugs

- During the breathing simulation motor suddenly stopped responding to control impulses. After diagnostic was made by using s specialized servomotor drive software encoder error was identified. Motor was stuck in "between position" which an encoder was not able to evaluate. Solution to this problem is to manual (using force) move the motor into different position. Described phenomena occurred twice during whole period of simulator testing (6 months).
- There is no dedicated place inside the thoracic box to attached the humidity and temperature sensors. Metal plate must be added.
- Manual movement of piston is sometimes required when reaching upper or down limit position.

Acknowledgement

I LABORATORY EXPERIMENT

Experiment BER-303
"Active Mechanical Lung Simulation"

Course:
Biomedical Engineering in Respiration

Study Program:
Master Biomedical Engineering Sciences

1. Problem Definition

1.1. Familiarize yourself with the *Spirobank II Basic* spirometer and the primary measurement setup.

1.2. Familiarize yourself with the *Active Mechanical Lung Simulator iLung 2.1.* and the setup required for experimental measurements.

1.3. Preform precise calibration of *iLung 2.1* Honeywell AWM720P1 flowmeters and pressure sensor. Set initial conditions according to human physiological values.

1.4. Measure *iLung 2.1* airflow and pressure characteristics during breathing simulations. Use *PI sin* and *PI breath* mode and two 3l Latex bags as a lung equivalent. Repeat measurements tree times for both modes.

1.5. Simultaneously with previous, step measure airflow characteristics during breathing simulation by *Spirobank II Basic* spirometer.

1.6. Analyse the data taken during breathing simulations from both, *iLung 2.1* Honeywell AWM720P1 flowmeters and *Spirobank II Basic* spirometer. Evaluate their comparability.

2. Basics

2.1. Lung Simulation

Study material: Course slides for BER-ILV-6 [1]

Several types of lung models such as electrical, mechanical and mathematical models hve been developed over the years in order to approximate a simulation of the behaviour of a human lung. Due to the difficulties of simulating a fully functional human lung high efforts have to be invested, either in computational power or in the complexity of the design. One of the most precise and reliable ways to simulate the behaviour and function of human lung is to use a mechanical lung simulator [2].

2.2. iLung 2.1

The Lung model 2.1, also called iLung, is next generation active mechanical lung simulator that offers the possibility to simulate physiological breathing patterns. The core element is the thoracic chamber, a PMMA (polymethylmethacrylate), in which different lung equivalents can be mounted. Via the connective flange the chamber is connected to a bellow system and a vacuum pump. The vacuum pump creates a constant negative pressure in order to achieve a more realistic anatomical and physiological breathing situation. The constant negative pressure represents the adhesion of the human lung to the thorax through the pleura. The bellow system induces differences of the pressure within the thoracic chamber due to the movement of the bellow. The bellow movement of compression and extension is in direct correlation to the ball screw in the middle of the bellow. A motor rotates the ball screw which has the effect that the bottom of the bellow is moved upward due to the threaded connection. The pressure changes within the thoracic chamber cause a in- and deflation of the used lung equivalent. Latex bags or porcine lung, which structure is similar to human lung, can be mounted into the simulator. Furthermore, with additional equipment, aerosol measurements are possible [4].

3. Experimental Instructions

3.1. Familiarize yourself with the *Spirobank II Basic* spirometer and the common measurement setup.

The Spirobank II Basic is a pocket spirometer in which a flow and volume measurement sensor is a digital turbine, based on the infrared interruption principal. This principal ensures the accuracy and the reproducibility of the measurements, without requiring a periodic calibration. It can operate in standalone mode and it can be connected to a PC using any one of several available methods: RS232, USB, Bluetooth. A quality control check is carried out internally on the measured parameters.

The Spirobank II Basic can be used with both re-usable and single-use disposable turbines. Re-usable turbines are used with standard adult one-way valve mouthpieces. The single-use disposable turbines have a pre-connected mouthpiece and are individually factory calibrated and packaged.

User manual and datasheet is available in respiration laboratory [3].

More Information can be also found at: http://www.spirometry.com/ENG/Products/spirobank2.asp

3.2. Familiarize yourself with the *Active Mechanical Lung Simulator iLung 2.1.* and the setup required for experimental measurements.

Before any manipulation with hardware or software, read carefully through the iLung 2.1 User Manual which should be available at experiment dedicated workplace. In case it is not, please advise the lecturer and it will be provided to you [5].

Basic setup:

1. Mount two 3l Latex bags as a lung equivalent into simulator thoracic chamber and seal it.
2. Place iLung 2.1 Honeywell AWM720P1 flowmeters at the top of simulated trachea of the simulator (orientation!). Connect flowmeters to the simulator front panel.
3. Connect dedicated PC at the experiment workplace and the simulator front panel via ethernet cable.
4. Place *Spirobank II Basic* spirometer also at the simulated trachea of the simulator (on top of iLung 2.1 flowmeters).
5. Power on the device.
6. Start LabView software and run the program.

3.3. Preform precise calibration of *iLung 2.1* flow and pressure sensors. Set initial conditions according to human physiological values.

After the start of LabView program calibration and initialization window is opened. This window is divided into two parts. The left side is used for calibration of flow and pressure sensors and the right side is used to set the initial conditions for simulation start.

1. Calibration

As the precision of calibration setting significantly affect measurement results, its necessary to devote enough time into the task [5].

Prior to actual measurements, sensor offset has to be set [mV]. Ensure zero flow throughout the sensors and set measured sensor values into corresponding boxes of a LabView program. Ideally Flow data calibration [V] and Pressure [mBar] graphs will be zero after you do so.

2. Initialization

Purpose of initialization is to set starting value of piston position and pressure inside thoracic box. The maximum value of piston position is 104000 (piston is the lowest point) and minimum is -104000 (piston is the highest point). Zero position is recommended for the test. Negative pressure value [mBar] is set according to experimenter requirements.

3.4. Measure iLung 2.1 airflow and pressure characteristics during breathing simulations. Use PI sin and PI breath mode and two 3l latex bags as a lung equivalent. Repeat measurements tree times for both modes.

Read task 3.5 before starting the measurements!

After calibration and initialization of a system is done, proceed with actual measurements by clicking *calibration finish* button. Program will automatically switch into the *Run mode.*

Measurements:

1. From scroll menu *movement* select *PI sin* mode and start measurements by clicking *stop move* button.
2. Record flow and pressure characteristic for at least 60 s.
3. Stop the measurements by clicking *stop move* button.
4. From scroll menu *movement* select *PI breath* mode and repeat tasks as in previous steps.
5. Repeat measurements three times for both breathing modes
6. After required measurements are taken stop bellow movement and exit the program by clicking *STOP* button.
7. Measured values of flow [l/min] and pressure [mBar] are displayed in corresponding graphs.

3.5. Simultaneously with previous step measure airflow characteristics during breathing simulation by *Spirobank II Basic* spirometer

For later analysis and comparison of both datasets measurements has to be taken simultaneously by both devices. Spirobank II Basic spirometer has to be placed at the simulated trachea, together with Honeywell AWM720P1 flowmeters.

3.6 Analyse the data taken during breathing simulations from both, iLung 2.1 Honeywell AWM720P1 flowmeters and Spirobank II Basic spirometer. Evaluate their comparability.

The acquired data has to be analysed separately in the first step. The data for each device and breath mode should be normalised and diagnosed. Possible anomalies should be identified and shown. In a subsequent step the data from iLung 2.1 Honeywell AWM720P1 flowmeters and Spirobank II Basic spirometer should be compared and objectively evaluated. The research question to solve is concerning the comparability of iLung 2.1 Honeywell AWM720P1 flowmeters with Spirobank II Basic spirometer which is certified for spirometry measurements. Also iLung 2.1 data should be compared and discussed in contrast to physiological breathing patterns values.

4. Experimental Setup

The experimental setup contains the following components:

- Spirobank II Basic spirometer
- Spirobank II Analysation Software
- iLung 2.1 and two Honeywell AWM720P1 flowmeters
- iLung 2.1 LabView Control Software
- Two 3l latex bags

The setup has to be placed and used at the defined working place in the laboratory. It is strictly prohibited to move the devices or change the given system setup. Additional tubing and connections will be provided for the experiment on demand.

5. Control Questions

1.1. Sketch and describe the basic setup of a turbine based flowmeter.

1.2 Explain basic types of lung simulation. What are the advantages and disadvantages of each approach?

1.3 Explain basic working principle of iLung 2.1. Don't forget to discuss control and information path.

References

[1] FORJAN, Mathias. *Course slides of BER ILV6.* 2015, [cit. 2015-12-12]. Available from: *https://moodle.technikum-wien.at/course/view.php?id=2509*.

[2] KACMAREK, Robert, James STOLLER a Albert HEUER. *Egan's fundamentals of respiratory care.* 10th ed. St. Louis, Mo: Elsevier, 2013, xvii, 1401 s. ISBN 978-0-323-08203-7.

[3] MEDICAL INTERNATIONAL RESEARCH. *Spirobank II: User Manual* [online]. 2015 [cit. 2016-04-07]. Dostupné z: http://www.spirometry.com/ENG/Products/SpiroBank2.asp.

[4] RWETC. S.R.O. *Lung model 2.1 simulator: Documentation Revision 2.1* Jihlava, 2014[cit. 2015-12-12].

[5] PASTEKA, Richard *iLung 2.1 User Manual* Revision 1.0. Vienna, 2016.